

**Investigating sources and sinks of organic aerosol:
NO₃-initiated oxidation of isoprene and
heterogeneous oxidation of organic aerosol**

Thesis by

Alan J. Kwan

In Partial Fulfillment of the Requirements for the degree of

Doctor of Philosophy



CALIFORNIA INSTITUTE OF TECHNOLOGY

Pasadena, California

2011

© 2011

Alan J. Kwan

All Rights Reserved

Acknowledgments

While only my name appears on the front of this work, it is the result of a collective effort studying a complex system, one involving instrumental development, laboratory and field studies, data analysis, and – as in many human experiences – tedium and drama, frustration and elation. I am honored to have navigated the scientific challenges and emotional vicissitudes with the support of a great team of collaborators and friends.

A constant force in the development of this work has been the intellectual vibrancy of Paul Wennberg and his group. In addition to Paul, John Crouse, David McCabe, Andreas Kürten, Jason St. Clair, Fabien Paulot, Nathan Eddingsaas, Melinda Beaver, and Coleen Roehl provided essential guidance on countless aspects of this work, although the support and encouragement of group members with whom I did not directly collaborate has been invaluable as well.

The Wennberg group's blatant ignorance of boundaries led me to collaborate with John Seinfeld, Richard Flagan, and their group at the Caltech environmental chamber. Here, Jesse Kroll, Nga Lee (Sally) Ng, Arthur Chan, Jason Surratt, Man Nin Chan, Puneet Chhabra, Shane Murphy, Armin Sorooshian, Scott Hersey, Havala Pye, Beth Kautzman, Lindsay Yee, and Christine Loza broadened my perspectives by introducing me to the practices of aerosol science and integrating me into their tight-knit community.

Outside of these two groups, I am also indebted to Janet Hering and Jared Leadbetter, who provided me with initial laboratory experience during my first year as a graduate student, Nathan Dalleska, who informed me with his analytical expertise, Rick Gerhardt, the glassblower who fixed many of my mistakes, and Rick Paniagua and his

team at the Physics machine shop, who taught me about the design and construction of the custom components that make much of this work possible. Outside of Caltech, I am also grateful for the opportunities to do field work sponsored by the National Aeronautics and Space Administration (NASA) and the National Oceanic and Atmospheric Administration (NOAA), which exposed me to different techniques and perspectives in atmospheric chemistry; my coauthors on Chapter 4 were especially helpful, but there are many other investigators whom I met during these missions and subsequent science team meetings who were generous with their time and knowledge to help me gain a foothold in a complicated field. Finally, my outside committee members, Mitchio Okumura and Alex Sessions, also deserve recognition for taking time out of their work to lend their fresh perspectives onto mine.

Lastly, this work is the result of efforts of many strangers, some recognized as Carlylian giants though most consigned to anonymity by history, whose struggles and ultimate successes have allowed me to live in an age and a place where living past one's 30th birthday is commonplace, and where I have the freedom to pursue my own dreams and make my own mistakes. Many in this world and in history have not shared my good fortune, often through no fault of their own. Regardless of this work's ultimate impact, I should be thankful that I had the opportunity to pursue it.

Brief mentions don't do justice to everyone's contributions, and I have likely neglected to mention many. Any omissions in acknowledgments, as well as any errors contained in the work that follows, are entirely my fault.

Abstract

Secondary organic aerosol (SOA) are important components in atmospheric processes and significantly impact human health. The complexity of SOA composition and formation processes has hampered efforts to fully characterize their impacts, and to predict how those impacts will be affected by changes in climate and human activity. Here, we explore SOA formation in the laboratory by coupling an environmental chamber with a suite of analytical tools, including a gas-phase mass spectrometry technique that is well suited for tracking the hydrocarbon oxidation processes that drive SOA formation. Focusing on the oxidation of isoprene by the nitrate radical, NO_3 , we find that reactions of peroxy radicals (RO_2) to form ROOR dimers is an important process in SOA formation. The other gas-phase products of these RO_2 reactions differ from what is expected from studies of simpler radicals, indicating that more studies are necessary to fully constrain RO_2 chemistry. Finally, we examine the role of heterogeneous oxidation as a sink of organic aerosol and a source of oxygenated volatile organic compounds in the free troposphere.

Table of Contents

Acknowledgments	iii
Abstract	v
Chapter 1: Introduction	1
References	6
Chapter 2: Secondary organic aerosol formation from the reaction of isoprene with nitrate radicals	15
Abstract	16
2.1 Introduction	16
2.2 Experimental	19
2.3 Results	24
2.3.1 Blank experiments	24
2.3.2 Aerosol yields	25
2.3.3 Gas-phase measurements	27
2.3.4 Chemical composition of SOA	30
2.3.4.1 Aerosol Mass Spectrometer (Q-AMS) measurements	30
2.3.4.2 Offline chemical analysis	31
2.4 Gas-phase chemistry and SOA formation	34
2.4.1 Formation of various gas-phase products	34
2.4.2 Effect of peroxy radical chemistry on SOA yield	37
2.4.3 Growth curves: multiple steps in SOA formation	39
2.4.4 Proposed mechanisms of SOA formation	41

2.5	Approximate estimate of global SOA production from isoprene + NO ₃	48
2.6	Implications	51
	Acknowledgments	54
	References	55
	Tables	72
	Figures	80
Chapter 3: Products of peroxy radical reactions from the NO₃-initiated oxidation of isoprene		98
	Abstract	99
3.1	Introduction	99
3.2	Experimental	102
3.3	Results and Discussion	105
3.3.1	Nitrate yield	106
3.3.2	Hydroxyl radical (OH) formation	109
3.3.3	RO ₂ -RO ₂ branching ratio	114
3.3.4	RO radical fate and HO ₂ production	116
3.3.5	Formation of dimer compounds	117
3.4	Implications	118
	Acknowledgments	124
	References	124

Tables	148
Figures	150
Chapter 4: The potential flux of oxygenated volatile organic compounds from organic aerosol oxidation	
Abstract	156
4.1 Introduction	157
4.2 Method	158
4.3 Results and Discussion	160
4.4 Implications	162
4.5 Conclusions and recommendations	164
Acknowledgments	165
References	165
Figures	173
Chapter 5: Conclusions and future directions	175
References	181
Appendix: List of authored and coauthored publications	184

List of Tables and Figures

Table 2.1: Initial conditions and results for isoprene-NO ₃ aerosol yield experiments	72
Table 2.2: Isoprene-NO ₃ SOA products identified with UPLC/(-)ESI-TOFMS	73
Table 2.3: Peroxide content of SOA formed by isoprene-NO ₃ reactions	78
Table 2.4: Global estimation of isoprene burdens and sinks using GEOS-Chem	79
Figure 2.1: Time profiles of aerosol volume and inorganic nitrate measured by PILS/IC, and nitrate signals from Q-AMS in a blank experiment (~1 ppm N ₂ O ₅ , ammonium sulfate seed, no isoprene)	80
Figure 2.2: Isoprene depletion and SOA formation for typical experiment	81
Figure 2.3: SOA yield data and yield curve for isoprene-NO ₃ reaction.	82
Figure 2.4: Time-dependent growth curves for the slow N ₂ O ₅ injection experiment and slow isoprene injection experiment	83
Figure 2.5: Time profiles of the major gas-phase products (<i>m/z</i> 230, 232, and 248) and the corresponding aerosol growth from the excess isoprene experiment	84
Figure 2.6: Time evolution of various gas-phase products in the staggered N ₂ O ₅ injection experiment	85
Figure 2.7: AMS spectrum for SOA formed in typical yield experiments	86
Figure 2.8: AMS spectra signal from the slow N ₂ O ₅ injection experiment versus a typical yield experiment	87

Figure 2.9: AMS spectra signal from the slow isoprene injection experiment versus a typical yield experiment	88
Figure 2.10: UPLC/(-)ESI-TOFMS base peak ion chromatograms (BPCs) for isoprene-NO ₃ oxidation experiments	89
Figure 2.11: Proposed mechanisms for the formation of various gas-phase intermediate product ions observed by CIMS	90
Figure 2.12: Time profiles of the major gas-phase products (<i>m/z</i> 230, 232, and 248) and the corresponding aerosol growth from the slow N ₂ O ₅ injection experiment	91
Figure 2.13: Time profiles of the major gas-phase products (<i>m/z</i> 230, 232, and 248) and the corresponding aerosol growth from the slow isoprene injection experiment	92
Figure 2.14: Proposed mechanism for SOA formation from the formation and decay of the C ₅ -hydroxynitrate gas-phase product formed from the isoprene + NO ₃ reaction	93
Figure 2.15: Proposed mechanism for SOA formation from the formation and decay of the CIMS <i>m/z</i> 377 gas-phase product formed from the isoprene + NO ₃ reaction	94
Figure 2.16: Proposed mechanism for SOA formation from the formation and decay of the CIMS <i>m/z</i> 393 gas-phase product formed from the isoprene + NO ₃ reaction	95

Figure 2.17: Proposed mechanism for SOA formation from the formation and decay of the C ₅ -nitrooxycarbonyl, C ₅ -hydroxycarbonyl, and C ₅ dinitrate first-generation products formed from the isoprene + NO ₃ reaction	97
Table 3.1: Gas-phase products of isoprene-NO ₃ reaction detected by GC-FID and CIMS	148
Table 3.2: Box model parameters for assessment of possible OH radical sources in isoprene-NO ₃ system	149
Figure 3.1: Generalized reaction mechanism for isoprene-NO ₃ system.	150
Figure 3.2: Formation of compounds resulting from isomerization of alkoxy radicals and seen by CIMS instrument at m/z 216, 246, 248, and 264	151
Figure 3.3: Formation mechanism of methyl vinyl ketone, methacrolein, 3-methylfuran, and hydroxycarbonyl, leading to release of NO ₂	152
Figure 3.4: Box model simulations for OH production in isoprene-NO ₃ system	153
Figure 3.5: Proposed formation mechanisms of products detected by CIMS at m/z 316, 330, 332, and 348	154
Figure 3.6: Formation mechanism of dinitrooxyepoxide and hydroxyl radical from oxidation of nitrooxyhydroperoxide	155
Figure 4.1: Mean elevation profiles of aerosol collision rates with OH, O ₃ , H ₂ O ₂ during INTEX-NA campaign	173

Figure 4.2: Modeled vs. measured elevation profiles for acetaldehyde and peroxyacetic acid during INTEX-NA campaign

Chapter 1

Introduction

Aerosols, liquid or solid particles suspended in air, are important components of the Earth's atmosphere. They affect the Earth's radiative balance both directly, through shortwave scattering and longwave absorption, and indirectly, through cloud formation, with consequences for global climate. Clouds in turn also impact atmospheric chemistry through their role in affecting photolysis reactions and mediating aqueous phase reactions that significantly alter the fate and distribution of trace gases (Cohan et al., 1999; Mari et al., 2000; Tie et al., 2003; Ervens et al., 2004; Sorooshian et al., 2006). Aerosols have also been implicated in respiratory and cardiovascular disease (Harrison and Yin, 2000; Davidson et al., 2005; Pope and Dockery, 2006).

Fully assessing aerosols' impact on the environment, and predicting future impacts driven by changes in emissions and climate, requires an understanding of aerosol sources, sinks, and composition that is currently lacking. Models of global aerosol burdens routinely underpredict field measurements (de Gouw et al., 2005; Heald et al., 2005; Volkammer et al., 2006), while analytical techniques have identified only ~ 10% of the mass of organic aerosols (Hallquist et al., 2009). Although aerosols are complex mixtures of inorganic (primarily sulfate) and organic components (Murphy et al., 2006; Zhang et al., 2007), most of the current uncertainties surrounding aerosol are probably linked to the organic portion, which is the more abundant fraction. Sulfur budgets have fewer uncertainties – estimates of global sulfur budgets are constrained to a factor of 2 (Barrie et al., 2001) – and less variation in chemical speciation than organic carbon.

Organic aerosol can be categorized as either primary (POA), i.e., directly emitted into the atmosphere, or secondary (SOA), i.e., formed from gaseous precursors, with SOA believed to be dominant (Goldstein and Galbally, 2007; Robinson et al., 2007;

Donahue et al., 2009; Hallquist et al., 2009). Currently, models apply laboratory determinations of SOA yields (aerosol mass formed divided by mass of precursor reacted) and precursor emission inventories to predict aerosol burdens. The significant underestimation by models can thus be due to many factors, including missing or underestimated precursor volatile organic compounds (VOCs) (Lewis et al., 2000; Di Carlo et al., 2004; Holzinger et al., 2005; Hamilton et al., 2009), missing SOA formation pathways such as heterogeneous esterification and polymerization reactions (Iinuma et al., 2004; Surratt et al., 2006, 2007ab, 2008), or that laboratory conditions are not representative of the atmosphere with respect to certain crucial parameters (Kroll and Seinfeld, 2008; Hallquist et al., 2009).

Increased understanding of SOA formation processes will help resolve the current discrepancy between models and measurements. Experimental studies of SOA typically fall into one of three complementary categories: flow tube studies, environmental chamber studies, and field studies. Flow tube studies are useful for isolating individual reaction pathways and quantifying fundamental parameters such as rate constants and accommodation coefficients, but are typically performed on too short a time scale (~seconds) to capture the chemical aging processes relevant to SOA formation. Field studies represent real atmospheric conditions, but important conditions such as emissions, wind patterns, and temperature are uncontrolled, which complicates data interpretation, and important species in both the gas and aerosol phases are often at low concentrations, which presents analytical challenges. Environmental chambers bridge these two scales, facilitating studies under conditions that are more atmospherically relevant than those of flow tubes and more controlled than those of field studies. Chamber studies also have

limitations; for example, they are usually performed at reagent concentrations that are higher than ambient, which can affect both the thermodynamics and kinetics of SOA formation (Odum et al., 1996; Presto and Donahue, 2006; Chan et al., 2007; Kroll et al., 2007), and most chambers can only run experiments that last about 1 day, which may not capture all processes relevant to SOA formation and loss. Nonetheless, in concert with other experimental and modeling techniques, they can provide important insights into SOA formation.

When performing chamber studies, the complexity of SOA precursors, components, and formation mechanisms necessitates having a wide suite of instrumentation to provide multiple, complementary perspectives on the evolution of gas and particle phase species during an experiment, as there is no single instrument that is capable of providing a complete characterization. A recent addition to the instrumental suite of the Caltech environmental chamber is a chemical ionization mass spectrometer (CIMS) (Crouse et al., 2006), which utilizes the CF_3O^- ion to selectively cluster compounds with high fluorine affinity. Two characteristics of the CIMS make it particularly suited for SOA studies. First, unlike common ionizing agents such as electrons or protons, CF_3O^- ionizes “softly,” i.e., with minimal fragmentation of the analyte, so that the analyte’s mass can be determined unambiguously. Second, polar compounds, such as acids, peroxides, and multifunctional carbonyls, have high fluorine affinity and are thus detectable by the CIMS. As VOCs are oxidized, they tend to gain polarity which in turn lowers their vapor pressure. Therefore, the CIMS provides previously missing information about the sources and fate of polar compounds which are

important components of VOC degradation mechanisms and key intermediates to SOA formation.

The selectivity, versatility, and time resolution of the CIMS makes it a good alternative to other techniques that measure a similar set of compounds. Acid and peroxide measurements typically involve collecting samples in water, which are then analyzed with chromatographic separation (Cofer et al., 1985; Lee et al., 1995). These techniques involve significant sample handling, which increase the chance of artifacts, and have poor time resolution. Nitrates, which are important VOC oxidation products in anthropogenically influenced environments, are often measured with Fourier transform infrared (FT-IR) (Barnes et al., 1990; Skov et al., 1992; Bernt and Böge, 1997), or thermal dissociation-laser induced fluorescence (TD-LIF) (Perring et al., 2009; Rollins et al., 2009), which measure only total nitrate, but don't speciate between different nitrate compounds.

The following work demonstrates insights into SOA formation and VOC degradation mechanisms that have been gained by coupling the CIMS to the Caltech environmental chamber. It focuses on studies of the reaction between the nitrate radical (NO_3) and isoprene (C_5H_8). Isoprene is a highly reactive VOC and is the most abundant VOC in the atmosphere after methane. Because of its reactivity and abundance, it is an important compound in atmospheric oxidation chemistry, and in the last decade it has also been recognized as an important source of SOA during photooxidation (i.e., daytime oxidation by OH, the hydroxyl radical). Its nighttime chemistry has been studied less extensively, so studies with the NO_3 radical, an important nighttime oxidant, are important to fully understand its fate and impact in the atmosphere.

In the following chapter, we demonstrate that the NO_3 -initiated oxidation of isoprene can produce a significant yield of SOA, and that a key parameter in determining the yield is the fate of the peroxy radical (RO_2) that forms in the initial oxidation step. In particular, if an RO_2 reacts with another RO_2 , it can dimerize into an ROOR compound, which is an efficient pathway for lowering vapor pressure.

Next, we perform a detailed gas-phase product study of RO_2 - RO_2 reactions in the isoprene- NO_3 system. Despite the potential importance of RO_2 - RO_2 reactions, only a limited suite of these reactions has been studied due to experimental challenges. In these studies, the RO_2 are typically small ($< \text{C}_3$) and are alkyl-, hydroxy-, acetyl-, or halogenated peroxy radicals. No studies of large, nitrooxy, or allylic peroxy radicals, such as those in the isoprene- NO_3 system, have been performed, and our study shows that these peroxy radicals lead to a significantly different product distribution than what is suggested by previous work, indicating that more studies on a greater variety of peroxy radical reactions are necessary to produce accurate chemical models.

Finally, the fate of organic aerosols after emission or formation are also important, so we speculate on organic aerosol sinks using data from the airborne NASA INTEX-NA field campaign. Specifically, we examine heterogeneous oxidation by OH, O_3 , and H_2O_2 as a potential source of oxygenated VOC into the upper troposphere, which is another current controversy in atmospheric chemistry.

References

Barrie, L. A., Yi, Y., Leaitch, W. R., Lohmann, U., Kasibhatla, P., Roelofs, G. J., Wilson, J., McGovern, F., Benkovitz, C., Melieres, M. A., Law, K., Prospero, J., Kritz, M., Bergmann, D., Bridgeman, C., Chin, M., Christensen, J., Easter, R., Feichter, J., Land, C.,

Jeuken, A., Kjellstrom, E., Koch, D., and Rasch, P.: A comparison of large-scale atmospheric sulphate aerosol models (COSAM): overview and highlights, *Tellus Series B-Chemical and Physical Meteorology*, 53, 615-645, 2001.

Berndt, T., and Boge, O.: Gas-phase reaction of NO_3 radicals with isoprene: A kinetic and mechanistic study, *International Journal of Chemical Kinetics*, 29, 755-765, 1997.

Chan, A. W. H., Kroll, J. H., Ng, N. L., and Seinfeld, J. H.: Kinetic modeling of secondary organic aerosol formation: effects of particle- and gas-phase reactions of semivolatile products, *Atmospheric Chemistry and Physics*, 7, 4135-4147, 2007.

Cofer, W. R., Collins, V. G., and Talbot, R. W.: Improved aqueous scrubber for collection of soluble atmospheric trace gases, *Environmental Science & Technology*, 19, 557-560, 1985.

Cohan, D. S., Schultz, M. G., Jacob, D. J., Heikes, B. G., and Blake, D. R.: Convective injection and photochemical decay of peroxides in the tropical upper troposphere: Methyl iodide as a tracer of marine convection, *Journal of Geophysical Research-Atmospheres*, 104, 5717-5724, 1999.

Crouse, J. D., McKinney, K. A., Kwan, A. J., and Wennberg, P. O.: Measurement of gas-phase hydroperoxides by chemical ionization mass spectrometry, *Analytical Chemistry*, 78, 6726-6732, 10.1021/ac0604235, 2006.

Davidson, C. I., Phalen, R. F., and Solomon, P. A.: Airborne particulate matter and human health: A review, *Aerosol Science and Technology*, 39, 737-749, 10.1080/02786820500191348, 2005.

de Gouw, J. A., Middlebrook, A. M., Warneke, C., Goldan, P. D., Kuster, W. C., Roberts, J. M., Fehsenfeld, F. C., Worsnop, D. R., Canagaratna, M. R., Pszenny, A. A. P., Keene, W. C., Marchewka, M., Bertman, S. B., and Bates, T. S.: Budget of organic carbon in a polluted atmosphere: Results from the New England Air Quality Study in 2002, *Journal of Geophysical Research-Atmospheres*, 110, D16305, 10.1029/2004jd005623, 2005.

Di Carlo, P., Brune, W. H., Martinez, M., Harder, H., Leshner, R., Ren, X. R., Thornberry, T., Carroll, M. A., Young, V., Shepson, P. B., Riemer, D., Apel, E., and Campbell, C.: Missing OH reactivity in a forest: Evidence for unknown reactive biogenic VOCs, *Science*, 304, 722-725, 2004.

Donahue, N. M., Robinson, A. L., and Pandis, S. N.: Atmospheric organic particulate matter: From smoke to secondary organic aerosol, *Atmospheric Environment*, 43, 94-106, 10.1016/j.atmosenv.2008.09.055, 2009.

Ervens, B., Feingold, G., Frost, G. J., and Kreidenweis, S. M.: A modeling study of aqueous production of dicarboxylic acids: 1. Chemical pathways and speciated organic mass production, *Journal of Geophysical Research-Atmospheres*, 109, D15205

10.1029/2003jd004387, 2004.

Goldstein, A. H., and Galbally, I. E.: Known and unexplored organic constituents in the earth's atmosphere, *Environmental Science & Technology*, 41, 1514-1521, 2007.

Hallquist, M., Wenger, J. C., Baltensperger, U., Rudich, Y., Simpson, D., Claeys, M., Dommen, J., Donahue, N. M., George, C., Goldstein, A. H., Hamilton, J. F., Herrmann, H., Hoffmann, T., Iinuma, Y., Jang, M., Jenkin, M. E., Jimenez, J. L., Kiendler-Scharr, A., Maenhaut, W., McFiggans, G., Mentel, T. F., Monod, A., Prevot, A. S. H., Seinfeld, J. H., Surratt, J. D., Szmigielski, R., and Wildt, J.: The formation, properties and impact of secondary organic aerosol: current and emerging issues, *Atmospheric Chemistry and Physics*, 9, 5155-5236, 2009.

Hamilton, J. F., Lewis, A. C., Carey, T. J., Wenger, J. C., Garcia, E. B. I., and Munoz, A.: Reactive oxidation products promote secondary organic aerosol formation from green leaf volatiles, *Atmospheric Chemistry and Physics*, 9, 3815-3823, 2009.

Harrison, R. M., and Yin, J. X.: Particulate matter in the atmosphere: which particle properties are important for its effects on health?, *Science of the Total Environment*, 249, 85-101, 2000.

Heald, C. L., Jacob, D. J., Park, R. J., Russell, L. M., Huebert, B. J., Seinfeld, J. H., Liao, H., and Weber, R. J.: A large organic aerosol source in the free troposphere missing from

current models, *Geophysical Research Letters*, 32, L18809, 10.1029/2005gl023831, 2005.

Holzinger, R., Lee, A., Paw, K. T., and Goldstein, A. H.: Observations of oxidation products above a forest imply biogenic emissions of very reactive compounds, *Atmospheric Chemistry and Physics*, 5, 67-75, 2005.

Iinuma, Y., Boge, O., Gnauk, T., and Herrmann, H.: Aerosol-chamber study of the alpha-pinene/O₃ reaction: influence of particle acidity on aerosol yields and products, *Atmospheric Environment*, 38, 761-773, 10.1016/j.atmosenv.2003.10.015, 2004.

Kroll, J. H., Chan, A. W. H., Ng, N. L., Flagan, R. C., and Seinfeld, J. H.: Reactions of semivolatile organics and their effects on secondary organic aerosol formation, *Environmental Science & Technology*, 41, 3545-3550, 10.1021/es062059x, 2007.

Kroll, J. H., and Seinfeld, J. H.: Chemistry of secondary organic aerosol: Formation and evolution of low-volatility organics in the atmosphere, *Atmospheric Environment*, 42, 3593-3624, 10.1016/j.atmosenv.2008.01.003, 2008.

Lee, M., Noone, B. C., O'Sullivan, D., and Heikes, B. G.: Method for the collection and HPLC analysis of hydrogen peroxide and C-1 and C-2 hydroperoxides in the atmosphere, *Journal of Atmospheric and Oceanic Technology*, 12, 1060-1070, 1995.

Lewis, A. C., Carslaw, N., Marriott, P. J., Kinghorn, R. M., Morrison, P., Lee, A. L., Bartle, K. D., and Pilling, M. J.: A larger pool of ozone-forming carbon compounds in urban atmospheres, *Nature*, 405, 778-781, 2000.

Murphy, D. M., Cziczo, D. J., Froyd, K. D., Hudson, P. K., Matthew, B. M., Middlebrook, A. M., Peltier, R. E., Sullivan, A., Thomson, D. S., and Weber, R. J.: Single-particle mass spectrometry of tropospheric aerosol particles, *Journal of Geophysical Research-Atmospheres*, 111, D23s32, 10.1029/2006jd007340, 2006.

Odum, J. R., Hoffmann, T., Bowman, F., Collins, D., Flagan, R. C., and Seinfeld, J. H.: Gas/particle partitioning and secondary organic aerosol yields, *Environmental Science & Technology*, 30, 2580-2585, 1996.

Perring, A. E., Wisthaler, A., Graus, M., Wooldridge, P. J., Lockwood, A. L., Mielke, L. H., Shepson, P. B., Hansel, A., and Cohen, R. C.: A product study of the isoprene+NO₃ reaction, *Atmospheric Chemistry and Physics*, 9, 4945-4956, 2009.

Pope, C. A., and Dockery, D. W.: Health effects of fine particulate air pollution: Lines that connect, *Journal of the Air & Waste Management Association*, 56, 709-742, 2006.

Presto, A. A., and Donahue, N. M.: Investigation of alpha-pinene plus ozone secondary organic aerosol formation at low total aerosol mass, *Environmental Science & Technology*, 40, 3536-3543, 10.1021/es052203z, 2006.

Robinson, A. L., Donahue, N. M., Shrivastava, M. K., Weitkamp, E. A., Sage, A. M., Grieshop, A. P., Lane, T. E., Pierce, J. R., and Pandis, S. N.: Rethinking organic aerosols: Semivolatile emissions and photochemical aging, *Science*, 315, 1259-1262, 10.1126/science.1133061, 2007.

Rollins, A. W., Kiendler-Scharr, A., Fry, J. L., Brauers, T., Brown, S. S., Dorn, H. P., Dube, W. P., Fuchs, H., Mensah, A., Mentel, T. F., Rohrer, F., Tillmann, R., Wegener, R., Wooldridge, P. J., and Cohen, R. C.: Isoprene oxidation by nitrate radical: alkyl nitrate and secondary organic aerosol yields, *Atmospheric Chemistry and Physics*, 9, 6685-6703, 2009.

Skov, H., Hjorth, J., Lohse, C., Jensen, N. R., and Restelli, G.: Products and mechanisms of the reactions of the nitrate radical (NO_3) with isoprene, 1,3-butadiene and 2,3-dimethyl-1,3-butadiene in air, *Atmospheric Environment Part A-General Topics*, 26, 2771-2783, 1992.

Sorooshian, A., Varutbangkul, V., Brechtel, F. J., Ervens, B., Feingold, G., Bahreini, R., Murphy, S. M., Holloway, J. S., Atlas, E. L., Buzorius, G., Jonsson, H., Flagan, R. C., and Seinfeld, J. H.: Oxalic acid in clear and cloudy atmospheres: Analysis of data from International Consortium for Atmospheric Research on Transport and Transformation 2004, *Journal of Geophysical Research-Atmospheres*, 111, D23s45, 10.1029/2005jd006880, 2006.

Surratt, J. D., Murphy, S. M., Kroll, J. H., Ng, N. L., Hildebrandt, L., Sorooshian, A., Szmigielski, R., Vermeylen, R., Maenhaut, W., Claeys, M., Flagan, R. C., and Seinfeld, J. H.: Chemical composition of secondary organic aerosol formed from the photooxidation of isoprene, *Journal of Physical Chemistry A*, 110, 9665-9690, 10.1021/jp061734m, 2006.

Surratt, J. D., Kroll, J. H., Kleindienst, T. E., Edney, E. O., Claeys, M., Sorooshian, A., Ng, N. L., Offenberg, J. H., Lewandowski, M., Jaoui, M., Flagan, R. C., and Seinfeld, J. H.: Evidence for organosulfates in secondary organic aerosol, *Environmental Science & Technology*, 41, 517-527, 10.1021/es062081q, 2007a.

Surratt, J. D., Lewandowski, M., Offenberg, J. H., Jaoui, M., Kleindienst, T. E., Edney, E. O., and Seinfeld, J. H.: Effect of acidity on secondary organic aerosol formation from isoprene, *Environmental Science & Technology*, 41, 5363-5369, 10.1021/es0704176, 2007b.

Surratt, J. D., Gomez-Gonzalez, Y., Chan, A. W. H., Vermeylen, R., Shahgholi, M., Kleindienst, T. E., Edney, E. O., Offenberg, J. H., Lewandowski, M., Jaoui, M., Maenhaut, W., Claeys, M., Flagan, R. C., and Seinfeld, J. H.: Organosulfate formation in biogenic secondary organic aerosol, *Journal of Physical Chemistry A*, 112, 8345-8378, 10.1021/jp802310p, 2008.

Tie, X. X., Madronich, S., Walters, S., Zhang, R. Y., Rasch, P., and Collins, W.: Effect of clouds on photolysis and oxidants in the troposphere, *Journal of Geophysical Research-Atmospheres*, 108, 4642, 10.1029/2003jd003659, 2003.

Volkamer, R., Jimenez, J. L., San Martini, F., Dzepina, K., Zhang, Q., Salcedo, D., Molina, L. T., Worsnop, D. R., and Molina, M. J.: Secondary organic aerosol formation from anthropogenic air pollution: Rapid and higher than expected, *Geophysical Research Letters*, 33, L17811, 10.1029/2006gl026899, 2006.

Zhang, Q., Jimenez, J. L., Canagaratna, M. R., Allan, J. D., Coe, H., Ulbrich, I., Alfarra, M. R., Takami, A., Middlebrook, A. M., Sun, Y. L., Dzepina, K., Dunlea, E., Docherty, K., DeCarlo, P. F., Salcedo, D., Onasch, T., Jayne, J. T., Miyoshi, T., Shimo, A., Hatakeyama, S., Takegawa, N., Kondo, Y., Schneider, J., Drewnick, F., Borrmann, S., Weimer, S., Demerjian, K., Williams, P., Bower, K., Bahreini, R., Cottrell, L., Griffin, R. J., Rautiainen, J., Sun, J. Y., Zhang, Y. M., and Worsnop, D. R.: Ubiquity and dominance of oxygenated species in organic aerosols in anthropogenically-influenced Northern Hemisphere midlatitudes, *Geophysical Research Letters*, 34, L13801, 10.1029/2007gl029979, 2007.

Chapter 2

Secondary organic aerosol formation from reaction of isoprene with nitrate radical¹

¹ Adapted from Ng, N. L., Kwan, A. J., Surratt, J. D., Chan, A. W. H., Chhabra, P. S., Sorooshian, A., Pye, H. O. T., Crouse, J. D., Wennberg, P. O., Flagan, R. C., and Seinfeld, J. H.: Secondary organic aerosol (SOA) formation from reaction of isoprene with nitrate radicals (NO₃), *Atmospheric Chemistry and Physics*, 8, 4117-4140, 2008.

Abstract

Secondary organic aerosol (SOA) formation from the reaction of isoprene with nitrate radicals (NO_3) is investigated in the Caltech indoor chambers. Experiments are performed in the dark and under dry conditions ($\text{RH} < 10\%$) using N_2O_5 as a source of NO_3 radicals. For an initial isoprene concentration of 18.4 to 101.6 ppb, the SOA yield (defined as the ratio of the mass of organic aerosol formed to the mass of parent hydrocarbon reacted) ranges from 4.3% to 23.8%. By examining the time evolutions of gas-phase intermediate products and aerosol volume in real time, we are able to constrain the chemistry that leads to the formation of low-volatility products. Although the formation of ROOR from the reaction of two peroxy radicals (RO_2) has generally been considered as a minor channel, based on the gas-phase and aerosol-phase data it appears that $\text{RO}_2 + \text{RO}_2$ reaction (self reaction or cross-reaction) in the gas phase yielding ROOR products is a dominant SOA formation pathway. A wide array of organic nitrates and peroxides are identified in the aerosol formed and mechanisms for SOA formation are proposed. Using a uniform SOA yield of 10% (corresponding to $M_0 \cong 10 \mu\text{g m}^{-3}$), it is estimated that ~ 2 to 3 Tg yr^{-1} of SOA results from isoprene + NO_3 . The extent to which the results from this study can be applied to conditions in the atmosphere depends on the fate of peroxy radicals in the nighttime troposphere.

2.1 Introduction

Isoprene has the largest emissions of any non-methane hydrocarbon ($\sim 500 \text{ Tg yr}^{-1}$) (Guenther et al., 1995; Guenther et al., 2006). In the troposphere, isoprene reacts with hydroxyl radicals (OH), ozone (O_3), and nitrate radicals (NO_3). Owing to its high

concentration and reactivity with OH radicals, isoprene plays an important role in the photochemistry occurring within the atmospheric boundary layer. Recently, it has been shown that the photooxidation of isoprene leads to the formation of low volatility species that condense to form SOA (Claeys et al., 2004; Edney et al., 2005; Kroll et al., 2005; Dommen et al., 2006; Kroll et al., 2006; Surratt et al., 2006); SOA yields as high as ~ 3% have been observed (Kroll et al., 2005; Kroll et al., 2006). Global SOA production from isoprene photooxidation has been estimated to be about 13 Tg yr⁻¹ (Henze et al., 2007).

Although emission of isoprene from vegetation is triggered by sunlight and increases with light intensity and temperature (e.g., Sharkey et al., 1996), the isoprene mixing ratio has been observed to peak in early evening in several field studies, with a measured mixing ratio up to a few ppb (Curren et al., 1998; Starn et al., 1998; Stroud et al., 2002; Steinbacher et al., 2005). After sunset, the isoprene mixing ratio drops rapidly, and it has been suggested that the reaction with nitrate radicals, NO₃, is a major contributor to isoprene decay at night (Curren et al., 1998; Starn et al., 1998; Stroud et al., 2002; Steinbacher et al., 2005). Typical NO₃ radical mixing ratios in boundary layer continental air masses range between ~10 to ~100 ppt (Platt and Janssen, 1995; Smith et al., 1995; Heintz et al., 1996; Carslaw et al., 1997). Concentrations as high as several hundred ppt have been observed over northeastern USA and Europe, however (Platt et al., 1981; von Friedeburg et al., 2002; Brown et al., 2006; Penkett et al., 2007). Given the rapid reaction rate between isoprene and NO₃ radicals ($k_{\text{NO}_3} = 7 \times 10^{-13} \text{ cm}^3 \text{ molecule}^{-1} \text{ s}^{-1}$ at $T = 298 \text{ K}$, IUPAC), it is likely that NO₃ radicals play a major role in the nighttime chemistry of isoprene.

The kinetics and gas-phase products of the isoprene-NO₃ reaction have been the subject of several laboratory and theoretical studies (Jay and Stieglitz, 1989; Barnes et al., 1990; Skov et al., 1992; Kwok et al., 1996; Berndt and Böge, 1997; Suh et al., 2001; Zhang et al., 2002; Fan et al., 2004). In many studies, C₅-nitrooxycarbonyl is identified as the major first-generation gas-phase reaction product (Jay and Stieglitz, 1989; Skov et al., 1992; Kwok et al., 1996; Berndt and Böge, 1997). Other compounds such as C₅-hydroxynitrate, C₅-nitrooxyhydroperoxide, and C₅-hydroxycarbonyl have also been identified (Kwok et al., 1996); C₅-hydroxynitrate has also been measured in ambient air with concentrations in the lower ppt range at a few ng m⁻³ (Werner et al., 1999). According to the experimental study by Barnes et al. (1990), the yield for nitrate-containing compounds from the reaction of isoprene and NO₃ radicals can be as high as 80%. A recent modeling study in conjunction with observations from the ICARTT field campaign suggests that ~50% of the total isoprene nitrates production occurs via reaction of isoprene and NO₃ radicals (Horowitz et al., 2007).

Little is known beyond the formation of the first-generation products of the reaction of NO₃ with isoprene. The isoprene nitrates and other first-generation products still contain a double bond, and it is likely that the further oxidation of these species will lead to low volatility products that can contribute to SOA formation at nighttime.

In this work, SOA formation from the reaction of isoprene with NO₃ radicals is investigated. Laboratory chamber experiments are performed in the dark using N₂O₅ as a source of NO₃ radicals. Aerosol yields are obtained over a range of initial isoprene concentrations (mixing ratios). By examining the time evolutions of aerosol volume and different intermediate gas-phase products, we are able to constrain the chemistry that

leads to the formation of low-volatility products. Mechanisms for SOA formation are proposed and chemical composition data of the SOA formed are also presented.

2.2 Experimental

Experiments are carried out in the Caltech dual 28 m³ Teflon chambers. A detailed description of the facility is provided elsewhere (Cocker et al., 2001; Keywood et al., 2004). Before each experiment, the chambers are flushed continuously for over 24 h. Aerosol number concentration, size distribution, and volume concentration are measured by a Differential Mobility Analyzer (DMA, TSI model 3081) coupled with a condensation nucleus counter (TSI model 3760). All aerosol growth data are corrected for wall loss, in which size-dependent particle loss coefficients are determined from inert particle wall loss experiments (Keywood et al., 2004). Temperature, relative humidity (RH), O₃, NO, and NO_x are continuously monitored. Experiments are performed in the dark at room temperature (20-21°C) and under dry conditions (RH < 10%).

In most experiments, seed aerosols are introduced into the chamber to act as a substrate onto which the gas-phase products may condense. Seed aerosols are generated by atomizing an aqueous solution with a constant-rate atomizer. The seed solution consists of 0.015 M (NH₄)₂SO₄. In a few experiments, acidic seed is used, consisting of 0.03 M MgSO₄ and 0.05 M H₂SO₄. The initial particle number concentration is ~20,000 particles cm⁻³, with a geometric mean diameter of ~50 nm. The initial seed volume is 10-12 μm³ cm⁻³. In some experiments, no seed particles are added and aerosols are formed via nucleation. After introduction of the seed aerosols (in seeded experiments), a known volume of isoprene (Aldrich, 99%) is injected into a glass bulb and introduced into the

chamber by an air stream. The mixing ratio of isoprene is monitored with a gas chromatograph equipped with a flame ionization detector (GC-FID, Agilent model 6890N). The column used is a bonded polystyrene-divinylbenzene based column (HP-PLOT Q, 15 m × 0.53 mm, 40 μm thickness, J&W Scientific). The oven temperature is held at 60°C for 0.5 min, ramped at 35°C min⁻¹ to 200°C, and held constant for 3.5 min.

The thermal decomposition of N₂O₅ serves as a source of NO₃ radicals in these experiments. N₂O₅ is prepared and collected offline by mixing a stream of nitric oxide (≥99.5%, Matheson Tri Gas) with a stream of ozone in a glass bulb (Davidson et al., 1978):



Ozone is generated by flowing oxygen through an ozonizer (OREC model V10-0, Phoenix, AZ) at ~1 L min⁻¹. The mixing ratio of ozone is measured by a UV/VIS spectrometer (Hewlett Packard model 8453) to be ~2%. The flow rate of nitric oxide into the glass bulb is adjusted until the brown color in the bulb disappears. The N₂O₅ is trapped for 2 h in an acetone-dry ice bath (approximately at -80°C; cold enough to trap N₂O₅ but not O₃, as condensed O₃ can explode upon warming and is extremely dangerous) as a white solid, and stored between experiments under liquid nitrogen temperature. Once the seed and isoprene concentrations in the chamber stabilize, reaction is initiated by vaporizing N₂O₅ into an evacuated 500 mL glass bulb and introduced into the chamber with an air stream of 5 L min⁻¹. The amount of N₂O₅ injected is estimated based on the vapor pressure in the glass bulb, which is measured

using a capacitance manometer (MKS); this amount corresponds to an initial mixing ratio of ~ 1 ppm in the chamber. The thermal decomposition of N_2O_5 forms NO_2 and NO_3 radicals. Impurities in the N_2O_5 starting material are quantified by FTIR spectroscopy (Nicolet model Magna 550). N_2O_5 is vaporized into an evacuated pyrex cell (18 cm in length and 300 cm^3) with CaF_2 windows. Spectra are collected immediately upon addition over the 1000 cm^{-1} to 4000 cm^{-1} window allowing for quantification of NO_2 (1616 cm^{-1} band) and HNO_3 (3550 cm^{-1} band) impurities.

A custom-modified Varian 1200 Chemical Ionization Mass Spectrometer (CIMS) is used to continuously monitor the concentrations of various gas-phase intermediates and products over the course of the experiments. The CIMS instrument is operated mainly in negative mode using CF_3O^- as a reagent ion, which selectively clusters with compounds having high fluorine affinity (e.g., acidic compounds and many hydroxy- and nitrooxy-carbonyls), forming ions at m/z $\text{MW} + 85$. In some experiments, the CIMS instrument is also operated in the positive mode using $\text{H}_2\text{O}\cdot\text{H}^+$ as a reagent ion forming ions at m/z $\text{MW} + 1$. The ionization schemes are as follows:

Negative chemical ionization: $\text{CF}_3\text{O}^- + \text{HB} \rightarrow \text{CF}_3\text{O}^- \cdot \text{HB}$

Positive chemical ionization: $\text{H}_2\text{O}\cdot\text{H}^+ + \text{D} \rightarrow \text{D}\cdot\text{H}^+ + \text{H}_2\text{O}$ (where D has a proton affinity $> \text{H}_2\text{O}$)

The term “product ion” is used throughout this manuscript to describe the ionized products formed through the above chemical reaction schemes. Typically, we scan from m/z 50 to 400. More details about the CIMS technique are given in Crouse et al. (2006) and Ng et al. (2007a). Because authentic standards are not available for the major products, sensitivities are not experimentally determined. We estimate the collision rate

of CF_3O^- with these products (which determines the sensitivity) with the empirical method of Su and Chesnavich (1982), which bases its predictions on an analyte's dipole moment and polarizability. Dipole moments and polarizabilities are calculated with the Spartan06 quantum package, and are based on molecular structures optimized with the B3LYP/6-31G(d) method. Further details on estimating CIMS sensitivities based on quantum calculations are described in Paulot et al. (2008). As isomers would have different polarities and hence different sensitivities, in estimating the concentrations it is assumed that the NO_3 attack at C_1 -position to C_4 -position is 5.5:1 (See Section 2.4.1).

Aerosol physical and chemical properties are monitored by many instruments. Real-time particle mass spectra are obtained with an Aerodyne quadrupole Aerosol Mass Spectrometer (Q-AMS) (Jayne et al., 2000). A Particle-Into-Liquid Sampler (PILS, Brechtel Manufacturing, Inc.) coupled with ion chromatography (IC) is employed for quantitative measurements of water-soluble ions in the aerosol phase (Sorooshian et al., 2006). Duplicate Teflon filters (PALL Life Sciences, 47-mm diameter, 1.0- μm pore size, teflo membrane) are collected from a selected number of experiments for offline chemical analysis. Filter sampling is initiated when the aerosol volume reaches its maximum value. Depending on the total volume concentration of aerosol in the chamber, the filter sampling time is 2-4 h, which results in $\sim 2\text{-}5\text{ m}^3$ of total chamber air sampled. Teflon filters used for high-resolution electrospray ionization-time-of-flight mass spectrometry (ESI-TOFMS) analysis are extracted in 5 mL of high-purity methanol (LC-MS CHROMASOLV-Grade, Sigma-Aldrich) by 45 minutes of sonication. Methanol sample extracts are then blown dry under a gentle N_2 stream (without added heat) once the filters are removed and archived at $-20\text{ }^\circ\text{C}$. Dried residues are then reconstituted with

500 mL of a 1:1 (v/v) solvent mixture of 0.1% acetic acid in water (LC-MS CHROMASOLV-Grade, Sigma-Aldrich) and 0.1% acetic acid in methanol (LC-MS CHROMASOLV-Grade, Sigma Aldrich). All resultant filter extracts are analyzed by a Waters ACQUITY ultra performance liquid chromatography (UPLC) system, coupled to a Waters LCT Premier XT time-of-flight mass spectrometer (TOFMS) equipped with an ESI source that is operated in the negative (-) ionization mode. Detailed operating conditions for the UPLC/(-)ESI-TOFMS instrument have been described previously (Ng et al., 2007a). A Waters ACQUITY UPLC HSS column is selected to separate the SOA components because of its increased retention of water-soluble polar organics; separation is achieved as a result of trifunctionally-bonded (T3) C₁₈ alkyl residues on this column, which prevent stationary phase collapse when a 100% aqueous mobile phase is used and result in better retention of water-soluble polar organic compounds. In addition to the UPLC/(-)ESI-TOFMS analysis, all remaining Teflon filters are extracted and analyzed for total peroxide content (sum of ROOR and ROOH) by using an iodometric-spectroscopic method (Docherty et al., 2005; Surratt et al., 2006).

To study the mechanism of SOA formation, in several experiments the experimental protocols are slightly modified: (1) An excess amount of isoprene (relative to N₂O₅ concentration) is injected into the chamber to prevent the further reaction of first-generation gas-phase products, allowing these products to be detected more readily; (2) After the addition of isoprene, pulses of N₂O₅ are introduced into the chamber to study the evolution of different intermediate gas-phase products; (3) With isoprene well mixed in the chamber, N₂O₅ is introduced slowly to maximize the self-reaction of peroxy radicals (see section 2.4.2). This is achieved by first injecting N₂O₅ into a 65 L Teflon

bag; then an air stream of 1 L min^{-1} is passed through the Teflon bag to introduce N_2O_5 into the chamber over a 7-h period. We refer to this as the “slow N_2O_5 injection experiment”; and (4) With N_2O_5 well mixed in the chamber, isoprene is introduced slowly to maximize the reaction between peroxy radicals and nitrate radicals (see section 2.4.2). This is achieved by first injecting isoprene into a 65 L Teflon bag, and then introduced into the chamber with an air stream of 1 L min^{-1} for 7 h. We refer to this as the “slow isoprene injection experiment”.

Experimental conditions and results are given in Table 2.1. In calculating SOA yield (defined as the ratio of the organic aerosol mass formed to the mass of parent hydrocarbon reacted), knowledge of the SOA density is required. By comparing volume distributions from the DMA and mass distributions from the Q-AMS, the effective density for the SOA formed can be estimated (Bahreini et al., 2005; Alfarra et al., 2006).

2.3 Results

2.3.1 Blank experiments

Blank experiments are performed to ensure that the aerosol growth observed is from the reaction of isoprene with NO_3 radicals. In these experiments, $\sim 1 \text{ ppm}$ N_2O_5 is introduced into chamber after the addition of ammonium sulfate seed aerosol (with no isoprene present). As shown in Figure 2.1, aerosol volume increases by $\sim 2 \mu\text{m}^3 \text{ cm}^{-3}$ within an hour after the introduction of N_2O_5 . About $2.5 \mu\text{g m}^{-3}$ of inorganic nitrate is measured by PILS/IC, which agrees well with the amount of nitrates detected by Q-AMS. FTIR analysis indicates the presence of $\sim 10\%$ HNO_3 and 4% NO_2 impurity in the N_2O_5 prepared, thus the nitrates measured by PILS/IC and Q-AMS likely arise from the

partitioning or reactive uptake of gas-phase HNO_3 into the aerosol phase, or HNO_3 produced from heterogeneous hydrolysis of N_2O_5 . As in the Q-AMS analysis, no organic species are detected in the filter samples collected from these blank experiments.

2.3.2 Aerosol yields

A series of experiments with different initial isoprene concentrations are carried out (these are referred to as “typical yield experiments” hereafter). The initial isoprene concentration ranged from 18.4 to 203.4 ppb. Figure 2.2 shows the reaction profile of the oxidation of an initial mixture containing 203.4 ppb isoprene. Since the chamber is NO_x -free at the beginning of the experiment, once N_2O_5 is introduced into the chamber the equilibrium in Reaction (2.3) favors the formation of NO_3 . This generates a relatively high concentration of NO_3 radicals and results in rapid isoprene decay. Aerosol growth is observed and aerosol volume continues to increase even after all the isoprene is consumed. Owing to the rapid isoprene decay and the relatively long time between each GC measurement (12 min), the isoprene decay over time is captured only in experiments in which the initial isoprene concentration is > 100 ppb. Based on the observed isoprene decay in these experiments and the isoprene- NO_3 rate constant k_{NO_3} , the average NO_3 concentration in the chamber is estimated to be ~ 140 ppt.

The SOA yield of each experiment (Table 2.1) is shown in Figure 2.3. The density of the SOA is determined to be 1.42 g cm^{-3} . The amount of inorganic nitrate detected by PILS/IC in each experiment ranges from 1.6 to $2.6 \mu\text{g m}^{-3}$, which is approximately equal to that measured in the blank experiments. In calculating SOA yield, the organic aerosol mass is corrected for the amount of inorganic nitrate measured

in each experiment. For convenience, SOA yields can be parameterized by a semi-empirical model based on absorptive gas-particle partitioning of two semivolatile products (Odum et al., 1996, 1997ab):

$$Y = \Delta M_o \left[\frac{\alpha_1 K_{om,1}}{1 + K_{om,1} M_o} + \frac{\alpha_2 K_{om,2}}{1 + K_{om,2} M_o} \right] \quad (2.4)$$

in which Y is the aerosol yield, ΔM_o is the organic aerosol mass produced, M_o is the organic aerosol mass present (equal to ΔM_o in chamber experiments with no absorbing organic mass present initially), α_i is the mass-based gas-phase stoichiometric fraction for semivolatile species i , and $K_{om,i}$ is the gas-particle partitioning coefficient for species i . With this two-product model, Eq. (2.4) is fit to the experimental yield data (data with $\Delta M_o < 100 \mu\text{g m}^{-3}$) and the yield parameters obtained are: $\alpha_1 = 0.089$, $\alpha_2 = 0.203$, $K_{om,1} = 0.182 \text{ m}^3 \mu\text{g}^{-1}$, and $K_{om,2} = 0.046 \text{ m}^3 \mu\text{g}^{-1}$. For an organic aerosol mass of $\sim 10 \mu\text{g m}^{-3}$, the aerosol yield is $\sim 10\%$.

Also shown in Figure 2.3 are aerosol yields from the slow isoprene/ N_2O_5 injection experiments. Since the PILS/IC is not employed in these experiments, in calculating SOA yields it is assumed that the amount of inorganic nitrate formed in these slow injection experiments is roughly the same as that in other experiments. For the slow isoprene injection experiment, no isoprene is observed by GC-FID, indicating that once the isoprene enters the chamber, it is quickly consumed by reaction with NO_3 . The time profile of isoprene injection is obtained in a separate experiment, in which the same amount of isoprene is added into the chamber without N_2O_5 present. Assuming the amount of isoprene injected into the chamber is the same as the isoprene reacted, the amount of isoprene reacted over the course of the slow isoprene experiment can be

deduced. As seen in Figure 2.3, the SOA yield from the slow N_2O_5 injection experiment is roughly the same as those in the other yield experiments; the yield from the slow isoprene injection experiment, however, is lower.

The time-dependent “growth curves” (organic aerosol, ΔM_o , as a function of hydrocarbon reacted, ΔHC) over the course of the slow N_2O_5 injection experiment and the slow isoprene injection experiment are shown in Figure 2.4. As hydrocarbon measurements are made with a lower frequency than particle volume, the isoprene concentrations shown are obtained by interpolating GC-FID measurements. In both experiments about 40 ppb of isoprene is consumed, the only difference being the order of isoprene/ N_2O_5 injection. From Figure 2.4 it is clear that as the reaction proceeds, more aerosol is formed in the slow isoprene injection experiment for the same amount of isoprene reacted. However, the final SOA yield under the slow N_2O_5 injection conditions is higher due to continued aerosol formation even after the complete consumption of isoprene. The presence of a “hook” at the end of the growth curve for the slow N_2O_5 injection experiment indicates that further reactions are contributing to aerosol growth after isoprene is consumed (Ng et al., 2006). Higher generation products also contribute to the aerosols formed in the slow isoprene injection experiment; however, their contributions are not readily observed in the growth curve owing to the way the experiment is conducted. This is further discussed in section 2.4.3.

2.3.3 Gas-phase measurements

The CIMS technique measures the concentrations of different gas-phase products over the course of the experiments. A series of experiments is carried out to study the

mechanisms of SOA formation by varying the relative amount of isoprene and N_2O_5 injected and monitoring the time evolution of the intermediate products. Shown in Figure 2.5 are the time profiles of three major gas-phase products and the corresponding aerosol growth from the excess isoprene experiment. In this experiment, ~ 120 ppb of N_2O_5 is first injected into the chamber, followed by the introduction of ~ 800 ppb isoprene. The initial concentration of isoprene is estimated based on the volume of the isoprene injected and the chamber volume. Once isoprene is injected, a number of product ions are formed immediately, with m/z 230, 232, and 248 being the most dominant ones. Several minor product ions at m/z 185, 377, and 393 are also observed (not shown). With the presence of excess isoprene, it is expected that the three major products detected are first-generation products. Their further reaction is suppressed, as indicated by the relatively constant concentrations of the product ions once they are formed. At the end of the experiment, 725 ppb of isoprene is measured by GC-FID. A small amount of aerosol is formed instantaneously, likely from the condensation of relatively nonvolatile first-generation products, or from further generation products that are formed at a relatively rapid rate.

To study further the evolution of the gas-phase products, an experiment is performed in which pulses of N_2O_5 are introduced into the chamber (with isoprene present) (Figure 2.6). The top panel shows the isoprene decay and aerosol formation; the middle panel shows the time profiles of the three major first-generation products (m/z 230, 232, and 248); the bottom panel shows the time profiles of three minor products (m/z 185, 377, and 393). In this experiment, 179 ppb of isoprene is first injected into the chamber, followed by the addition of 3 pulses of N_2O_5 ($\sim 120, 50, 210$ ppb). The

observations after the addition of the first pulse of N_2O_5 are similar to the excess isoprene experiment described above. With the addition of ~ 120 ppb N_2O_5 , 97 ppb of isoprene is reacted away, m/z 230, 232, and 248 are formed with concentrations of 49.8 ppb, 26.1 ppb, and 17.3 ppb, respectively. Because of the lack of authentic standards, the concentrations are uncertain. Because the sum of the ion concentrations derived from our estimated sensitivities is equal to the reacted isoprene, our estimated sensitivity must represent a lower limit for the actual sensitivity of the CIMS technique to these compounds. Similar to the data in Figure 2.5, the concentrations of these product ions stay relatively constant owing to the presence of excess isoprene. The minor products at m/z 185, 377, and 393, are formed with the concentrations 1.4 ppb, 0.9 ppb, and 0.9 ppb, respectively. It is noted that the m/z 393 ion is formed with a relatively slower rate than all other product ions. A small amount of aerosol is observed. At $t = 15:40$, a second pulse of N_2O_5 (~ 50 ppb) is introduced into the chamber and the remaining 82 ppb isoprene is completely consumed. As seen from Figure 2.6, the concentrations of all intermediate products increase accordingly and more aerosol is produced. The last pulse of N_2O_5 (~ 210 ppb) is added at $t = 19:00$. Since all isoprene has been consumed, the additional NO_3 radicals react mainly with the first-generation products, as indicated by the decay of m/z 230, 232, and 248, 185, 377, and 393 ions. Of all of the observed products, it appears that m/z 232 and 377 ions are the most reactive with NO_3 radicals, and their decays in excess NO_3 are strongly correlated with aerosol growth. The rest of the product ions display relatively slower decay kinetics. The decay of the major product ion at m/z 230 does not appear to correlate with aerosol growth, as the concentration of the m/z 230 ion continues to decrease throughout the experiment but there is no further

aerosol growth. Since the CIMS instrument has only 0.5 AMU resolution and it cannot distinguish products of similar or identical molecular weight, it is likely that many of observed ions comprise isomers formed from the NO_3 attack at different positions. The fact that many of the observed product ions show two distinct decay time scales indicates that these isomers have substantially different reactivity towards NO_3 radicals.

2.3.4 Chemical composition of SOA

2.3.4.1 Aerosol Mass Spectrometer (Q-AMS) measurements

Figure 2.7 shows the AMS spectrum of SOA formed in the typical yield experiments. Each mass fragment is normalized by the total signal. The SOA exhibits relatively high signals at m/z 30, 43, and 46. The signals at m/z 30 and 46 likely correspond to NO^+ (30) and NO_2^+ (46) fragments from the nitrates in the aerosol. The spectrum shown in Figure 2.7 is obtained when aerosol volume reaches its maximum value; the spectrum obtained several hours after aerosol volume peaks shows minimal changes in the mass fractions of different fragments, indicating that the aerosol composition is not changing significantly over time.

Figure 2.8 shows the mass spectrum of the slow N_2O_5 injection experiment versus a typical yield experiment; Figure 9 shows the mass spectrum of the slow isoprene injection experiment versus a typical yield experiment. As shown in both figures, the mass fragments fall on the 1:1 line, suggesting a similar SOA composition under the three different experimental conditions. At higher mass to charge ratios the plots drift below the one-to-one line and it appears that the typical experiments have stronger

signals at higher m/z 's. However, the signals at these masses (>165) are strongly dominated by noise and cannot be interpreted as differences between the spectra.

2.3.4.2 Offline chemical analysis

Figure 2.10 shows the representative UPLC/(-)ESI-TOFMS base peak ion chromatograms (BPCs) for different types of experiments conducted. The numbers denoted above the selected chromatographic peaks correspond to the most abundant negative ions observed in their respective mass spectra. Comparison of the BPCs shown in Figure 2.10 indicates that the compositions of the SOA are quite similar for the typical yield experiment, slow isoprene injection experiment, and the acid seed experiment, suggesting a common SOA formation pathway. The SOA composition from the excess isoprene experiment, however, is different from these experiments. This will be discussed further in section 2.4.4.

Accurate mass measurements for all ions observed by the UPLC/(-)ESI-TOFMS technique for a typical yield experiment are listed in Table 2.2. The error between the measured mass and theoretical mass is reported in two different ways, ppm and mDa. Overall, the error between the measured and theoretical masses is found to be less than ± 2 mDa and ± 5 ppm, allowing for generally unambiguous identification of molecular formulae. None of the listed ions is observed in solvent blanks and control filters. By combining the elemental SOA composition (i.e., TOFMS suggested ion formula) data and the gas-phase data from CIMS, structures for each of the SOA components are also proposed. As shown in Table 2.2, the types of compounds formed included nitrooxy-organic acids, hydroxynitrates, nitrooxy-organic peroxides (e.g., nitrooxy-

hydroxyperoxides), and nitrooxy-organosulfates. It should be noted that the data presented in Table 2.2 are also applicable to all other types of experiments conducted in this study; however, none of the organosulfates are observed in the nucleation experiments, consistent with previous work (Liggio et al., 2005; Liggio et al., 2006; Surratt et al., 2007ab; Iinuma et al., 2007ab). Surprisingly, previously characterized organosulfates of the 2-methyltetrols and the 2-methyltetrol mono-nitrates detected at m/z 215 and m/z 260 (not listed in Table 2), respectively, which are produced from the photooxidation of isoprene in the presence of acidified sulfate seed aerosol (Surratt et al., 2007ab; Gómez-González et al., 2007), are also observed in the acid seed experiment shown in Figure 2.10, suggesting that nighttime oxidation of isoprene in the presence of acidic seed may also be a viable pathway for these known ambient tracer compounds.

Owing to the implementation of reverse-phase chromatography, the SOA components that are more hydrophilic elute from the column the earliest, while the more hydrophobic components elute the latest. It is clear from Table 2.2 that compounds with the same carbon number and general functionality (i.e., carboxylic acid, alcohol, or organosulfate), but differing number of nitrooxy groups, exhibit distinctly different chromatographic behaviors. The presence of more nitrooxy groups appears to increase the retention time of the SOA compound. For example, it is found that m/z 194 organic acid compound ($C_5H_8NO_7^-$) containing one nitrooxy group elutes earlier than that of the m/z 239 organic acid compounds ($C_5H_7N_2O_9^-$) containing two nitrooxy groups. Similarly, the m/z 305 organosulfate ($C_5H_9N_2O_{11}S^-$) elutes earlier than that of the m/z 349 organosulfate ($C_5H_8N_3O_{13}S^-$).

SOA components that are either nitrooxy-organic acids or nitrooxy-organosulfates are detected strongly as the $[M - H]^-$ ion, consistent with previous work (Surratt et al., 2006; Surratt et al., 2007ab; Gao et al., 2004ab; Gao et al., 2006), whereas the hydroxynitrates and nitrooxy-hydroxyperoxides are detected as both the $[M - H]^-$ and $[M - H + C_2H_4O_2]^-$ ions, with the latter acetic acid adduct ion, in most cases, being the base peak ion (i.e., dominant ion). The acetic acid adduct ions for the hydroxynitrates and the nitrooxy-hydroxyperoxides are formed owing to the presence of acetic acid in the UPLC mobile phase. Previous studies have shown that non-acidic hydroxylated species (such as the 2-methyltetrols) and organic peroxides formed from the photooxidation of isoprene (Claeys et al., 2004; Edney et al., 2005; Surratt et al., 2006) are either undetectable or yield weak negative ions when using (-)ESI-MS techniques. However, it appears that the co-presence of nitrooxy groups in the hydroxylated SOA components allow for these compounds to become acidic enough to be detected by the UPLC/(-)ESI-TOFMS technique, or allow for adduction with acetic acid. Further confirmation for the presence of organic peroxides in the isoprene SOA produced from NO_3 oxidation is provided by the iodometric-spectroscopic measurements shown in Table 2.3. Based upon the UPLC/(-) ESI-TOFMS measurements shown in Table 2.2, an average molecular weight of 433 for the organic peroxides is assumed for the calculations shown in Table 2.3. The contribution of organic peroxides to the SOA mass concentration is found to be fairly reproducible for duplicate typical experiments (i.e., 8/22/07 and 10/24/07). The amount of organic peroxides in the excess isoprene experiment is below detection limits. Owing to the lack of authentic standards, there are large uncertainties associated with the

quantification of these products in the aerosol phase. This is further discussed in section 2.4.4.

2.4 Gas-phase chemistry and SOA formation

2.4.1 Formation of various gas-phase products

As seen from Figure 2.5 and Figure 2.6, the three major first-generation products formed from isoprene-NO₃ reaction are the m/z 230, 232, and 248 ions. Since the CIMS technique uses CF₃O⁻ (anionic mass 85 Da) as the reagent ion, compounds are detected at a m/z value of their molecular weight (MW) plus 85. The product ions at m/z 230, 232, and 248 likely correspond to C₅-nitrooxycarbonyl (MW 145), C₅-hydroxynitrate (MW 147), and C₅-nitrooxyhydroperoxide (MW 163). These products have been observed in previous studies (Jay and Stieglitz, 1989; Skov et al., 1992; Kwok et al., 1996; Berndt and Böge, 1997) and their formation from the isoprene-NO₃ reaction is relatively straightforward (Figure 2.11). The reaction proceeds by NO₃ addition to the C=C double bond, forming four possible nitrooxyalkyl radicals depending on the position of the NO₃ attack. Previous studies suggest that NO₃ radicals predominantly attack isoprene in the 1-position, with a branching ratio (C₁-position/C₄-position) varying between 3.5 and 7.4 (Skov et al., 1992; Berndt and Boge, 1997; Suh et al., 2001). As mentioned before, the average branching ratio (5.5:1) is used in estimating the sensitivities of the compounds measured by CIMS. In Figure 2.11, only the nitrooxyalkyl radical formed from the C1 attack is shown. The nitrooxyalkyl radicals then react with O₂ to form RO₂ radicals, which react further with HO₂, RO₂, or NO₃ radicals under the experimental conditions in this study. The reaction of RO₂ radicals and HO₂ radicals leads to the formation of C₅-

nitrooxyhydroperoxide (m/z 248). The reaction of two RO_2 radicals (self reaction or cross reaction) has three different possible channels:



The second channel results in the formation of C_5 -nitrooxycarbonyl (m/z 230) and C_5 -hydroxynitrate (m/z 232). According to channel (2.5b), these two products should be formed with a 1:1 ratio; however, C_5 -nitrooxycarbonyl can also be formed from alkoxy radicals (alkoxy radicals formed through $\text{RO}_2 + \text{RO}_2$ reaction or $\text{RO}_2 + \text{NO}_3$ reaction). In Figure 2.6, 49.8 ppb of C_5 -nitrooxycarbonyl and 26.1 ppb of C_5 -hydroxynitrate are formed after the addition of the first pulse of N_2O_5 , indicating ~ 24 ppb of C_5 -nitrooxycarbonyl is formed from the reaction of alkoxy radicals. The branching ratios for the reaction of small peroxy radicals have been investigated in previous studies. It is found that the branching ratio for channel (5a) for methylperoxy and ethylperoxy radicals is ~ 0.3 - 0.4 and ~ 0.6 , respectively (Lightfoot et al., 1992; Wallington et al., 1992; Tyndall et al., 1998). It is likely that the isoprene peroxy radicals react via this pathway to form alkoxy radicals and contribute to the “extra” 24 ppb of C_5 -nitrooxycarbonyl. This observation is indicative that most RO_2 radicals react with other RO_2 radicals instead with NO_3 or HO_2 radicals.

Other than C_5 -nitrooxycarbonyl, C_5 -hydroxynitrate, and C_5 -nitrooxyhydroperoxide, three other minor products (m/z 185, 377 and 393 ions) are also observed as intermediate products. The proposed mechanisms for the formation of these gas-phase products are also shown in Figure 2.11. Although channel (2.5c) in the $\text{RO}_2 +$

RO₂ reaction is found to be minor for small peroxy radicals such as methylperoxy and ethylperoxy radicals (Kan et al., 1980; Niki et al., 1981; Niki et al., 1982; Wallington et al., 1989; Tyndall et al., 1998; Tyndall et al., 2001), the product ion at *m/z* 377 could be the corresponding ROOR product formed from the self reaction of isoprene peroxy radicals. The product ion at *m/z* 185 likely corresponds to the C₅-hydroxycarbonyl. It has been observed in previous studies and it likely arises from the isomerization of nitrooxyalkoxy radicals through a 6-member transition state to form a hydroxynitrooxy alkyl radical, which then decomposes to form NO₂ and C₅-hydroxycarbonyl (Kwok et al., 1996). Such isomerization has also been proposed to occur in the photooxidation of isoprene (Paulson and Seinfeld, 1992; Carter and Atkinson, 1996; Dibble, 2002). It is possible that the hydroxynitrooxy alkyl radical formed proceeds to react with O₂ to form a peroxy radical, which then reacts with the isoprene peroxy radical to form the product ion *m/z* at 393. The product ion at *m/z* 393 shows a slower rate of formation (Figure 2.6) compared to other product ions suggesting that it might also be formed from the further oxidation of a first-generation product. 2-methyl-2-vinyl-oxirane has been observed from isoprene-NO₃ reaction in previous studies at 20 mbar in helium (Berndt and Böge, 1997) and 20 Torr in argon (Skov et al., 1994), respectively. When operated in positive mode with H₂O·H⁺ as the reagent ion (products are observed at *m/z* = MW + 1), CIMS shows a protonated molecule at *m/z* 85. Although the epoxide yield is found to be <1% of the total reacted isoprene at atmospheric pressure (Skov et al., 1994), the signal at *m/z* 85 can arise in part from the epoxide. The further oxidation of the epoxide results in the formation of an epoxide peroxy radical, which can react with the isoprene peroxy radical to form the peroxide at *m/z* 393. It is noted that a product ion at *m/z* 246 is detected in

CIMS, which could arise from the corresponding carbonyl product formed from the reactions of two epoxide peroxy radicals, or from the fragmentation of the epoxide alkoxy radicals. Unlike m/z 393, which decays after the addition of the last pulse of N_2O_5 , m/z 246 stays relatively constant suggesting that it is not being further oxidized by NO_3 radicals. To examine further the possibility of peroxide formation (m/z 377 and 393) in the gas phase, an experiment is conducted using 1,3-butadiene as the parent hydrocarbon. The analogous product ions for the 1,3-butadiene system, i.e., m/z 349 and 365, are observed in CIMS, providing further indication that the formation of ROOR products from two RO_2 radicals is occurring in the gas phase. Further details of the gas-phase chemistry of isoprene and 1,3-butadiene will be forthcoming in a future manuscript.

2.4.2 Effect of peroxy radical chemistry on SOA yield

The SOA yield ranges from 4.3% to 23.8% for an initial isoprene concentration of 18.4 to 101.6 ppb in the typical yield experiments. While the SOA yield from the slow N_2O_5 injection experiment is roughly the same as that in the typical yield experiments, the SOA yield from the slow isoprene injection experiment is lower (Figure 2.3). In both cases, ~ 40 ppb of isoprene is consumed, the main difference being the relative importance of $RO_2 + RO_2$ reaction versus $RO_2 + NO_3$ reaction in each system. In the slow N_2O_5 injection experiment, a relatively small amount of NO_3 is available in the chamber. Once RO_2 radicals are formed, it is expected that they would react primarily with other RO_2 radicals instead of NO_3 radicals owing to the presence of a relatively higher isoprene concentration in the chamber. On the other hand, the slow isoprene

injection experiment favors $\text{RO}_2 + \text{NO}_3$ reaction owing to the presence of excess N_2O_5 in the chamber. Thus the higher SOA yield observed in the slow N_2O_5 injection experiment suggests the products formed via $\text{RO}_2 + \text{RO}_2$ reaction partition more readily into the aerosol phase, or the $\text{RO}_2 + \text{RO}_2$ reaction forms products that further react and contribute significantly to aerosol growth. The fact that the SOA yield from the slow N_2O_5 injection experiment is roughly the same as in the typical yield experiments implies that $\text{RO}_2 + \text{RO}_2$ reaction dominates in typical yield experiments.

The time profile for the three major first-generation gas phase products and SOA growth from the slow N_2O_5 injection experiment and slow isoprene injection experiment are shown in Figure 2.12 and Figure 2.13, respectively. It is noted that this pair of experiments has a higher initial isoprene concentration (~ 200 ppb) compared to the pair of experiments shown in Figure 2.4. In both cases, once the first-generation products are formed they can react further with NO_3 radicals, making it difficult to estimate the formation yields of these products based on the measured concentrations. The extent to which these products react further is expected to be higher in the slow isoprene injection experiment owing to the presence of excess NO_3 in chamber; this is consistent with the relatively lower concentrations of first-generation products observed. As mentioned before, it is possible that the CIMS signal at the observed m/z comprises isomers formed from the NO_3 attack at positions other than the C1 carbon. Such isomers have slightly different structures but they could exhibit a very different reaction rate towards NO_3 radicals. For instance, studies have shown that the reaction rates of NO_3 radicals with unsaturated alcohols and unsaturated carbonyl compounds can vary by several orders of magnitude depending on the position of the substituted methyl group (Noda et al., 2002;

Canosa-Mas et al., 2005). It is possible that the minor products formed from NO_3 attack at other positions react much slower with NO_3 radicals, hence the concentrations of the observed product ions do not decay to zero towards the end of the experiment. At the end of the experiment, about 8 ppb and 3 ppb of C_5 -hydroxynitrate is left in the slow N_2O_5 injection experiment and slow isoprene injection experiment, respectively. Assuming the amount of reactive isomers and unreactive (or relatively slow reacting) isomers are formed in the same ratio in the slow N_2O_5 injection experiment and the slow isoprene injection experiment, we can deduce that a relatively higher concentration of reactive C_5 -hydroxynitrate (as well as the two other first-generation products) is formed in the slow N_2O_5 injection experiment. This is consistent with the larger extent of $\text{RO}_2 + \text{RO}_2$ reaction (which forms C_5 -hydroxynitrate) and the higher SOA yield observed in the slow N_2O_5 injection experiment, as it appears that C_5 -hydroxynitrate is an effective SOA precursor (Figure 2.6).

2.4.3 Growth curves: multiple steps in SOA formation

By examining the time-dependent growth curves (organic aerosol, ΔM_o , as a function of hydrocarbon reacted, ΔHC) we can gain insights into the general mechanisms of SOA formation (Ng et al., 2006, 2007ab). Figure 2.4 shows the time-dependent growth curves for the slow N_2O_5 injection experiment and the slow isoprene injection experiment, respectively. For the slow N_2O_5 injection experiment, the initial aerosol growth likely arises from the condensation of first-generation products as the presence of excess isoprene in the chamber suppresses their further oxidation. If higher generation products do contribute to SOA formation, they would have to be formed at relatively fast

rates. After isoprene is consumed, aerosol mass continues to increase and results in a “hook” in the growth curve. This indicates that secondary products (or higher generation products) also contribute significantly to SOA formation. The same observation can be made if we examine the reaction profile of a typical yield experiment (Figure 2.2): there is further SOA growth after all isoprene is reacted away, indicating that the further oxidation of first generation products are contributing to SOA formed. These observations are consistent with the fact that the decay of first-generation products observed in CIMS (especially the m/z 232 and m/z 377 ions) is strongly anticorrelated with further SOA growth (Figure 2.6). On the other hand, the slow isoprene injection experiment does not allow us to differentiate the contribution of first- and second-generation products to SOA formation. With the presence of excess NO_3 radicals in the chamber, the first-generation products formed in the slow isoprene injection experiment would be further oxidized once they are formed. The SOA growth observed throughout this experiment is from the partitioning of these highly oxidized and nonvolatile products. Hence, at the beginning of the experiment, for the same amount of ΔHC , the amount of SOA formed in this experiment is higher than that in the slow N_2O_5 injection experiment, in which the aerosol growth is probably from the condensation of relatively more volatile first-generation products. Both the AMS data and filter sample data (Figures 2.8, 2.9, and 2.10) show a very similar composition for the final SOA formed in slow N_2O_5 injection experiment and the slow isoprene injection experiment, suggesting a common SOA forming channel. Based on the previous discussion on the effect of peroxy radical chemistry on SOA yields, it is likely that the $\text{RO}_2 + \text{RO}_2$ reaction is the SOA-forming

channel in both cases; such a reaction occurs to a large extent in the slow N_2O_5 injection experiments and results in the formation of more SOA.

2.4.4 Proposed mechanisms of SOA formation

The combination of CIMS gas-phase data and elemental SOA composition data provides substantial insights into the mechanisms of SOA formation. Shown in Figures 2.14-2.17 are the proposed SOA formation mechanisms from the further oxidation of the various gas-phase products measured by CIMS. The compounds in the boxes are the SOA products detected by UPLC/(-)ESI-TOFMS. Owing to multiple chromatographic peaks observed in the UPLC/(-)ESI-TOFMS extracted ion chromatograms (EICs) for the negative ions of the proposed SOA products, structural isomers are likely; however, for simplicity we show only one possible isomer for each product formed from a particular reaction pathway. Many of the SOA products detected are formed from the further oxidation of first- or higher-generation products, which is consistent with the observation of continual SOA growth after the complete consumption of isoprene (hence a “hook” in the growth curve). With the large number of nitrate-substituted compounds detected by UPLC/(-)ESI-TOFMS technique, it is also not surprising that AMS shows strong signals at m/z 30 (NO^+) and m/z 46 (NO_2^+).

Shown in Figures 2.14 and 2.15 are the proposed SOA formation pathways from the further oxidation of the m/z 232 (i.e., C_5 -hydroxynitrate) and 377 gas-phase product ions (as detected by CIMS). The decay of these two products has been found to be strongly correlated with aerosol growth (Figure 2.6), which is consistent with the large number of SOA products formed from their further oxidation. The further oxidation of

these two gas-phase products also yields SOA compounds of the same molecular weight (compounds of MW 371 and 450). Although m/z 393 is a minor gas-phase product, the further oxidation of this compound leads to formation of several SOA products (Figure 2.16). As mentioned before, there are two possible formation routes for m/z 393, and the further oxidation of both products is shown in Figure 2.16. The further oxidation of the m/z 393 ion appears to yield SOA products that are specific only to this gas-phase product: these include the SOA products of MW 387 and 467.

Figure 2.17 shows the proposed SOA formation mechanisms from three other gas-phase products (m/z 185, m/z 230, and m/z 277); the further oxidation of these product ions leads to relatively minor SOA products. Although C_5 -nitrooxycarbonyl (m/z 230) is the most abundant gas-phase product detected by CIMS, its further oxidation is not well correlated with aerosol growth (Figure 2.6). The further oxidation of m/z 230 yields an SOA product at MW 240. This organic acid product is found to be quite minor when examining the peak area in its corresponding extracted ion chromatogram (EIC). It is noted that no SOA products are detected from the further oxidation of the C_5 -nitrooxyhydroperoxide (m/z 248) (also a major gas-phase product); it is possible that these hydroperoxide products are not acidic enough to be detected by the UPLC/(-)ESI-TOFMS technique, or degrade during sample workup and/or analysis procedures. It has been shown that hydroxycarbonyl plays a key role in SOA formation from the reaction of linear alkenes with NO_3 radicals (Gong et al., 2005), however, in the isoprene- NO_3 system, the further oxidation of the minor gas-phase product C_5 -hydroxycarbonyl (m/z 185) leads to the formation of only one minor aerosol product at MW 195. Some evidence for the formation of a C_5 -dinitrate first-generation gas-phase product is

indicated from the CIMS and UPLC/(-)ESI-TOFMS data. This first-generation gas-phase product has been observed previously by Werner et al. (1997). The CIMS shows a weak signal at m/z 277, which could be associated to the dinitrate product; we do not know, however, whether the negative ion efficiently clusters with such compounds. Further evidence for the dinitrate gas-phase product is provided by the UPLC/(-)ESI-TOFMS detection of an SOA product at MW 495, which could result from the further oxidation of a C_5 -dinitrate precursor. The precursor compound before the last oxidation step shown in this mechanism in Figure 2.17 may exist in the particle phase; however, this compound is not likely to be detected by the UPLC/(-)ESI-TOFMS technique owing to the lack of acidic hydrogens from neighboring hydroxyl and/or carboxyl groups.

The SOA products highlighted in Figures 2.14-2.17 are observed in all major experiments conducted; however, not all of these products are strongly detected in the excess isoprene experiment (Figure 2.10c). With the presence of excess isoprene, further oxidations of first-generation products should be minimal and no significant SOA formation is expected. The reaction rate of isoprene and NO_3 radicals is $k_{NO_3} = 7 \times 10^{-13} \text{ cm}^3 \text{ molecule}^{-1} \text{ s}^{-1}$. To our knowledge, the reaction rate of the first-generation products and NO_3 radicals has not been studied. The structure of m/z 232 (C_5 -hydroxynitrate) is similar to 3-methyl-2-buten-1-ol (MBO321), except that the γ -carbon has one nitro group and one methyl group substitution instead of two methyl group substitutions. The reaction rate coefficient of MBO321 and NO_3 radicals is $k_{NO_3} = 1 \times 10^{-12} \text{ cm}^3 \text{ molecule}^{-1} \text{ s}^{-1}$. It is found that the reaction rate with NO_3 radicals increases with increasing number of methyl groups at the γ -carbon (Noda et al., 2002), which is in accordance with the stabilization theory for leaving groups discussed in Atkinson (1997) and Noda et al.

(2000). With reference to this, we would expect the reaction rate of C₅-hydroxynitrate and NO₃ radicals to be slower than that of MBO321 due to the presence of the electron withdrawing nitro group. Hence, it is likely that the reaction rate of isoprene and NO₃ radicals and C₅-hydroxynitrate and NO₃ radicals are roughly in the same range. The relative production rate of first- and second-generation products will then be the ratio of the concentrations of isoprene and first-generation products, and aerosol can be formed either from the condensation of relatively non-volatile first-generation products (e.g., *m/z* 393) or higher generation products that are formed relatively fast in the gas-phase. It appears from the UPLC/(-)ESI-TOFMS data that enough RO₂ + RO₂ chemistry is occurring to yield many of the products shown in Figures 2.14-2.17. When comparing the UPLC/(-) ESI-TOFMS BPCs (Figure 2.10) of all experiments, it is clear that the *m/z* 430 and *m/z* 446 are the dominant ions in the excess isoprene experiment, while *m/z* 333 is the dominant chromatographic peak in other experiments. The chromatographic peak at *m/z* 430 corresponds to the acetic acid cluster ion for the compound at MW 371, which can be formed from the further oxidation of CIMS *m/z* 232 and 377 ions (Figures 2.14 and 2.15). The chromatographic peak at *m/z* 446 corresponds to the acetic acid cluster ion for the compound at MW 387, which is formed from the further oxidation of CIMS *m/z* 393 (Figure 2.16). The detection of these two SOA products (MW 371 and MW 387) suggests that further oxidation of *m/z* 232, 377, and 393 is occurring in the excess isoprene experiment and contributing to SOA growth. Studies have shown that NO₃ uptake on organic surfaces (even to saturated organic surfaces) be quite rapid (Moise et al., 2002; Knopf et al., 2006; Rudich et al., 2007). Hence, it is also possible that CIMS *m/z* 393 (a first-generation product according to one of the formation routes) is

nonvolatile enough that it partitions into the aerosol phase and its further oxidation proceeds heterogeneously. Chromatographic peaks such as m/z 333 (associated with MW 271 compound), 449 (MW 450 compound) and 554 (MW 495 compound) are not as strong in the excess isoprene experiment owing to the fact there is not enough NO_3 in the system to allow for the formation of these highly oxidized compounds.

From the UPLC/(-)ESI-TOFMS (Table 2.2) and PILS/IC measurements, it appears that organic acids are not a major contributor to SOA formation from the oxidation of isoprene by NO_3 radicals. The UPLC/(-)ESI-TOFMS technique detects only two minor organic acids at MW 195 and 240. Additionally, the PILS/IC technique does not detect large quantities of any small organic acids. The sum of formate, acetate, glycolate, lactate, oxalate, and pyruvate are usually between $0.01 - 0.50 \mu\text{g m}^{-3}$. These observations are different from the SOA produced in the photooxidation of isoprene (under high- and low- NO_x conditions), in which a large number of organic acids, such as 2-methylglyceric, formic, and acetic acid, are observed (Surratt et al., 2006; Szmigielski et al., 2007). In the photooxidation experiments, the level of organic acids detected under low- NO_x conditions is lower than under high- NO_x conditions. The low- NO_x isoprene SOA was previously found to also have a significant amount of organic peroxides, as detected in the current study (Table 2.3); however, organic peroxides detected previously in low- NO_x isoprene SOA were not structurally elucidated through MS techniques performed in the present study (Table 2.2, Figures 2.14-2.17), possibly owing to the lack of nitrooxy groups which seem to induce acidity and/or increase the adductive abilities of organic peroxides with acetic acid during the ESI-MS analysis. Overall, it appears that the isoprene- NO_3 SOA is much more similar to the previously studied low- NO_x isoprene

SOA. More specifically, it appears that both contain a large amount of organic peroxides, organosulfates (if conducted in the presence of sulfate seed aerosol), and neutral hydroxylated compounds, such as the hydroxynitrates observed in Figure 2.14 (e.g., MW 226 and 271 products).

As discussed earlier, the formation yields of ROOR from the reaction of two peroxy radicals is very low for small peroxy radicals (Kan et al., 1980; Niki et al., 1981, 1982; Wallington et al., 1989; Tyndall et al., 1998, 2001). However, according to both gas-phase and aerosol-phase data in this study, it appears that the RO_2+RO_2 reaction (self reaction or cross-reaction) in the gas phase yielding ROOR products is an important SOA formation pathway. Such reaction has been proposed to form low-volatility diacyl peroxides in the SOA formed from cyclohexene ozonolysis (Ziemann, 2002). In the case of self-reaction of peroxy radicals, the molecular weight of the product is essentially doubled, providing an efficient way to form products of low volatility. Based on the iodometric spectroscopic method the contributions of peroxides (ROOH + ROOR) to the total SOA formed is 17-32% (Table 2.3). We can estimate the mass yield of peroxides based on their percentage contribution to total SOA and the SOA yield for each of the experiments in Table 2.3. It is found that the mass yield of peroxides range from ~6-10%. For the two experiments (i.e., 8/22/07 and 10/24/07) that are carried out under similar conditions as those in the yield experiments, the mass yield of peroxide is 8%.

Based on the shape of the Odum yield curve (Figure 2.3), it is expected that the products are semivolatile. Hence, the relatively large contribution of nonvolatile peroxides in the aerosol phase appears to be inconsistent with the observed yield curve behavior. It is evident from the UPLC/(-)ESI-TOFMS data that there exists a wide array

of peroxides in the aerosol composition, however, we need to caution that there are large uncertainties associated with the quantification of peroxides owing to the lack of authentic standards. Based on the standard deviations of the measurements, the uncertainty is at least 10%, yet if we take into account of the following factors it is expected that the true uncertainty would be larger. In estimating the percentage contribution of peroxides, an average molecular weight of 433 for peroxides is used. The peroxides formed would largely depend on the branching ratio of various reactions and this number may not reflect the molecular weights of the wide array of peroxides formed. Also, the iodometric spectroscopic method does not allow the distinction between ROOH and ROOR products. Hence, the contribution of the low volatility ROOR products may not be as high as estimated. ROOH standards were run in the ESI-TOFMS to examine the possibility of ROOH further reacting in the mass spectrometer to form ROOR and no ROOR products were detected. As mentioned before, it appears that the presence of nitrooxy groups in ROOR products aids their detection in the MS. Since the ROOH standards used do not have a nitrooxy group, unfortunately, we cannot rule out the possibility that ROOR products are formed but just not being detected. Finally, it is worth noting that the initial isoprene concentrations in the yield experiments are much lower than those experiments in which SOA composition is measured. In performing the yield experiments, the initial isoprene concentrations are kept relatively low so as to be closer to atmospheric levels. Because of the lower initial isoprene concentration (hence lower aerosol loading), the partitioning of various products would be different and it is likely that level of peroxides would be lower in the yield experiments. Nevertheless, the

higher concentration experiments are necessary to produce enough aerosols filter analysis and to map out the complete spectrum of oxidation products.

To fully elucidate the relationship between the actual products identified and those inferred from fitting the yield data would require a modeling study that is beyond the scope of this work. However, we emphasize that there are large uncertainties associated with the quantification of peroxides and it is likely that their contributions to total SOA can be overestimated. Indeed, if the mass yield for these nonvolatile peroxides were lower (for instance, ~2%), this would agree well with the observed yield curve behavior. The measurement of peroxides certainly warrants further study. This work serves as a good example in showing that caution must be taken when interpreting experiments with low aerosol yields, especially when a relatively minor pathway may be responsible for forming the aerosols.

2.5 Approximate estimate of global production of SOA from isoprene + NO₃

The global chemical transport model GEOS-Chem (v. 7-04-11) (<http://www-as.harvard.edu/chemistry/trop/geos/>) is used to estimate, roughly, global SOA formation from the isoprene + NO₃ reaction. The current version of GEOS-Chem treats mechanistically SOA formation from isoprene + OH, monoterpenes and sesquiterpenes, and aromatics; here we will estimate SOA formation from isoprene + NO₃ by using an approximate, uniform SOA yield of 10% (corresponding to $M_0 \cong 10 \mu\text{g m}^{-3}$ in Figure 2.3). It is noted that this yield is quite uncertain and the importance of peroxy radical self reactions in this study suggest that the SOA yield in the atmosphere will be highly sensitive to the nature of the nighttime peroxy radical chemistry. Here, we seek to obtain

only a “back-of-the-envelope” estimate.

Two global isoprene emissions are available in GEOS-Chem: GEIA (Global Emission Inventory Activity) (Guenther et al., 1995) and MEGAN (Model of Emissions and Gases from Nature) (Guenther et al., 2006). Both models require, as input, meteorological data such as temperature to calculate the amount isoprene emitted. For the present estimate, the meteorological fields employed by Wu et al. (2007), generated by the Goddard Institute for Space Studies (GISS) General Circulation Model III, are used. Meteorological conditions correspond approximately to those of year 2000.

Table 2.4 presents the annual emissions of isoprene as predicted by each of the emission models, together with the amount of isoprene predicted to react via OH, O₃, and NO₃, the global burden, and lifetime. We note that there is a significant difference between the annual isoprene emissions predicted by the earlier and newer emission models. Isoprene + OH accounts for 300 to 400 Tg yr⁻¹ of isoprene consumption. Henze et al. (2007) predict that annual SOA production from isoprene + OH is about 13 Tg yr⁻¹ (based on the MEGAN inventory and GEOS-4 meteorological fields, which are assimilated fields from actual year 2004). Note that SOA production from isoprene + OH, or any other pathway for that matter, is sensitive to the production of SOA from other hydrocarbon precursors since gas-aerosol partitioning depends on the total organic aerosol mass.

If we take as a rough estimate a 10% SOA yield from the isoprene + NO₃ pathway from the results in Table 2.4, 2 to 3 Tg yr⁻¹ of SOA results from isoprene + NO₃. This rate of production would make SOA from isoprene + NO₃ as significant as that from sesquiterpenes, biogenic alcohols, and aromatics, each of which is estimated to produce

about 2 to 4 Tg yr⁻¹ of SOA based on yields measured in chamber studies (Henze et al., 2007). As a reference, the global SOA production is estimated to be 10–70 Tg yr⁻¹ (Kanakidou et al., 2005). Recently, Goldstein and Galbally (2007) provided several alternative approaches to estimate global SOA production: 510–910 Tg C yr⁻¹ based on the global mass balance of VOC removal, 225–575 Tg C yr⁻¹ based on SOA deposition plus oxidation, 140–540 Tg C yr⁻¹ based on comparison with the sulfate budget, and 223–615 Tg C yr⁻¹ required to maintain the assumed global mean vertical SOA distribution. If we assume mass carbon/mass organics = 0.5, the lower limit for SOA production from these estimates would be 280 Tg yr⁻¹, which is much larger than that estimated from chamber SOA yields. Still, the 3 Tg yr⁻¹ of SOA estimated for the isoprene + NO₃ system is worth noticing. Owing to efficient photodissociation, NO₃ achieves its highest concentrations at night. By contrast, isoprene emissions are assumed to be zero at night in both emission models. Consequently, the isoprene + NO₃ reaction occurs only at night, involving isoprene that remains unreacted after each daytime period.

We caution that the estimates above are obtained at the crudest level of approximation, in which a globally uniform SOA yield of 10% from isoprene + NO₃ is applied. As we note from Table 2.4, there is also a substantial difference between predictions of the two available isoprene emission models; the more recent MEGAN model represents an improved level of understanding over the earlier GEIA model. Predictions of SOA formation from the isoprene + NO₃ pathway are, of course, highly dependent on ambient NO₃ radical concentrations. Nitrate radical concentrations predicted in the current simulations vary from about 0.1 ppt in remote regions of South America to 20 ppt or more in the southeastern USA (in August). Future work will

address the simulation of SOA formation from isoprene + NO₃ following the microphysical treatment in GEOS-Chem.

2.6 Implications

We report a series of chamber experiments investigating the formation of secondary organic aerosols from the reaction of isoprene with nitrate radicals. For an initial isoprene concentration of 18.4 to 101.6 ppb, the SOA yield ranges from 4.3% to 23.8% (typical yield experiments). The SOA yield from the slow N₂O₅ injection experiment (RO₂ + RO₂ reaction dominates) is much higher than that from the slow isoprene injection experiment (RO₂ + NO₃ dominates), implying that RO₂ + RO₂ is a more effective channel of forming SOA. The SOA yield from the slow N₂O₅ experiment is roughly the same as that in the typical yield experiments, suggesting that SOA yields obtained in this study likely represent conditions in which peroxy-peroxy radical reactions are favored. Using a uniform SOA yield of 10% (corresponding to M₀ ≅ 10 μg m⁻³), ~2 to 3 Tg yr⁻¹ of SOA results from isoprene + NO₃, which is about 1/4 of the amount of SOA estimated to be formed from isoprene + OH (~13 Tg yr⁻¹) (Henze et al., 2007).

The extent to which the results from this study can be applied to conditions in the atmosphere depends on the relative importance of the various reaction pathways of peroxy radicals in the nighttime atmosphere: RO₂+RO₂, RO₂+NO₃, RO₂+NO, and RO₂+HO₂. However, the fate of peroxy radicals in the atmosphere is uncertain owing to the large uncertainties in the reaction rate constants and ambient concentrations of the radicals (Skov et al., 1992; Kirchner and Stockwell, 1996; Bey et al., 2001ab; Vaughan et al., 2006). For instance, a modeling study by Kirchner and Stockwell (1996) suggests

that the RO_2+NO_3 reaction is the dominant pathway at night; 77% and 90% of the total RO_2 at night is predicted to react with NO_3 in polluted atmosphere and rural air (mixed with aged air), respectively. The other pathways are not as important; while RO_2+RO_2 can account for about 8-23% of the total RO_2 reaction, RO_2+HO_2 only accounts for 6-10%, and RO_2+NO is minimal (0-1%) (Kirchner and Stockwell, 1996). These results are at odds with the study by Bey et al. (2001ab), which suggests that NO_3 radicals are not involved significantly in the propagation of RO_2 radicals (<5%). Instead, RO_2+NO (77%) and RO_2+RO_2 (40%) are dominant in the mixed layer in the urban and rural areas, respectively. Although there is no definite conclusion as which reaction pathway dominates in the nighttime atmosphere, both studies seem to suggest that RO_2+HO_2 is relatively not as important. In this work, we investigated situations in which either RO_2+RO_2 or RO_2+NO_3 dominates. In both cases the RO_2+HO_2 reaction is expected to be a minor channel and thus this is in line with the modeling studies. Although RO_2+NO is not considered in this study, this reaction produces the same alkoxy radical as in the RO_2+NO_3 reaction. It is likely that it would result in similar products as those in the case where the RO_2+NO_3 reaction dominates. Currently, only the reaction rate constants for small, relatively simple RO_2 radicals with NO_3 radicals have been reported (e.g., Biggs et al., 1994; Daele et al., 1995; Canosa-Mas et al., 1996; Vaughan et al., 2006) and they are roughly in the range of $(1-3) \times 10^{-12} \text{ cm}^3 \text{ molecule}^{-1} \text{ s}^{-1}$. With the oxidation of various volatile organic compounds by O_3 and NO_3 under nighttime conditions, it is expected that multi-functional peroxy radicals would be prevalent; the reaction rates of these complex peroxy radicals warrant future study. Furthermore, more field measurements on the

concentrations of various radicals would also help to constrain the relative importance of the different reaction pathways.

In this study, we have shown that the formation of ROOR from the reaction of two peroxy radicals is an effective SOA-forming channel based on gas-phase data and elemental SOA composition data. If the results from this study can be applied to other systems (i.e., the reaction of NO_3 radicals with other volatile organic compounds), the organic peroxides could possibly be formed in all systems; they may not have been identified previously owing to the lack of suitable analytical techniques such as accurate mass measurements from high resolution MS. Since the formation of ROOR from two peroxy radicals has always been considered as a minor channel, the reaction has not been widely studied. Ghigo et al. (2003) ruled out the direct formation of products (RO, ROH, RCHO) from the tetroxide intermediate ROOOOR. Instead, they proposed that the tetroxide breaks up into a weakly bound complex of two RO radicals and O_2 , which then fall apart or undergoes intersystem crossing to form the corresponding alcohol and carbonyl products. The formation of ROOR was not discussed in Ghigo et al. (2003) owing to little experimental evidence for the production of ROOR. However, the observation of ROOR formation in this study suggests that this reaction does occur and is potentially important for aerosol formation. As pointed out by Dibble (2008), the mechanism proposed by Ghigo (2003) would seem to allow for easy production of ROOR from the RO-RO- O_2 complex. Therefore, it appears that there are at least two possible pathways for ROOR formation: it can either be formed through the RO-RO- O_2 complex as suggested by Dibble (2008), or there may exist a direct pathway for ROOR

formation from ROO + ROO. Certainly more work is needed regarding the formation, detection, and quantification of ROOR products.

It is also worth noting that while most NO₃ chemistry occurs at night, it can also be important during the day at specific locations. Recently, a study by Fuentes et al. (2007) suggested substantial formation of NO₃ radicals can take place in forested environments with moderate to high levels of BVOC production, resulting in a significant oxidation of isoprene and terpenes by NO₃ radicals. For instance, approximately 60% of the terpenes react with NO₃ radicals within the canopy. Clearly, more study is needed to evaluate the importance of NO₃ chemistry of biogenic hydrocarbons under different environments and time of the day.

Acknowledgments

This research was funded by U.S. Department of Energy Biological and Environmental Research Program DE-FG02-05ER63983. This material is based in part on work supported by the National Science Foundation (NSF) under grant ATM-0432377. The Waters LCT Premier XT time-of-flight mass spectrometer interfaced to a Waters UPLC system was purchased in 2006 with a grant from the National Science Foundation, Chemistry Research Instrumentation and Facilities Program (CHE-0541745). The LCQ Ion Trap mass spectrometer was purchased in 1997 with funds from the National Science Foundation through the CRIF program (CHE-9709233). J. D. Surratt is supported in part by the U.S. EPA under the STAR Graduate Fellowship Program. A. J. Kwan and H. O. T. Pye acknowledge the support of NSF graduate research fellowships. The authors would like to thank C. D. Vecitis, J. Cheng, and M. R.

Hoffmann for use of and aid with their ozonizer and UV-VIS spectrometer, K. Takematsu and M. Okumura for helpful advice on preparing N_2O_5 , J. H. Kroll and M. Claeys for helpful discussions and suggestions, M. N. Chan for assistance with filter sample collection, H. G. Kjaergaard and F. Paulot for performing the quantum calculations and estimating the sensitivities of CIMS to various gas-phase products, and Y. Yu and the reviewers for helpful comments on the manuscript.

References

- Alfarra, M. R., Paulsen, D., Gysel, M., Garforth, A. A., Dommen, J., Prevot, A. S. H., Worsnop, D. R., Baltensperger, U., and Coe, H.: A mass spectrometric study of secondary organic aerosols formed from the photooxidation of anthropogenic and biogenic precursors in a reaction chamber, *Atmos. Chem. Phys.*, 6, 5279-5293, 2006.
- Bahreini, R., Keywood, M. D., Ng, N. L., Varutbangkul, V., Gao, S., Flagan, R. C., and Seinfeld, J. H. Measurements of secondary organic aerosol (SOA) from oxidation of cycloalkenes, terpenes, and m-xylene using an Aerodyne aerosol mass spectrometer. *Environ. Sci. Technol.*, 39, 5674-5688, 2005.
- Barnes, I., Bastian, V., Becker, K. H. and Tong, Z.: Kinetics and products of the reactions of NO_3 with monoalkenes, dialkenes, and monoterpenes, *J. Phys. Chem.*, 94, 2413-2419, 1990.
- Berndt, T. and Böge, O.: Gas-Phase reaction of NO_3 radicals with isoprene: A kinetic and

mechanistic study, *Inter. J. Chem. Kinet.*, 29, 755-765, 1997.

Bey, I., Aumont, B. and Toupance, G.: A modeling study of the nighttime radical chemistry in the lower continental troposphere. 1. Development of a detailed chemical mechanism including nighttime chemistry, *J. Geophys. Res.*, 106, D9, 9959-9990, 2001a.

Bey, I., Aumont, B. and Toupance, G.: A modeling study of the nighttime radical chemistry in the lower continental troposphere. 2. Origin and evolution of HO_x, *J. Geophys. Res.*, 106, D9, 9991-10001, 2001b.

Bey, I., Jacob, D. J., Yantosca, R. M., Logan, J. A., Field, B. D., Fiore, A. M., Li, Q. B., Liu, H. G. Y., Mickley, L. J. and Schultz, M. G.: Global modeling of tropospheric chemistry with assimilated meteorology: Model description and evaluation, *J. Geophys. Res.*, 106, D19, 23073-23095, 2001c .

Biggs, P., Canosa-Mas, C. E., Fracheboud, J. M., Shallcross, D. E. and Wayne, R. P.: Investigation into the kinetics and mechanisms of the reaction of NO₃ with CH₃ and CH₃O at 298K between 0.6 Torr and 8.5 Torr – is there a chain decomposition mechanism in operation, *J. Chem. Soc., Faraday Trans.*, 90, 1197-1204, 1994.

Brown, S. S., Ryerson, T. B., Wollny, A. G., Brock, C. A., Peltier, R., Sullivan, A. P., Weber, R. J., Dube, W. P., Trainer, M., Meagher, J. F., Fehsenfeld, F. C. and Ravishankara, A. R.: Variability in nocturnal nitrogen oxide processing and its role in

regional air quality, *Science*, 311, 5757, 67-70, 2006.

Canosa-Mas, C. E., Flugge, M. L., King, M. D. and Wayne, R. P.: An experimental study of the gas-phase reaction of the NO₃ radical with α,β -unsaturated carbonyl compounds, *Phys. Chem. Chem. Phys.*, 7, 643-650, 2005.

Canosa-Mas, C. E., King, M. D., Lopez, R., Percival, C. J., Wayne, R. P., Shallcross, D. E., Pyle, J. A. and Daele, V.: Is the reaction CH₃C(O)O₂ and NO₃ important in the night-time troposphere? *J. Chem. Soc., Faraday Trans.*, 92, 2211-2222, 1996.

Carslaw, N., Carpenter, L. J., Plane, J. M. C., Allan, B. J., Burgess, R. A., Clemitshaw, K. C., Coe, H. and Penkett, S. A.: Simultaneous measurements of nitrate and peroxy radicals in the marine boundary layer, *J. Geophys. Res.*, 102, 18917-18933. 1997.

Carter, W. P. L. and Atkinson, R.: Development and evaluation of a detailed mechanism for the atmospheric reactions of isoprene and NO_x, *Int. J. Chem. Kinet.*, 28, 497-530, 1996.

Claeys, M., Graham, B., Vas, G., Wang, W., Vermeylen, R., Pashynska, V., Cafmeyer, J., Guyon, P., Andreae, M.O., Artaxo, P. and Maenhaut, W.: Formation of secondary organic aerosols through photooxidation of isoprene, *Science*, 303, 1173-1176, 2004.

Cocker III, D. R., Flagan, R. C., and Seinfeld, J. H.: State-of-the-art chamber facility for studying atmospheric aerosol chemistry, *Environ. Sci. Technol.*, 35, 2594-2601, 2001.

Crouse, J. D., McKinney, K. A., Kwan, A. J. and Wennberg, P. O.: Measurements of gas-phase hydroperoxides by chemical ionization mass spectrometry, *Anal. Chem.*, 78, 6726-6732, 2006.

Curren, K., Gillespie, T., Steyn, D., Dann, T. and Wang, D.: Biogenic isoprene in the Lower Fraser Valley, British Columbia, *J. Geophys. Res.*, 103, D19, 25467-25477, 1998.

Daele, V., Laverdet, G., Lebras, G. and Poulet, G.: Kinetics of the reactions of $\text{CH}_3\text{O}+\text{NO}$, $\text{CH}_3\text{O}+\text{NO}_3$, and $\text{CH}_3\text{O}_2+\text{NO}_3$, *J. Phys. Chem.*, 99, 1470-1477, 1995.

Davidson, J. A., Viggiano, A. A., Howard, C. J., Fehsenfeld, F. C., Albritton, D. L. and Ferguson, E. E.: Rate constants for the reaction of O_2^+ , NO_2^+ , NO^+ , H_3O^+ , CO_3^- , NO_2^- , and halide ions with N_2O_5 at 300K, *J. Chem. Phys.*, 68, 2085-2087, 1978.

Dibble, T. S.: Isomerization of OH-isoprene adducts and hydroxyalkoxy isoprene radicals, *J. Phys. Chem.*, 106, 28, 6643-6650, 2002.

Dibbe T. S.: Failures and limitations of quantum chemistry for two key problems in the atmospheric chemistry of peroxy radicals, *Atmos. Environ.*, in press, 2008.

Docherty, K., Wu, W., Lim, Y., Ziemann, P.: Contributions of Organic Peroxides to Secondary Aerosol Formed from Reactions of Monoterpenes with O₃, *Environ. Sci. Technol.*, 39, 4049-4059, 2005.

Dommen, J., Metzger, A., Duplissy, J., Kalberer, M., Alfarra, M. R., Gascho, A., Weingartner, E., Prevot, A. S. H., Verheggen, B. and Baltensperger, U.: Laboratory observation of oligomers in the aerosol from isoprene/NO_x photooxidation, *Geophys. Res. Lett.*, 33, L13805, doi:10.1029/2006GL026523, 2006.

Edney, E. O., Kleindienst, T. E., Jaoui, M., Lewandowski, M., Offenberg, J. H., Wang, W. and Claeys, M.: Formation of 2-methyl tetrols and 2-methylglyceric acid in secondary organic aerosol from laboratory irradiated isoprene/NO_x/SO₂/air mixtures and their detection in ambient PM_{2.5} samples collected in the eastern United States, *Atmos. Environ.*, 39, 5281-5289, 2005.

Fan, J. and Zhang, R.: Atmospheric oxidation mechanism of isoprene, *Environ. Chem.*, 1, 140-149, doi:10.1071/EN04045, 2004.

Fuentes, J. D., Wang, D., Rowling, D. R., Potosnak, M., Monson, R. K., Goliff, W. S., and Stockwell, W. R.: Biogenic hydrocarbon chemistry within and above a mixed deciduous forest, *J. Atmos. Chem.*, 56, 165-185. 2007.

Gao, S., Keywood, M. D., Ng, N. L., Surratt, J. D., Varutbangkul, V., Bahreini, R.,

Flagan, R. C., and Seinfeld, J. H.: Low molecular weight and oligomeric components in secondary organic aerosol from the ozonolysis of cycloalkenes and α -pinene, *J. Phys. Chem. A*, 108, 10147-10164, 2004a.

Gao, S., Ng, N. L., Keywood, M. D., Varutbangkul, V., Bahreini, R., Nenes, A., He, J., Yoo, K. Y., Beauchamp, J. L., Hodyss, R. P., Flagan, R. C., and Seinfeld, J. H.: Particle phase acidity and oligomer formation in secondary organic aerosol, *Environ. Sci. Technol.*, 38, 6582-6589, 2004b.

Gao, S., Surratt, J. D., Knipping, E. M., Edgerton, E. S., Shahgholi, M., and Seinfeld, J. H.: Characterization of polar organic components in fine aerosols in the southeastern United States: Identity, origin, and evolution, *J. Geophys. Res.*, 111, D14314, doi:10.1029/2005JD006601, 2006.

Ghigo, G., Maranzana, A., Tonachini, G.: Combustion and atmospheric oxidation of hydrocarbons: Theoretical study of the methyl peroxy self-reaction, *J. Chem. Phys.*, 118, 23, 2003.

Goldstein, A. H. and Galbally, I. E.: Known and unexplored organic constituents in the earth's atmosphere, *Environ. Sci. Technol.*, 41, 1514-1521, 2007.

Gong, H., Matsunaga, A. and Ziemann, P.: Products and mechanism of secondary organic aerosol formation from reactions of linear alkenes with NO_3 radicals, *J. Phys.*

Chem., 109, 4312-4324, 2005.

Gómez-González, Y., Surratt, J. D., Cuyckens, F., Szmigielski, R., Vermeulen, R., Jaoui, M., Lewandowski, M., Offenberg, J. H., Kleindienst, T. E., Edney, E. O., Blockhuys, F., Van Alsenoy, C., Maenhaut, W. and Claeys, M.: Characterization of organosulfates from the photooxidation of isoprene and unsaturated fatty acids in ambient aerosol using liquid chromatography/(-) electrospray ionization mass spectrometry, *J. Mass Spectrom.*, doi:10.1002/jms.1329, 2007.

Guenther, A., Hewitt, C. N., Erickson, D., Fall, R., Geron, C., Graedel, T., Harley, P., Klinger, L., Lerdau, M., McKay, W. A., Pierce, T., Scholes, B., Steinbrecher, R., Tallamraju, R., Taylor, J. and Zimmerman, P.: A global-model of natural volatile organic compound emissions, *J. Geophys. Res.*, 100 (D5), 8873-8892, 1995.

Guenther, A., Karl, T., Harley, P., Wiedinmyer, C., Palmer, P. I. and Geron, C.: Estimates of global terrestrial isoprene emissions using MEGAN (Model of Emissions of Gases and Aerosols from Nature), *Atmos. Chem. Phys.*, 6, 3181-3210, 2006.

Heintz, F., Platt, U., Flentje, H. and Dubois, R.: Long-term observation of nitrate radicals at the tor station, Kap Arkona (Rugen), *J. Geophys. Res.*, 101, D17, 22891-22910, 1996.

Henze, D. K., Seinfeld, J. H., Ng, N. L., Kroll, J. H., Fu, T. M., Jacob, D. J. and Heald, C. L.: Global modeling of secondary organic aerosol formation from aromatic

hydrocarbons: High- vs low-yield pathways, *Atmos. Chem. Phys. Discuss.*, 7, 14569-14601, 2007.

Horowitz, L. W., Fiore, A. M., Milly, G. P., Cohen, R. C., Perring, A., Wooldridge, P. J., Hess, P.G., Emmons, L. K. and Lamarque, J.: Observational constraints on the chemistry of isoprene nitrates over the eastern United States, *J. Geophys. Res.*, 112, D12S08, doi:10.1029/2006JD007747, 2007.

Iinuma, Y., Müller, C., Berndt, T., Böge, O., Claeys, M. and Herrmann, H.: Evidence for the existence of organosulfates from β -pinene ozonolysis in ambient secondary organic aerosol, *Environ. Sci. Technol.*, 41, 6678-6683, 2007b.

Iinuma, Y., Müller, C., Böge, O., Gnauk, T. and Herrmann, H.: The formation of organic sulfate esters in the limonene ozonolysis secondary organic aerosol (SOA) under acidic conditions, *Atmos. Environ.*, 41, 5571-5583, 2007a.

Jay, K. and Stieglitz, L.: The gas phase addition of NO_x to olefins, *Chemosphere*, 19, 1939-1950, 1989.

Jayne, J. T., Leard, D. C., Zhang, X., Davidovits, P., Smith, K. A., Kolb, C. E., and Worsnop, D. W.: Development of an Aerosol Mass Spectrometer for size and composition analysis of submicron particles, *Aerosol Sci. Technol.*, 33, 49-70, 2000.

Kan, C. S., Calvert, J. G. and Shaw, J. H.: Reactive channels of the $\text{CH}_3\text{O}_2\text{-CH}_3\text{O}_2$ reaction, *J. Phys. Chem.*, 84, 3411-3417, 1980.

Kanakidou, M., et al.: Organic aerosol and global climate modeling: A review, *Atmos. Chem. Phys.*, 5, 1053-1123, 2005.

Keywood, M. D., Varutbangkul, V., Bahreini, R., Flagan, R. C., and Seinfeld, J. H.: Secondary organic aerosol formation from the ozonolysis of cycloalkenes and related compounds, *Environ. Sci. Technol.*, 38, 4157-4164, 2004.

Kirchner, F. and Stockwell, W. R.: Effect of peroxy radical reactions on the predicted concentrations of ozone, nitrogenous compounds, and radicals, *J. Geophys. Res.*, 101, D15, 21007-21022, 1996.

Knopf, D. A., Mak, J., Gross, S., Bertram, A. K.: Does atmospheric processing of saturated hydrocarbon surfaces by NO_3 lead to volatilization?, *Geophys. Res. Lett.*, 33, L17816, doi:10.1029/2006GL026884, 2006.

Kroll, J. H., Ng, N. L., Murphy, S. M., Flagan, R. C., and Seinfeld, J. H.: Secondary organic aerosol formation from isoprene photooxidation under high- NO_x conditions, *J. Geophys. Res.*, 32, L18808, doi: 10.1029/2005GL023637, 2005.

Kroll, J. H., Ng, N. L., Murphy, S. M., Flagan, R. C., and Seinfeld, J. H.: Secondary organic aerosol formation from isoprene photooxidation, *Environ. Sci. Technol.*, 40, 1869-1877, 2006.

Kwok, E. S. C., Aschmann, S. M., Arey, J. and Atkinson, R.: Product formation from the reaction of the NO_3 radical with isoprene and rate constants for the reactions of methacrolein and methyl vinyl ketone with the NO_3 radical, *Inter. J. Chem. Kinet.* 28, 925-934, 1996.

Liggio, J. and Li, S. M.: Organosulfate formation during the uptake of pinonaldehyde on acidic sulfate aerosols, *Geophys. Res. Lett.*, 33, L13808, doi: 10.1029/2006GL026079, 2006.

Liggio, J., Li, S. M. and McLaren, R.: Heterogeneous reactions of glyoxal on particulate matter: Identification of acetals and sulfate esters, *Environ. Sci. Technol.*, 39, 1532-1541, 2005.

Lightfoot, P. D., Cox, R.A., Crowley, J. N., Destriau, M. Hayman, G. D., Jenkin, M. E., Moortgat G. K. and Zabel, F.: Organic peroxy radicals – kinetics, spectroscopy and tropospheric chemistry, *Atmos. Environ.*, 26, 1805-1961, 1992.

Moise, T., Talukdar, R. K., Frost, G. J., Fox, R. W., and Rudich, Y.: Reactive uptake of NO_3 by liquid and frozen organics, *J. Geophys. Res.*, 107, D2, 4014, doi: ,

10.1029/2001JD000334, 2002.

Ng, N. L., Chhabra, P. S., Chan, A. W. H., Surratt, J. D., Kroll, J. H., Kwan, A. J., McCabe, D. C., Wennberg, P. O., Sorooshian, A., Murphy, S. M., Dalleska, N. F., Flagan, R. C. and Seinfeld, J. H.: Effect of NO_x level on secondary organic aerosol (SOA) formation from the photooxidation of terpenes, *Atmos. Chem. Phys.*, 7, 5159-5174, 2007a.

Ng, N. L., Kroll, J. H., Chan, A. W. H., Chhabra, P. S., Flagan, R. C. and Seinfeld, J. H.: Secondary organic aerosol formation from *m*-xylene, toluene, and benzene, *Atmos. Chem. Phys.*, 7, 3909-3922, 2007b.

Ng, N. L., Kroll, J. H., Keywood, M. D., Bahreini, R., Varutbangkul, V., Flagan, R. C., Seinfeld, J. H., Lee, A. and Goldstein, A. H.: Contribution of first- versus second-generation products to secondary organic aerosols formed in the oxidation of biogenic hydrocarbons, *Environ. Sci. Technol.*, 40, 2283-2297, 2006.

Niki, H, Maker, P. D., Savage, C. M. and Breitenbach L.P.: Fourier Transform Infrared studies of the self-reaction of CH_3O_2 radicals, *J. Phys. Chem.*, 85, 877-881, 1981.

Niki, H, Maker, P. D., Savage, C. M. and Breitenbach L.P.: Fourier Transform Infrared studies of the self-reaction of $\text{C}_2\text{H}_5\text{O}_2$ radicals, *J. Phys. Chem.*, 86, 3825-3829, 1982.

Noda, J., Nyman, G. and Langer S.: Kinetics of the gas-phase reaction of some unsaturated alcohols with the nitrate radical, *J. Phys. Chem.*, 106, 945-951, 2002.

Odum, J. R., Hoffmann, T., Bowman, F., Collins, D., R. C. Flagan, R. C., and Seinfeld, J. H.: Gas/particle partitioning and secondary organic aerosol yields, *Environ. Sci. Technol.*, 30, 2580-2585, 1996.

Odum, J. R., Jungkamp, T. P. W., Griffin, R. J., Flagan, R. C., and Seinfeld, J. H.: The atmospheric aerosol-forming potential of whole gasoline vapor, *Science*, 276, 96-99, 1997a.

Odum, J. R., Jungkamp, T. P. W., Griffin, R. J., Forstner, H. J. L., Flagan, R. C., and Seinfeld, J. H.: Aromatics, reformulated gasoline and atmospheric organic aerosol formation, *Environ. Sci. Technol.*, 31, 1890-1897, 1997b.

Paulot, F., Crouse, J.D., Kjaergaard, H. G., Kroll, J. H., Seinfeld, J. H., and Wennberg, P. O.: Isoprene photooxidation mechanism: resonance channels and implications for the production of nitrates and acids, submitted to *Atmos. Chem. Phys. Discuss.*, 2008.

Paulson, S. E. and Seinfeld, J. H.: Development and evaluation of a photooxidation mechanism for isoprene, *J. Geophys. Res.*, 97, D18, 20703-20715, 1992.

Penkett, S.A., Burgess, R.A., Coe, H., Coll, I., Hov, Ø., Lindskog, A., Schmidbauer, N.,

Solberg, S., Roemer, M., Thijssse, T., Beck, J. and Reeves C.E.: Evidence for large average concentrations of the nitrate radical (NO_3) in Western Europe from the HANSA hydrocarbon database, *Atmos. Environ.*, 41, 3465-3478, 2007.

Platt, U. and Janssen, C.: Observation and role of the free radicals NO_3 , ClO , BrO and IO in the troposphere, *Faraday Discuss.*, 100, 175-198, 1995.

Platt, U., Perner, D., Schroder, J., Kessler, C. and Toennissen, A.: The diurnal variation of NO_3 , *J. Geophys. Res.*, 86, 11965-11970, 1981.

Rudich, Y., Donahue, N. M., and Mentel, T. F.: Aging of organic aerosol: Bridging the gap between laboratory and field studies, *Annu. Rev. Phys. Chem.*, 58, 321-352, 2007.

Sharkey, T. D., Singaas, E. L., Vanderveer, P. J. and Geron, C.: Field measurements of isoprene emission from trees in response to temperature and light, *Tree Physiol.*, 16, 649-654, 1996.

Skov, H., Benter, Th., Schindler, R. N., Hjorth, J. and Restelli, G.: Epoxide formation in the reactions of the nitrate radical with 2,3-dimethyl-2-butene, cis- and trans-2-butene and isoprene, *Atmos. Environ.*, 28, 1583-1592, 1994.

Skov, H., Hjorth, J., Lohse, C., Jensen, N. R. and Restelli, G.: Products and mechanisms of the reactions of the nitrate radical (NO_3) with isoprene, 1,3-butadiene and 2,3-

dimethyl-1,3-butadiene in air, *Atmos. Environ.*, 26A, 15, 2771-2783, 1992.

Smith, N., Plane, J. M. C., Nien, C. F. and Solomon, P. A.: Nighttime radical chemistry in the San-Joaquin Valley, *Atmos. Environ.*, 29, 2887-2897, 1995.

Sorooshian, A., Brechtel F. J., Ma, Y. L., Weber R. J., Corless, A., Flagan, R. C., and Seinfeld, J. H.: Modeling and characterization of a particle-into-liquid sampler (PILS), *Aerosol Sci. Technol.*, 40, 396-409, 2006.

Starn, T. K., Shepson, P. B., Bertman, S. B., Riemer, D. D., Zika, R. G. and Olszyna, K.: Nighttime isoprene chemistry at an urban-impacted forest site, *J. Geophys. Res.*, 103, D17, 22437-22447, 1998.

Steinbacher, M., Dommen, J. Ordonez, C., Reimann, S., Gruebler, F. C., Staehelin, J., Andreani-Aksoyoglu, S. and Prevot, A. S. H.: Volatile organic compounds in the Po Basin. Part B: Biogenic VOCs, *J. Atmos. Chem.*, 51, 293-315, 2005.

Stroud, C. A., Roberts, J. M., Williams E. J., Hereid, D., Angevine, W. M., Fehsenfeld, F. C., Wisthaler, A., Hansel, A., Martinez-Harder, M., Harder, H., Brune, W. H., Hoenninger, G., Stutz, J. and White, A. B.: Nighttime isoprene trends at an urban forested site during the 1999 Southern Oxidant Study, *J. Geophys. Res.*, 107, D16, 4291, 10.1029/2001JD000959, 2002.

Su, T. and Chesnavich, W. J.: Parametrization of the ion–polar molecule collision rate constant by trajectory calculations, *The Journal of Chemical Physics*, 76, 5183, 1982.

Suh, I., Lei, W. and Zhang, R.: Experimental and theoretical studies of isoprene reaction with NO₃, *J. Phys. Chem.*, 105, 6471-6478, 2001.

Surratt, J. D., Kroll, J. H., Kleindienst, T. E., Edney, E. O., Claeys, M., Sorooshian, A., Ng, N. L., Offenberg, J. H., Lewandowski, M., Jaoui, M., Flagan, R. C. and Seinfeld, J. H.: Evidence for organosulfates in secondary organic aerosol, *Environ. Sci. Technol.*, 41, 517-527, 2007a.

Surratt, J. D., Lewandowski, M., Offenberg, J. H., Jaoui, M., Kleindienst, T. E., Edney, E. O. and Seinfeld, J. H.: Effect of acidity on secondary organic aerosol formation from isoprene, *Environ. Sci. Technol.*, 41, 5363-5369, 2007b.

Surratt, J. D., Murphy, S. M., Kroll, J. H., Ng, N. L., Hildebrandt, L., Sorooshian, A., Szmigielski, R., Vermeylen, R., Maenhaut, W., Claeys, M., Flagan, R. C. and Seinfeld, J. H.: Chemical composition of secondary organic aerosol formed from the photooxidation of isoprene, *J. Phys. Chem. A*, 110, 9665-9690, 2006.

Szmigielski, R., Surratt, J. D., Vermeylen, R., Szmigielska, K., Kroll, J. H., Ng, N. L., Murphy, S. M., Sorooshian, A., Seinfeld, J. H. and Claeys, M.: Characterization of 2-methylglyceric acid oligomers in secondary organic aerosol formed from the

photooxidation of isoprene using trimethylsilylation and gas chromatography/ion trap mass spectrometry, *J. Mass Spectrom.*, 42, 101-116, 2007.

Tyndall, G. S., Cox, R. A., Granier, C., Lesclaux, R., Moortgat, G. K., Pilling, M. J., Ravishankara, A. R. and Wallington, T. J.: Atmospheric chemistry of small peroxy radicals, *J. Geophys. Res.*, 106, D11, 12157-12182, 2001.

Tyndall, G. S., Wallington, T. J. and Ball, J. C.: FTIR product study of the reactions of $\text{CH}_3\text{O}_2 + \text{CH}_3\text{O}_2$ and $\text{CH}_3\text{O}_2 + \text{O}_3$, *J. Phys. Chem.*, 102, 2547-2554, 1998.

Vaughan, S. Canosa-Mas, C. E., Pfrang, C., Shallcross, D. E., Watson, L. and Wayne, R. P.: Kinetic studies of reactions of the nitrate radical (NO_3) with peroxy radicals (RO_2): an indirect source of OH at night? *Phys. Chem. Chem. Phys.*, 8, 3749–3760, 2006.

von Friedeburg, C., Wagner, T., Geyer, A., Kaiser, N., Platt, U., Vogel, B. and Vogel, H.: Derivation of tropospheric NO_3 profiles using off-axis differential optical absorption spectroscopy measurements during sunrise and comparison with simulations, *J. Geophys. Res.*, 107, D13, doi:10.1029/2001JD000481, 2002.

Wallington, T. J., Dagaut, P. and Kurylo, M. J.: Ultraviolet absorption cross-sections and reaction kinetics and mechanisms for peroxy radicals in the gas phase, *Chem. Rev.*, 92, 667-710, 1992.

Wallington, T. J., Gierczak, C. A., Ball, J. C. and Japar, S. M.: Fourier Transform Infrared studies of the self-reaction of $C_2H_5O_2$ radicals in air at 295K, *Int. J. Chem. Kinet.*, 21, 1077-1089, 1989.

Werner, G., Kastler, J., Looser, R. and Ballschmiter, K.: Organic nitrates of isoprene as atmospheric trace compounds, *Angew. Chem. Int. Ed.*, 38, 11, 1634-1637, 1999.

Wu, S. L., Mickley, L. J., Jacob, D. J. Logan, J. A., Yantosca, R. M. and Rind, D.: Why are there large differences between models in global budgets of tropospheric ozone? *J. Geophys. Res.*, 112, D5, D05302, doi: 10.1029/2006JD007801, 2007.

Zhang, D. and Zhang, R.: Unimolecular decomposition of nitrooxyalkyl radicals from NO_3 -isoprene reaction, *J. Chem. Phys.*, 116, 22, 9721-9728, 2002.

Ziemann, P.: Evidence for low-volatility diacyl peroxides as a nucleating agent and major component of aerosol formed from reactions of O_3 with cyclohexene and homologous compounds, *J. Phys. Chem.*, 106, 4390-4402, 2002.

Table 1. Initial conditions and results for yield experiments

Date	T (K)	RH (%)	ΔHC (ppb) ^a	ΔM_o ($\mu\text{g}/\text{m}^3$) ^b	SOA Yield (%)
8/9/07	294	5.1	101.6 ± 0.6	68.1 ± 1.1	23.8 ± 0.5
8/10/07	293	4.7	30.2 ± 0.1	11.5 ± 0.4	13.5 ± 0.5
8/11/07	294	5.4	67.1 ± 0.1	39.3 ± 1.2	20.8 ± 0.7
8/12/07	293	6.0	51.7 ± 0.2	26.7 ± 0.6	18.2 ± 0.5
8/13/07	294	5.7	18.4 ± 0.1	2.2 ± 0.2	4.3 ± 0.5
8/14/07	294	5.5	21.8 ± 0.1	4.8 ± 0.4	7.8 ± 0.6
10/4/2007 ^c	293	5.5	39.5 ± 0.1 ^d	7.9 ± 0.3	7.1 ± 0.6
10/25/2007 ^e	294	6.4	42.0 ± 0.1	16.6 ± 0.6	14.1 ± 0.7

^a Stated uncertainties (1σ) are from scatter in isoprene measurements.

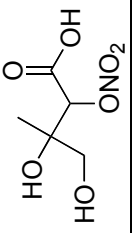
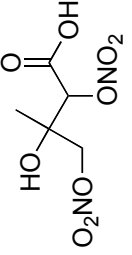
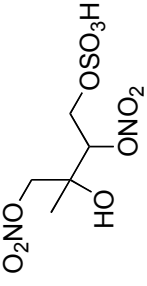
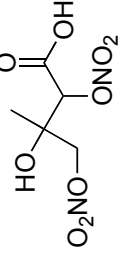
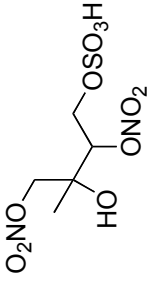
^b Stated uncertainties (1σ) are from scatter in particle volume measurements.

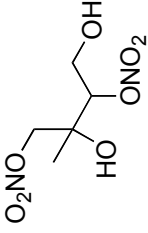
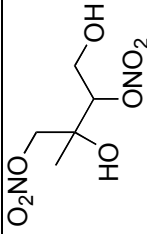
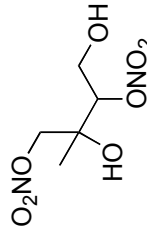
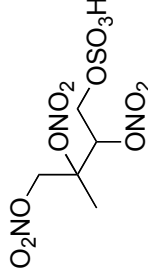
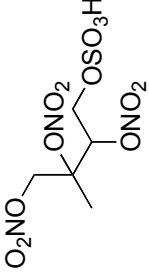
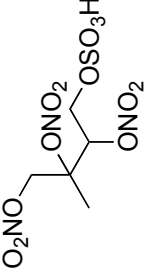
^c Slow isoprene injection experiment

^d Concentration estimated based on a separate calibration experiment (see Sect. 3.2); the uncertainty in the measured isoprene concentration is assumed to be the same as in the slow N_2O_5 experiment.

^e Slow N_2O_5 injection experiment

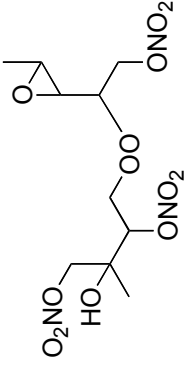
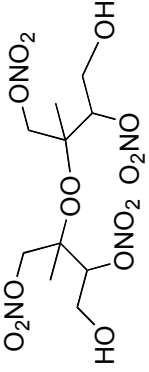
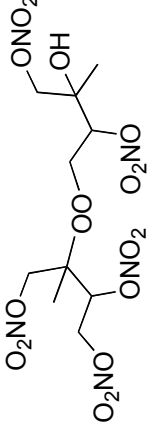
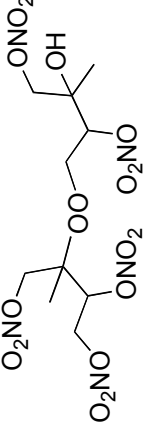
Table 2. SOA products identified using UPLC/(-)ESI-TOFMS.

Retention Time (min)	Measured [M - H] ⁻ Ion (m/z)	TOFMS Suggested [M - H] ⁻ Ion Formula	Error (mDa, ppm)	Measured [M - H + C ₂ H ₄ O ₂] ⁻ Ion (m/z)	TOFMS Suggested [M - H + C ₂ H ₄ O ₂] ⁻ Ion Formula	Error (mDa, ppm)	Proposed Structure ^a
3.68 ^b	194.0310	C ₅ H ₈ NO ₇ ⁻	0.9, 4.6	c			
4.52 ^b	239.0137	C ₅ H ₇ N ₂ O ₉ ⁻	-1.5, -6.3				
5.09 ^d	304.9946	C ₅ H ₉ N ₂ O ₁₁ S ⁻	1.9, 6.2				
5.24 ^b	239.0152	C ₅ H ₇ N ₂ O ₉ ⁻	0.0, 0.0				
5.43 ^d	304.9944	C ₅ H ₉ N ₂ O ₁₁ S ⁻	1.7, 5.6				

6.07	225.0350	$C_5H_9N_2O_8^-$	-0.9, -4.0				
6.12	225.0342	$C_5H_9N_2O_8^-$	-1.7, -7.6				
6.60	225.0375	$C_5H_9N_2O_8^-$	1.6, 7.1	285.0676	$C_7H_{13}N_2O_{10}^-$	0.6, 2.1	
7.75 ^d	349.9775	$C_5H_8N_3O_{13}S^-$	-0.3, -0.9				
7.85 ^d	349.9764	$C_5H_8N_3O_{13}S^-$	0.2, 0.6				
8.00 ^d	349.9784	$C_5H_8N_3O_{13}S^-$	-0.4, -1.1				

8.48 ^d	466.0268	$C_{10}H_{16}N_3O_{16}S^-$	1.7, 3.6				
8.54 ^d	466.0264	$C_{10}H_{16}N_3O_{16}S^-$	1.3, 2.8				
8.72 ^d	466.0237	$C_{10}H_{16}N_3O_{16}S^-$	-1.4, -3.0				
8.76 ^e	270.0199	$C_8H_8N_3O_{10}^-$	-1.1, -4.1	330.0393	$C_7H_{12}N_3O_{12}^-$	-2.8, -8.5	
8.81 ^d	466.0237	$C_{10}H_{16}N_3O_{16}S^-$	-1.4, -3.0				
8.85 ^e	270.0204	$C_8H_8N_3O_{10}^-$	-0.6, -2.2	330.0379	$C_7H_{12}N_3O_{12}^-$	-4.2, -12.7	

9.15	370.0734	$C_{10}H_{16}N_3O_{12}^-$	0.9, 2.4	430.0940	$C_{12}H_{20}N_3O_{14}^-$	-0.5, -1.2	
9.19	386.0678	$C_{10}H_{16}N_3O_{13}^-$	-0.5, -1.3	446.0888	$C_{12}H_{20}N_3O_{15}^-$	-0.6, -1.3	
9.24	370.0732	$C_{10}H_{16}N_3O_{12}^-$	-0.2, -0.5	430.0937	$C_{12}H_{20}N_3O_{14}^-$	-0.8, -1.9	
9.25	386.0683	$C_{10}H_{16}N_3O_{13}^-$	-0.2, -0.5	446.0893	$C_{12}H_{20}N_3O_{15}^-$	-0.1, -0.2	
9.37	449.0637	$C_{10}H_{17}N_4O_{16}^-$	-0.3, -0.7	509.0854	$C_{12}H_{21}N_4O_{18}^-$	0.3, 0.6	

9.41	386.0684	$C_{10}H_{16}N_3O_{13}^-$	0.1, 0.3	446.0903	$C_{12}H_{20}N_3O_{15}^-$	0.9, 2.0	
9.45	449.0653	$C_{10}H_{17}N_4O_{16}^-$	1.3, 2.9	509.0853	$C_{12}H_{21}N_4O_{18}^-$	0.2, 0.4	
9.90 ^f	494.0537	$C_{10}H_{16}N_5O_{18}^-$	4.7, 9.5	554.0669	$C_{12}H_{20}N_5O_{20}^-$	-3.3, -6.0	
9.98 ^f	494.0518	$C_{10}H_{16}N_5O_{18}^-$	2.8, 5.7	554.0676	$C_{12}H_{20}N_5O_{20}^-$	-2.6, -4.7	

^a Structural isomers containing nitrate, sulfate, or hydroxyl groups at other positions are likely; for simplicity, only one isomer is shown.

^b These compounds appear to be very minor SOA products due to very small chromatographic peak areas, confirming that the further oxidation of the nitrooxycarbonyl and hydroxycarbonyl first-generation gas-phase products do not yield significant quantities of SOA.

^c A blank cell indicates that the detected SOA product had no observable acetic acid adduct ion (i.e. $[M - H + C_2H_4O_2]^-$).

^d These organosulfate SOA products were observed only in experiments employing either $(NH_4)_2SO_4$ (i.e. neutral) or $MgSO_4 + H_2SO_4$ (i.e. acidic) seed aerosol. These organosulfate SOA products were also observed in the excess isoprene experiments.

^e In addition to the acetic acid adduct ion, these compounds also had a significant adduct ion at $[M - H + HNO_3]^-$ (m/z 333), indicating that these compounds are likely not very stable due to the fragmentation of one of the NO_3 groups during the MS analysis.

^f These compounds were only weakly detected in the excess isoprene experiments.

Table 3. Peroxide content of SOA formed by NO₃ oxidation of isoprene.

Experiment Date	Seeded/ ^a / Nucleation	[Isoprene] (ppb)	[N ₂ O ₅] (ppm)	SOA Volume Growth Observed ^b (μm ³ /cm ³)	Total SOA Mass Concentration ^c (μg/m ³)	Peroxide Aerosol Mass Concentration (μg/m ³)	Contribution of Peroxides to the SOA Mass Concentration Observed (%)
8/22/07	AS	200	1	102	145	46	32
8/30/07	AMS	200	1	123	174	40	23
10/22/07 ^d	AS	1200	0.7	70	100	b.d.l. ^e	f
10/23/07	nucleation	200	1	125	177	31	17
10/24/07	AS	200	1	111	158	47	30
10/27/07 ^g	AS	300	1	110	156	47	30

^a AS = ammonium sulfate seed, AMS = acidified magnesium sulfate seed.

^b Averaged over the course of filter sampling.

^c Assuming a SOA density of 1.42 g/cm³. This was based on DMA and Q-AMS measurements.

^d Excess isoprene experiment.

^e Below detection limits.

^f No observable contribution of organic peroxides to the SOA mass concentration.

^g Slow injection of isoprene in this experiment to enhance the RO₂ + NO₃ reaction pathway.

Table 4. Global estimation of isoprene using GEOS-Chem

	Emission Model	
	GEIA ^a	MEGAN ^b
Isoprene emission (Tg/y)	507	389
Global isoprene burden (Tg)	1.7	1.7
Isoprene lifetime (days)	1.2	1.6
Isoprene reacted (Tg/y) by		
Isoprene + OH	407	304
Isoprene + O ₃	69	62
Isoprene + NO ₃	29	21

^a Modification of GEIA for GEOS-Chem are described at Bey et al. (2001c).

Original GEIA reference is Guenther et al. (1995).

^b Guenther et al. (2006)

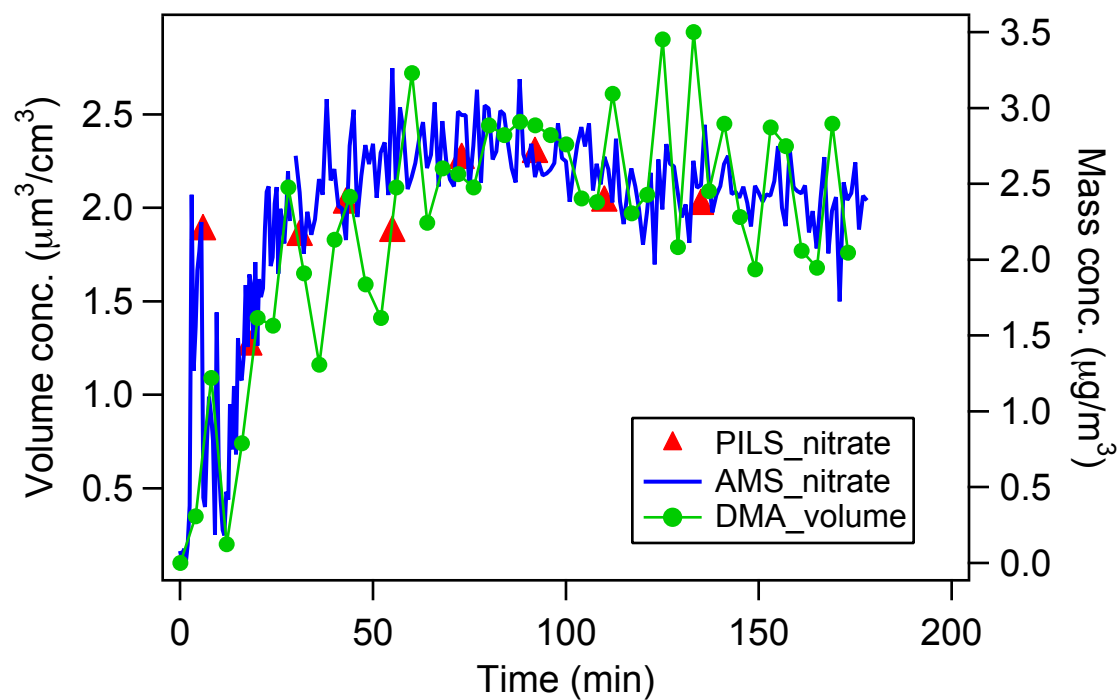


Figure 2.1. Time profiles of aerosol volume, inorganic nitrate measured by PILS/IC, and nitrate signals from Q-AMS in a blank experiment (~ 1 ppm N_2O_5 , ammonium sulfate seed, no isoprene).

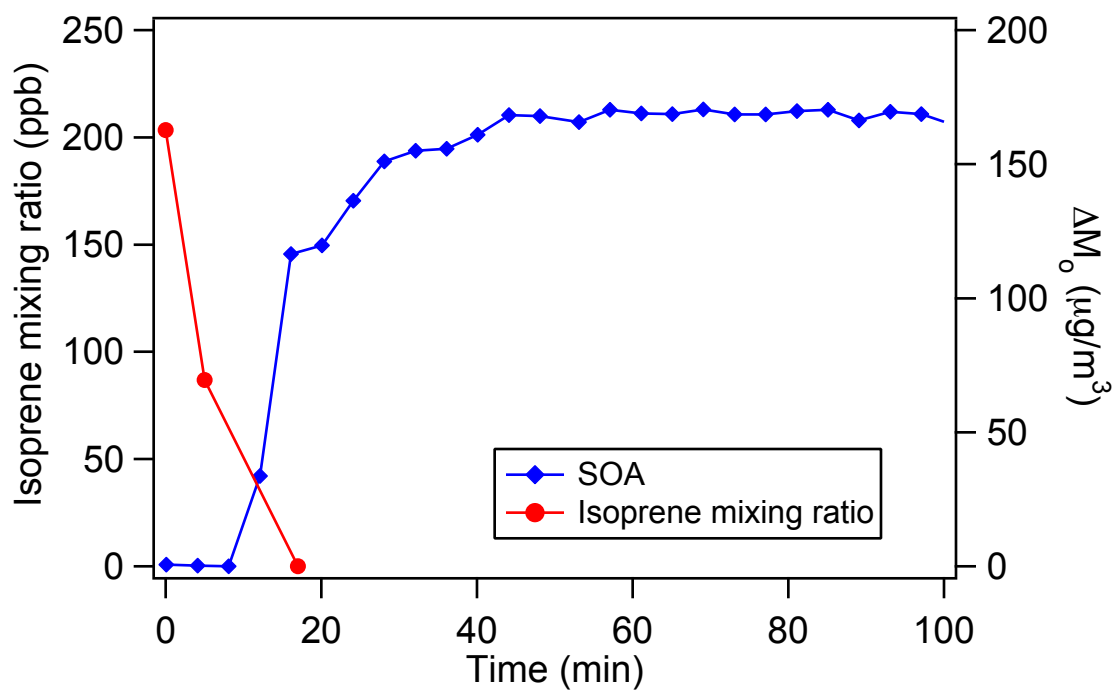


Figure 2.2. Isoprene depletion and SOA formation for typical experiment. Initial isoprene is 203.4 ppb ($573 \mu\text{g}/\text{m}^3$).

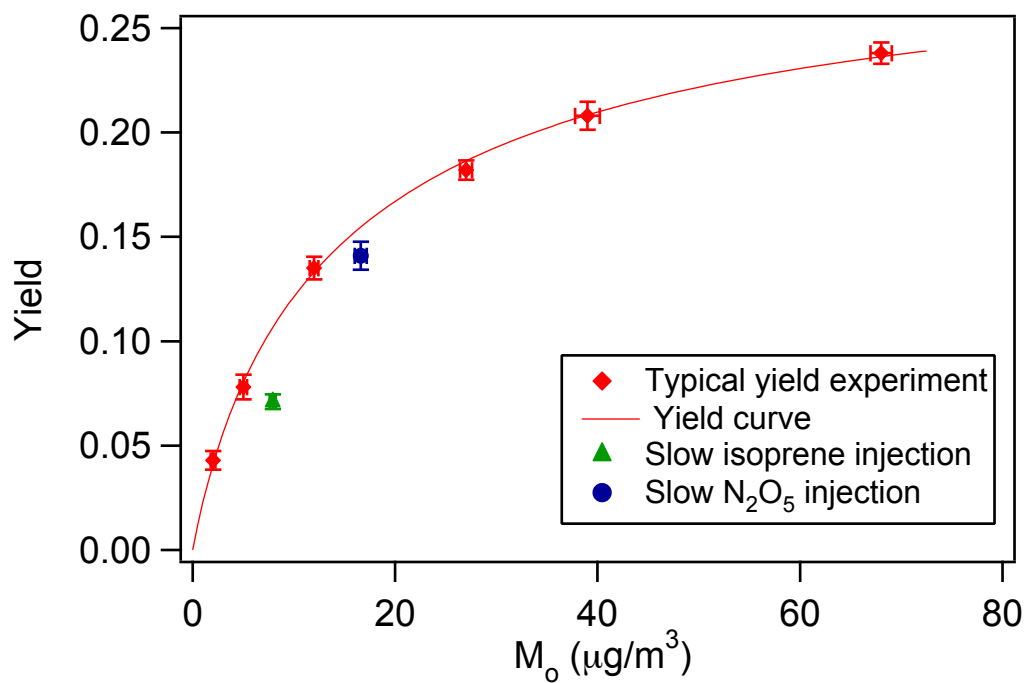


Figure 2.3. SOA yield data and yield curve for isoprene- NO_3 reaction. Also shown are SOA yields from the slow N_2O_5 injection experiment and slow isoprene injection experiment.

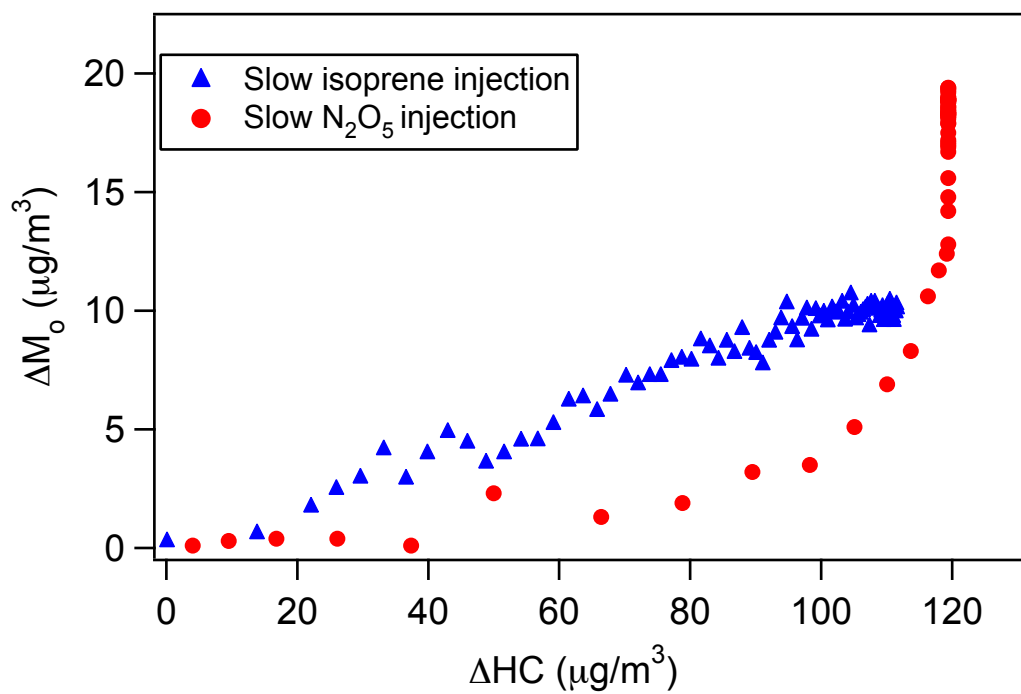


Figure 2.4. Time-dependent growth curves for the slow N_2O_5 injection experiment and slow isoprene injection experiment (last two experiments in Table 1).

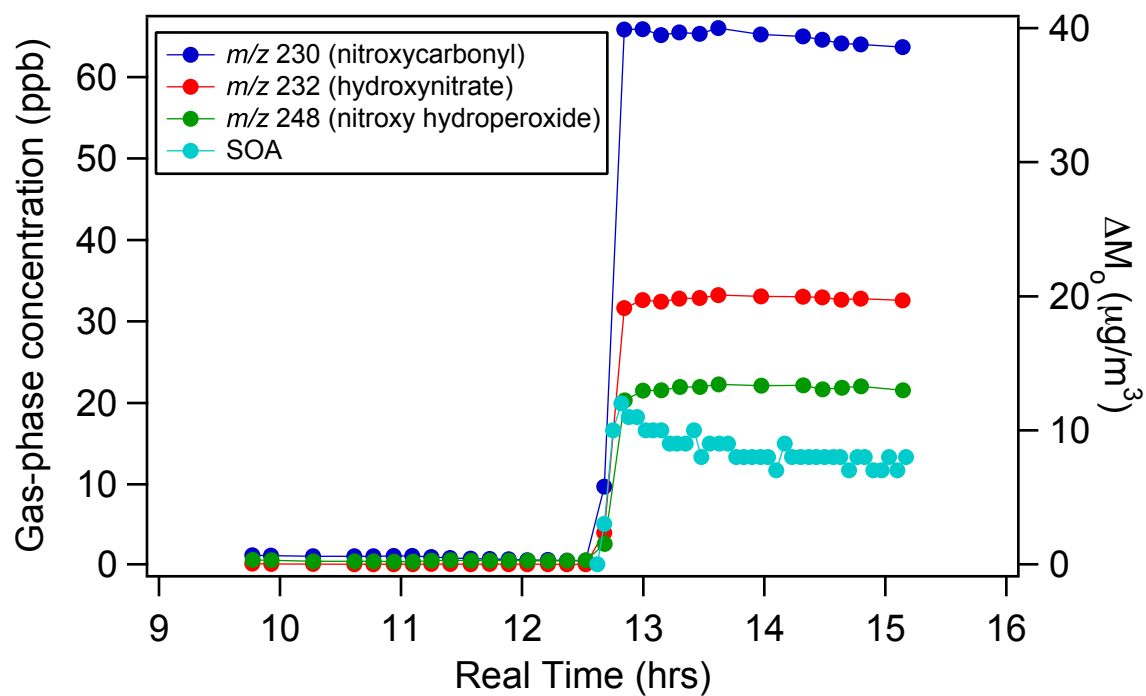


Figure 2.5. Time profiles of the major gas-phase products (m/z 230, 232, and 248) and the corresponding aerosol growth from the excess isoprene experiment.

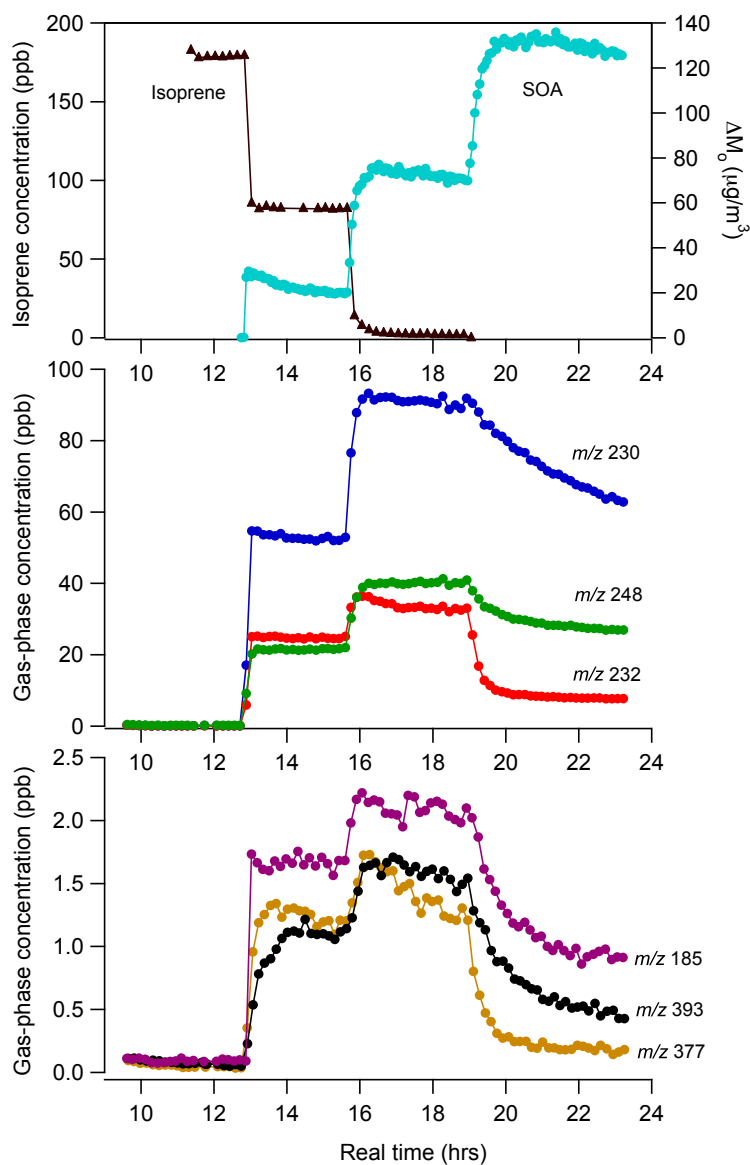


Figure 2.6. Time evolution of various gas-phase products in the staggered N_2O_5 injection experiment (Isoprene is first injected into the chamber, followed by the addition of 3 pulses of N_2O_5 : ~120, 50, and 210 ppb). The top panel shows the isoprene decay and aerosol formation; the middle panel shows the time profiles of the three major first-generation products (m/z 230, 232, and 248); the bottom panel shows the time profiles of three minor products (m/z 185, 377, and 393). (The likely identities for these products are shown in Fig. 11.)

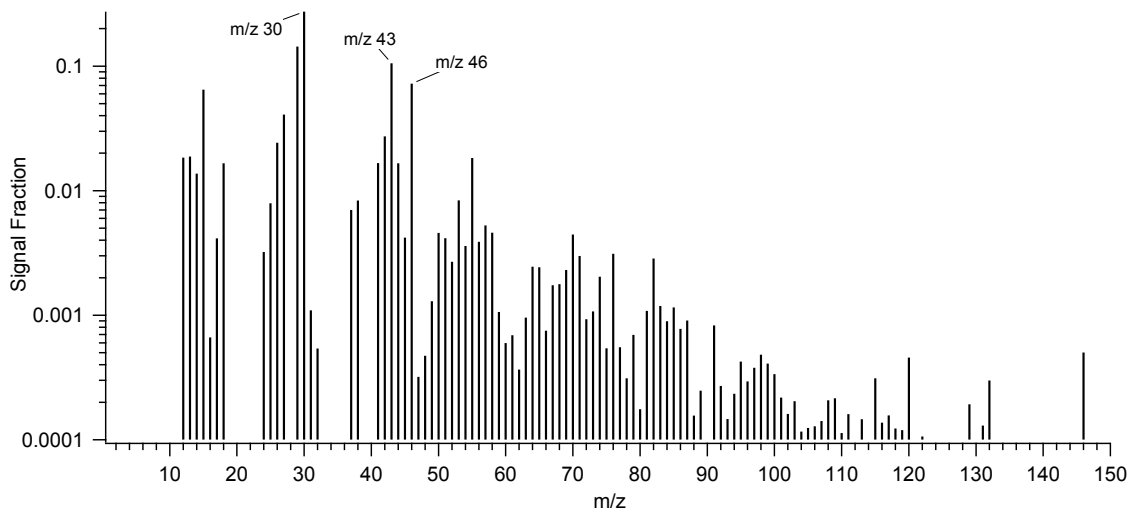


Figure 2.7. A typical AMS spectrum for SOA formed in typical yield experiments.

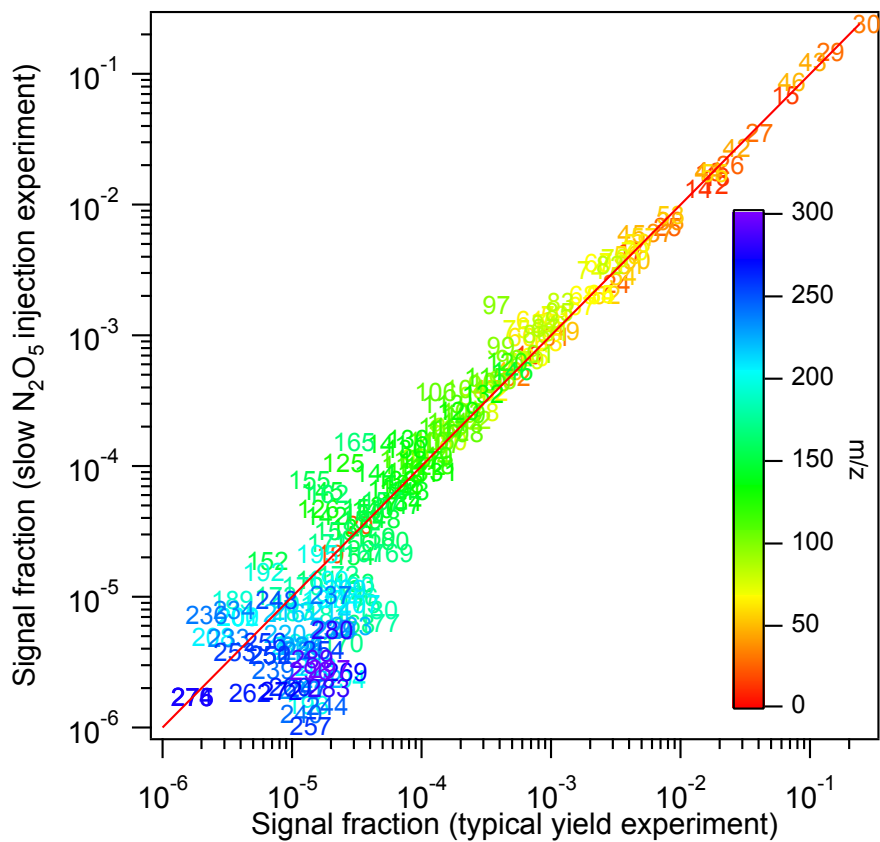


Figure 2.8. AMS spectra signal from the slow N_2O_5 injection experiment versus a typical yield experiment. Each mass fragment is normalized by the total signal. The solid red line is the 1:1 line. Note that the higher masses ($m/z > 165$) are dominated by noise.

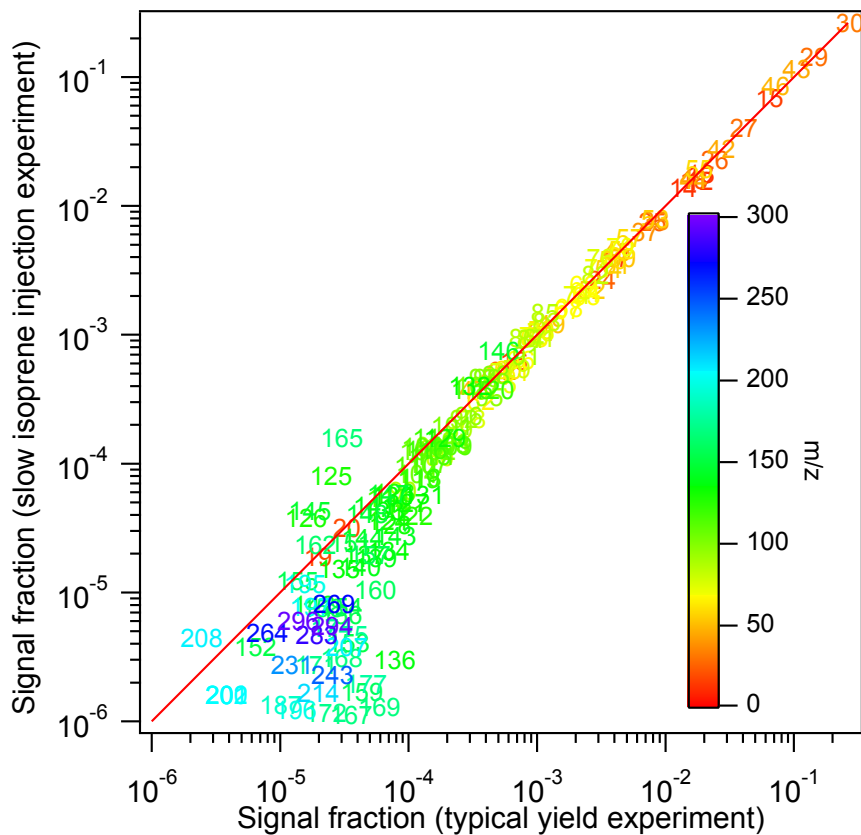


Figure 2.9. AMS spectra signal from the slow isoprene injection experiment versus a typical yield experiment. Each mass fragment is normalized by the total signal. The solid red line is the 1:1 line.

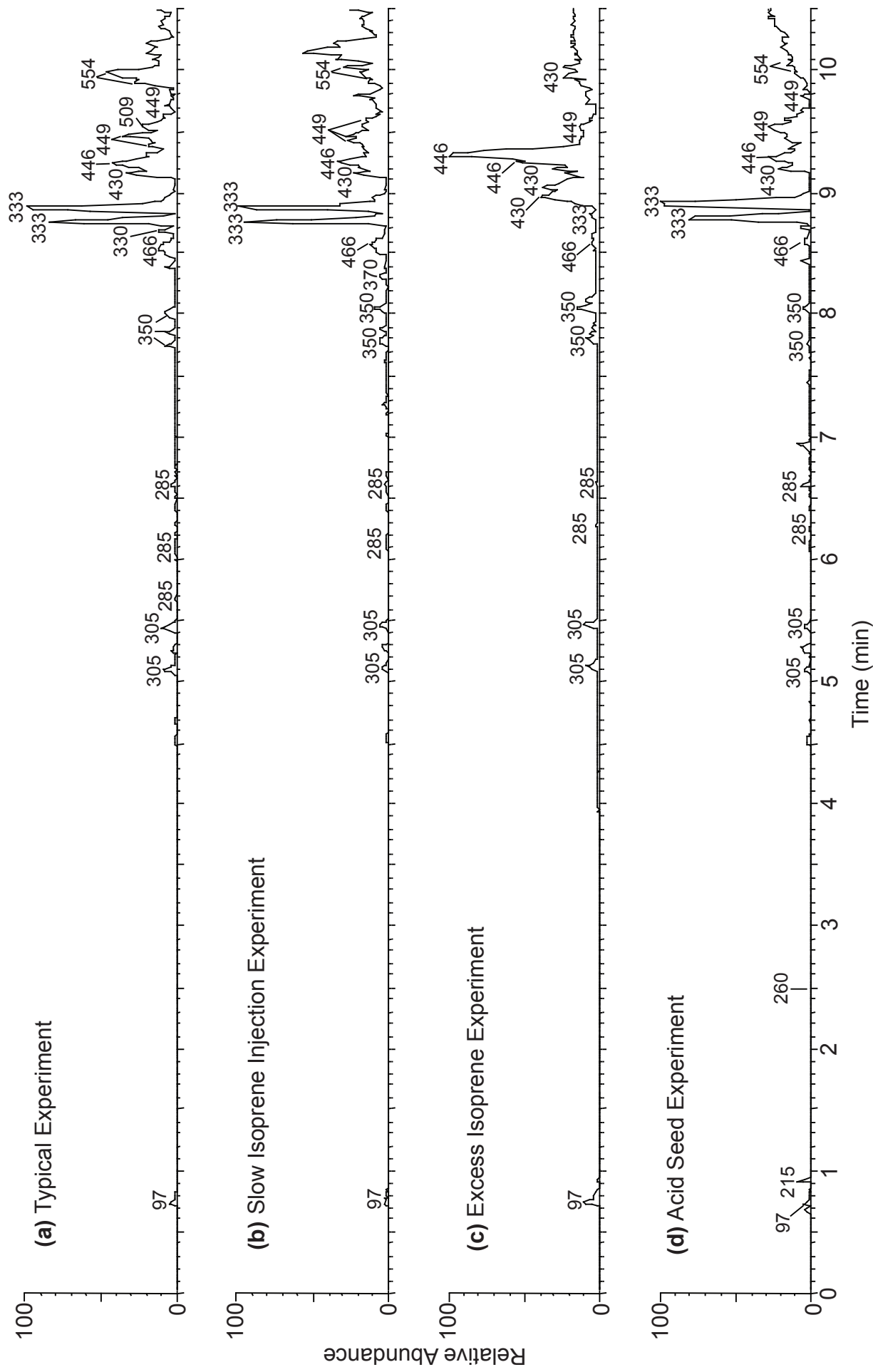


Figure 2.10. UPLC/(-)ESI-TOFMS base peak ion chromatograms (BPCs) for the following isoprene-NO₃ oxidation experiments: (a) 200 ppb isoprene + 1 ppm N₂O₅ + seed aerosol generated from 15 mM (NH₄)₂SO₄ atomizing solution; (b) 300 ppb isoprene + 1 ppm N₂O₅ + seed aerosol generated from 15 mM (NH₄)₂SO₄ atomizing solution; (c) 1.2 ppm isoprene + 700 ppb N₂O₅ + seed aerosol generated from 15 mM (NH₄)₂SO₄ atomizing solution; (d) 200 ppb isoprene + 1 ppm N₂O₅ + seed aerosol generated from 30 mM MgSO₄ + 50 mM H₂SO₄ atomizing solution. The numbers indicated above the selected chromatographic peaks correspond to the most abundant negative ion, and is either the [M - H]⁻ or [M - H + C₂H₄O₂]⁻ ions.

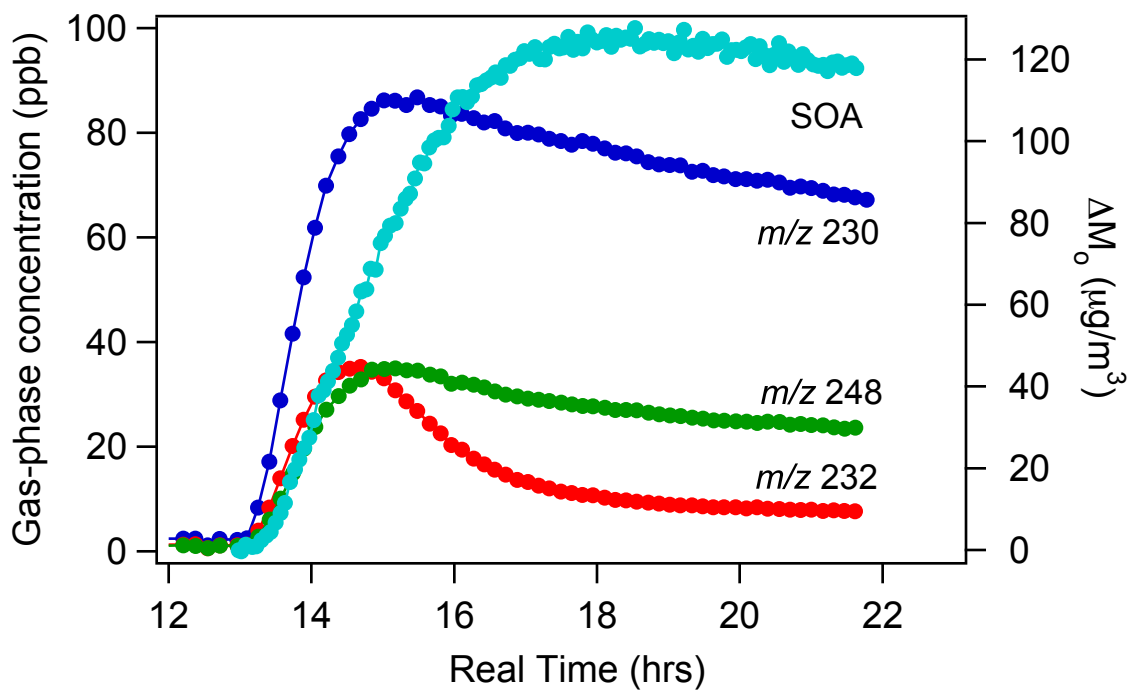


Figure 2.12. Time profiles of the major gas-phase products (m/z 230, 232, and 248) and the corresponding aerosol growth from the slow N_2O_5 injection experiment. Note that this experiment has a higher initial isoprene concentration (~ 200 ppb) compared to the one shown in Figure 2.4.

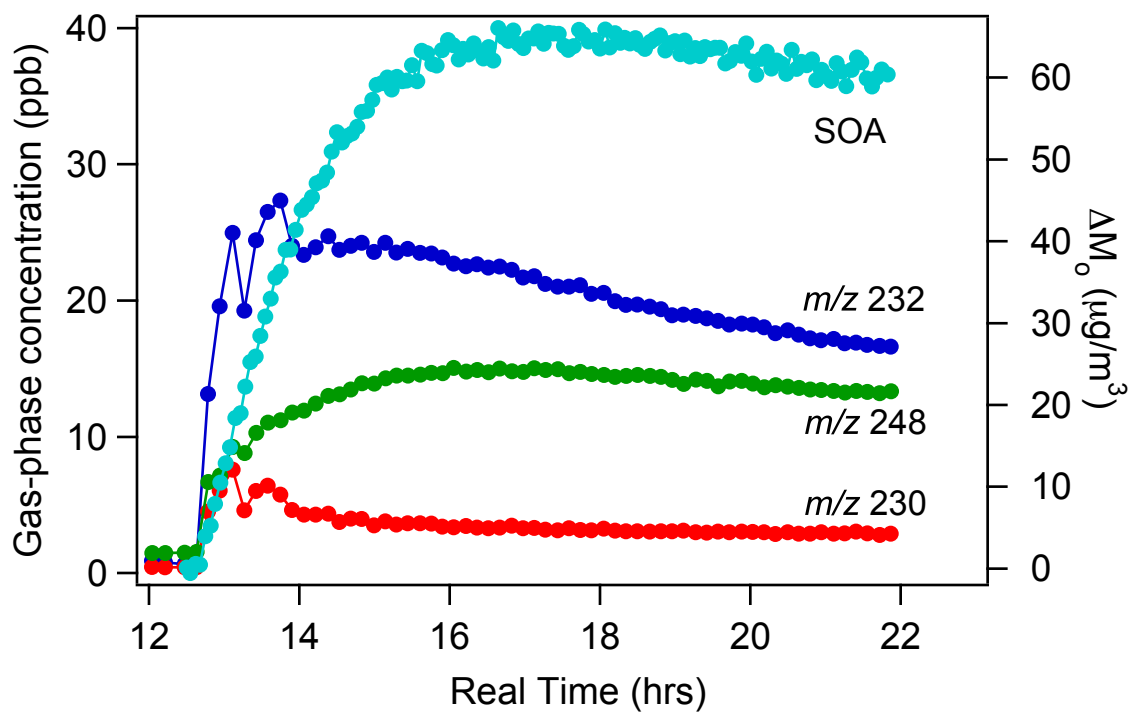


Figure 2.13. Time profiles of the major gas-phase products (m/z 230, 232, and 248) and the corresponding aerosol growth from the slow isoprene injection experiment. Note that this experiment has a higher initial isoprene concentration (~ 200 ppb) compared to the one shown in Figure 2.4.

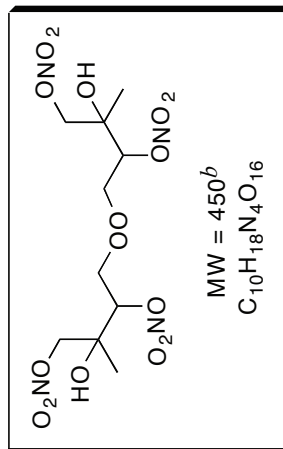
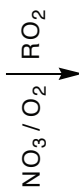
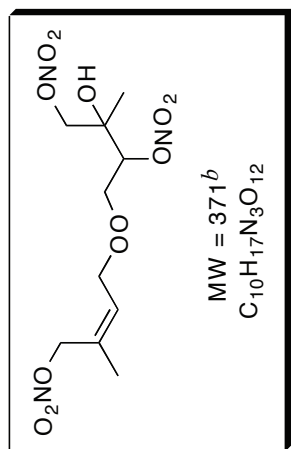
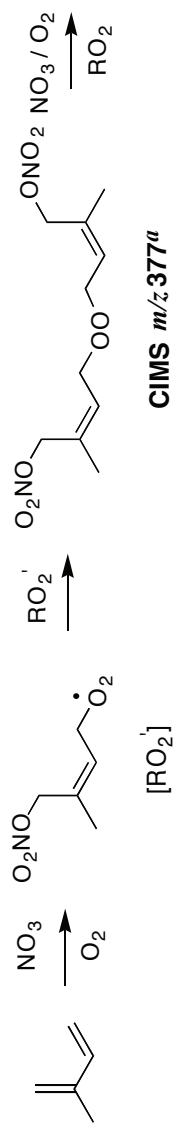


Figure 2.15. Proposed mechanism for SOA formation from the formation and decay of the CIMS m/z 377 gas-phase product formed from the isoprene + NO_3 reaction. Boxes indicate UPLC/(-)ESI-TOFMS detected SOA products; molecular formulas were confirmed by the accurate mass data provided by the UPLC/(-)ESI-TOFMS. Multiple structural isomers are possible, consistent with the multiple chromatographic peaks observed in the extracted ion chromatograms; however, only one structural isomer is shown for simplicity. ^a This first-generation gas-phase product was detected as the $[M + CF_3O]^-$ ion by the CIMS instrument. ^b These particle-phase compounds were detected as both their $[M - H]^-$ and $[M - H + C_2H_4O_2]^-$ ions; the acetic acid adduct ($[M - H + C_2H_4O_2]^-$) ion was, in most cases, the molecular ion (i.e. dominant ion).

Figure 2.16. Proposed mechanism for SOA formation from the formation and decay of the CIMS m/z 393 gas-phase product formed from the isoprene + NO₃ reaction. Boxes indicate UPLC/(-)ESI-TOFMS detected SOA products; molecular formulas were confirmed by the accurate mass data provided by the UPLC/(-)ESI-TOFMS. Multiple structural isomers are possible, consistent with the multiple chromatographic peaks observed in the extracted ion chromatograms; however, only one structural isomer is shown for simplicity. ^a This first-generation gas-phase product was detected as the [M + H]⁺ ion by the CIMS instrument; this gas-phase product was previously observed by Berndt and Bšge (1997) and could also be 2-(1-methylvinyl)oxirane. ^b This gas-phase product was detected as the [M + CF₃O]⁻ ion. ^c These particle-phase compounds were detected as both their [M - H]⁻ and [M - H + C₂H₄O₂]⁻ ions; the acetic acid adduct ([M - H + C₂H₄O₂]⁻) ion was, in most cases, the molecular ion (i.e. dominant ion). ^d This organosulfate compound was detected as its [M - H]⁻ ion and was observed only in the ammonium sulfate and acidified magnesium sulfate seeded experiments.

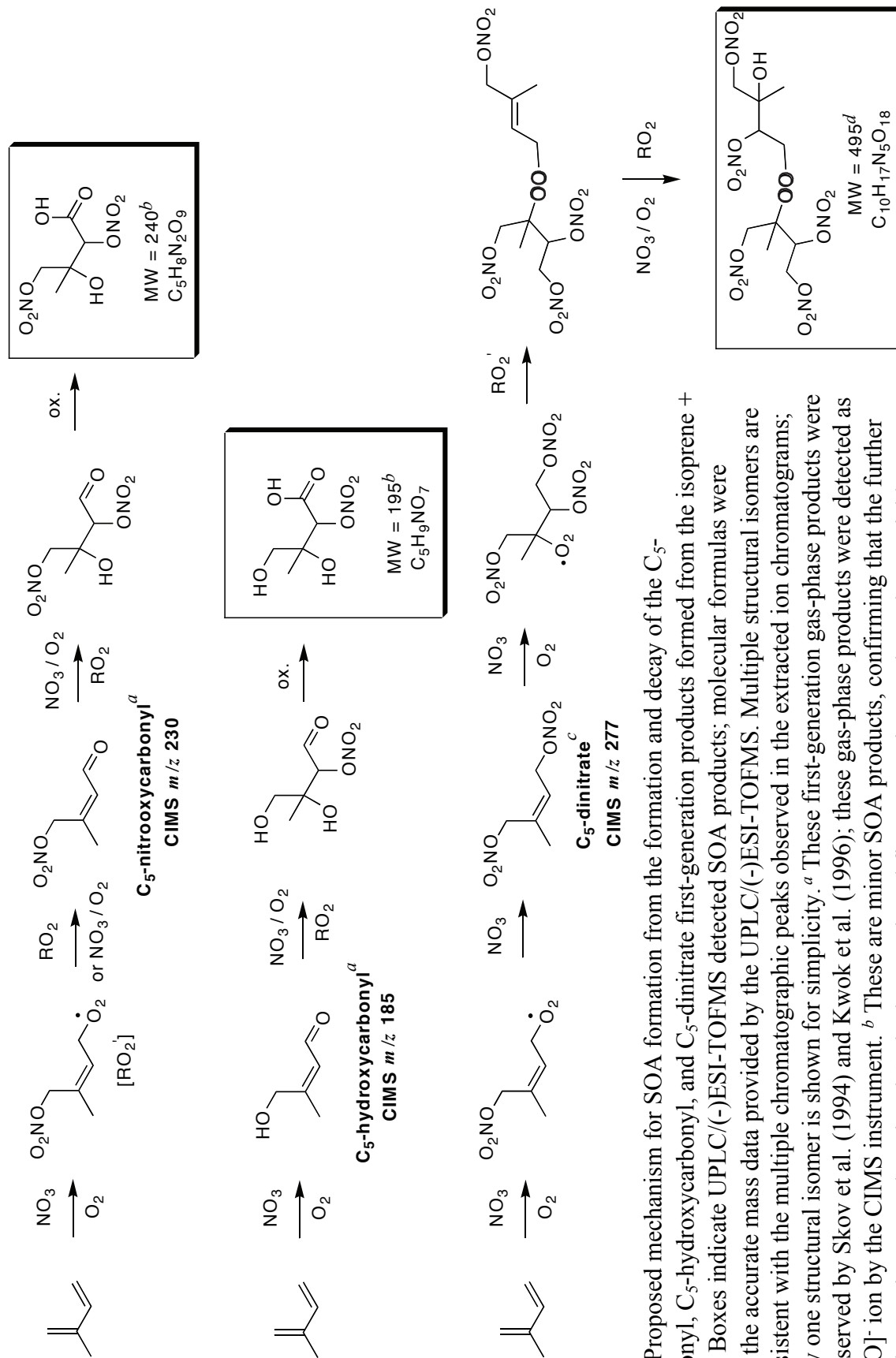


Figure 2.17. Proposed mechanism for SOA formation from the formation and decay of the C₅-nitrooxycarbonyl, C₅-hydroxycarbonyl, and C₅-dinitrate first-generation products formed from the isoprene + NO₃ reaction. Boxes indicate UPLC/(-)ESI-TOFMS detected SOA products; molecular formulas were confirmed by the accurate mass data provided by the UPLC/(-)ESI-TOFMS. Multiple structural isomers are possible, consistent with the multiple chromatographic peaks observed in the extracted ion chromatograms; however, only one structural isomer is shown for simplicity. ^a These first-generation gas-phase products were previously observed by Skov et al. (1994) and Kwok et al. (1996); these gas-phase products were detected as the [M + CF₃O]⁻ ion by the CIMS instrument. ^b These are minor SOA products, confirming that the further oxidation of the C₅-nitrooxycarbonyl and C₅-hydroxycarbonyl first-generation products do not yield significant amounts of SOA. ^c This first-generation gas-phase product was previously observed by Werner et al. (1999); this gas-phase product was also detected as the [M + CF₃O]⁻ ion by the CIMS instrument. ^d This particle-phase compound was detected as both its [M - H]⁻ and [M - H + C₂H₄O₂]⁻ ions; the acetic acid adduct ([M - H + C₂H₄O₂]⁻) ion was the molecular ion (i.e. dominant ion).

Chapter 3

Products of peroxy radical reactions from the NO₃-initiated oxidation of isoprene²

² Adapted from Kwan, A. J., Chan, A. W. H., Ng, N. L., Kjaergaard, H.G., Seinfeld, J. H., and Wennberg, P. O.: Products of peroxy radical reactions from the NO₃-initiated oxidation of isoprene, in preparation.

Abstract

Peroxy radical reactions ($\text{RO}_2\text{-RO}_2$) in the NO_3 -initiated oxidation of isoprene are studied with both gas chromatography and a chemical ionization mass spectrometry technique that allows for more specific speciation of products than in previous studies of this system. We find high nitrate yields ($> \sim 80\%$), consistent with other studies. We further see evidence of significant OH formation in this system, which we propose comes from $\text{RO}_2\text{-HO}_2$ reactions with a yield of 44-64%. The branching ratio of the radical propagating, carbonyl and alcohol forming, and dimer forming channels of the $\text{RO}_2\text{-RO}_2$ reaction are found to be 18-38%, 59-75%, and 7-10%, respectively. HO_2 formation in this system is lower than has been previously assumed. Reaction of RO_2 with isoprene is suggested as a possible route to the formation of several isoprene dimer compounds (ROOR). The nitrooxy, allylic, and C_5 peroxy radicals present in this system exhibit different behavior than the limited suite of peroxy radicals that have been studied to date.

3.1 Introduction

The global emissions of isoprene ($440\text{-}660 \text{ Tg yr}^{-1}$ (Guenther et al., 2006)) are larger than those of any other non-methane hydrocarbon. Because of its high abundance and reactivity towards atmospheric radicals, isoprene plays a major role in the oxidative chemistry of the troposphere (e.g., Chameides et al., 1988; Williams et al., 1997; Roberts et al., 1998; Horowitz et al., 1998; Paulot et al., 2009a) and is an important precursor for secondary organic aerosol (SOA) (e.g., Claeys et al., 2004; Kroll et al., 2005, 2006; Surratt et al., 2006, 2010; Carlton et al., 2009).

Nitrate radicals (NO_3), which form primarily from the reaction of NO_2 and O_3 , are likely the dominant oxidant of isoprene at night when photochemical production of hydroxyl radicals (OH) ceases. Although nighttime isoprene emissions are negligible (Sharkey et al., 1996; Harley et al., 2004), isoprene emitted late in the day, as OH concentrations drop, remains in the nighttime atmosphere (e.g., Starn et al., 1998; Stroud et al., 2002; Warneke et al., 2004; Steinbacher et al., 2005; Brown et al., 2009). The rate constant for the isoprene reaction with NO_3 is $\sim 50,000$ times higher than that with O_3 , the other major nighttime oxidant (Atkinson, 1997). Assuming an NO_3 mixing ratio of 10 ppt and an O_3 mixing ratio of 40 ppb, oxidation of isoprene by NO_3 will proceed more than an order of magnitude faster than by O_3 . Mixing ratios of NO_3 in the nighttime continental boundary layer generally exceed 10 ppt, being in the range of 10-100 ppt (Platt and Janssen, 1995; Smith et al., 1995; Heintz et al., 1996; Carslaw et al., 1997), though concentrations on the order of several hundred ppt have been reported (Platt et al., 1981; von Friedeburg et al., 2002; Brown et al., 2006; Penkett et al., 2007).

During the day, NO_3 is efficiently destroyed by photolysis and reaction with NO (Wayne et al., 1991), but significant daytime concentrations have been measured under conditions of sufficient O_x ($\text{O}_x = \text{O}_3 + \text{NO}_2$) and low actinic flux. NO_3 has been shown to reach concentrations of ~ 1 pptv and be responsible for $\sim 10\%$ of total isoprene oxidation in the daytime under clouds or in a forest canopy (Brown et al., 2005; Forkel et al., 2006; Fuentes et al., 2007). In Houston, with large concentrations of both NO_x and O_3 , NO_3 concentrations between 5-30 pptv in the hours before sunset have been measured (Geyer et al., 2003a).

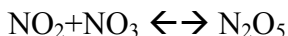
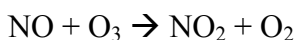
The reaction of isoprene and NO_3 can be significant to atmospheric carbon and nitrogen budgets – and subsequently ozone formation – particularly on a regional scale. Globally, it is estimated the isoprene- NO_3 reaction is responsible for ~ 6-7% of total isoprene oxidation (Horowitz et al., 2007; Ng et al., 2008) and ~ 15% of oxidized nitrogen consumption (Brown et al., 2009). Field studies in the northeastern United States, which has a mix of NO_x and isoprene sources, find that ~ 22% of isoprene oxidation in the residual daytime boundary layer, ~ 40% of isoprene oxidation in airmasses advected offshore within the marine boundary layer, and ~ 73% of NO_3 consumption can be attributed to this reaction (Warneke et al., 2004; Brown et al., 2009). In addition, the isoprene- NO_3 reaction is likely an important source of isoprene nitrates, which are significant NO_x -reservoir compounds affecting regional ozone formation (von Kuhlmann et al., 2004; Fiore et al., 2005; Horowitz et al., 1998, 2007).

The oxidation mechanism and products of the isoprene- NO_3 reaction have been the subject of numerous studies (Jay and Stieglitz, 1989; Barnes et al., 1990; Skov et al., 1992; Kwok et al., 1996; Berndt and Boge, 1997; Suh et al., 2001; Zhang et al., 2002; Fan et al., 2004; Ng et al., 2008, Perring et al., 2009; Rollins et al., 2009). The initial step in the reaction is addition to one of the double bonds, followed by addition of O_2 to make a nitrooxyalkyl peroxy radical (RO_2). The RO_2 radicals then react with NO_2 (to make short-lived peroxyxynitrate compounds), NO_3 , HO_2 , NO_2 , or another RO_2 , leading to a variety of 1st generation products (Figure 3.1). We neglect RO_2 reactions with NO , as NO concentrations are generally very low at night (and low in the chamber due to the rapid reaction $\text{NO}_3 + \text{NO} \rightarrow 2\text{NO}_2$).

In a previous study (Ng et al., 2008), we show that the SOA yield from the reaction of isoprene with NO_3 radicals is higher when experimental conditions favor RO_2 - RO_2 reactions over RO_2 - NO_3 reactions. This phenomenon is explained in part by the formation of low vapor pressure ROOR dimers from RO_2 - RO_2 reactions, a product channel that had previously been considered insignificant. In light of the potential importance of RO_2 - RO_2 reactions, we present here a detailed product study of the RO_2 - RO_2 reactions from the NO_3 -initiated oxidation of isoprene.

3.2 Experimental

This work presents a detailed product study of the “excess isoprene” experiment discussed in Ng et al. (2008). The thermal decomposition of N_2O_5 serves as the source of NO_3 radicals. N_2O_5 is synthesized by mixing streams of nitric oxide ($\geq 99.5\%$, Matheson Tri Gas) and ozone in a glass bulb, which forms N_2O_5 via the following reactions (Davidson et al., 1978):



Ozone is generated by flowing oxygen through an ozonizer (OREC V10-0); its mixing ratio is found to be $\sim 2\%$ as measured by a UV/VIS spectrometer (Hewlett-Packard 8453). The flow rate of nitric oxide into the glass bulb is adjusted until the brown color in the bulb disappears. The N_2O_5 is trapped for 2 hours in an acetone-dry ice bath at

approximately -80°C , cold enough to trap N_2O_5 but not O_3 , as condensed O_3 can explode upon warming. After synthesis, the bulb containing the N_2O_5 , a white solid, is stored in a liquid nitrogen dewar.

Experiments are performed in the Caltech dual 28 m^3 Teflon chambers (Cocker et al., 2001; Keywood et al., 2004). O_3 (Horiba, APOA 360), NO and NO_2 (Horiba, APNA 360), and temperature and relative humidity (RH) (Vaisala, HMP 233) are continuously monitored. The chambers are maintained in the dark at room temperature ($\sim 20\text{-}21^{\circ}\text{C}$) under dry conditions ($\text{RH} < 10\%$). Prior to an experiment, the chambers are continuously flushed for at least 24 hours. The N_2O_5 is removed from the liquid nitrogen and vaporizes into an evacuated 500 ml glass bulb, the pressure in which is continuously monitored by a capacitance manometer (MKS). Once a sufficient pressure of N_2O_5 has been achieved in the bulb, the bulb's contents are flushed into the chamber with a 5 L min^{-1} air stream. After waiting ~ 1 hour to allow the N_2O_5 to become well-mixed in the chamber, a known volume of isoprene (Aldrich, 99%) is injected into a glass bulb and flushed into the chamber with a 5 L min^{-1} air stream, which initiates the reaction.

The amount of isoprene added corresponds to a mixing ratio in the chamber of ~ 800 ppb, while the N_2O_5 concentration is ~ 150 ppb. The large excess of hydrocarbon with respect to N_2O_5 maximizes peroxy radical self- and cross- reactions and minimizes NO_3 reactions with both peroxy radicals and stable first generation products (i.e., species other than isoprene). This excess is magnified by adding the hydrocarbon after the N_2O_5 is well-mixed in the chamber: within the injected plume, hydrocarbon concentrations will be much greater than 800 ppb.

An Agilent 6890N gas chromatograph with flame ionization detector (GC-FID) measures isoprene and the oxidation products methyl vinyl ketone, methacrolein, and 3-methylfuran. The GC-FID, equipped with a bonded polystyrene-divinylbenzene based column (HP-Plot Q, 15 m x .53 mm, 40 μm thickness, J&W Scientific), is held at 60°C for 0.5 minutes, then ramped at 35°C min^{-1} to 200°C, after which the temperature is held steady for 3.5 min.

The other gas-phase products reported here are monitored with a custom-modified Varian 1200 chemical ionization mass spectrometer (CIMS) (Ng et al., 2007; Paulot et al., 2009b), which selectively clusters CF_3O^- with compounds having a high fluoride affinity (e.g., acids, peroxides, and multifunctional nitrooxy- and hydroxy- compounds), forming ions detected at m/z $\text{MW} + 85$ (Crouse et al., 2006). The quadrupole mass filter scans from m/z 50 to m/z 425, with a dwell time of 0.5 s per mass. The CIMS enables more specific speciation of organic nitrates than other techniques that have been employed to study the isoprene- NO_3 system: Fourier transform infrared (FT-IR) (Barnes et al., 1990; Skov et al., 1992; Berndt and Böge, 1997), thermal dissociation-laser induced fluorescence (TD-LIF) (Perring et al., 2009; Rollins et al., 2009), and proton transfer reaction mass spectrometry (PTR-MS) (Kwok et al., 1996; Perring et al., 2009; Rollins et al., 2009). FT-IR and TD-LIF measure the amount of a certain functionality (e.g., nitrates), but in complex mixtures it is difficult to distinguish compounds sharing a common functional group (e.g., nitrooxycarbonyls and hydroxynitrates). The PTR-MS allows for identification of individual compounds, but does so with significant fragmentation and water clustering, which leads to complex mass spectra and an increased probability of mass analog confusion. In contrast, the CIMS does not lead to

significant fragmentation or water clustering under these experimental conditions, which simplifies interpretation of mass spectra.

Because authentic standards for the major products are unavailable, we estimate the sensitivity of the CIMS to these products using the empirical method described by Su and Chesnavich (1982) and Garden et al. (2009). This method estimates the collision rate of CF_3O^- and an analyte based on the analyte's dipole moment and polarizability, which are calculated with the Spartan06 quantum package based on molecular structures optimized with the B3LYP/6-31G(d) method. While this theoretical approach compares favorably with experimentally derived sensitivities for many compounds (Garden et al., 2009; Paulot et al., 2009ab), it represents the largest source of uncertainty ($\pm 25\%$) for the CIMS data.

3.3 Results and Discussion

Because the isoprene- NO_3 reaction is rapid, the low time resolution of our measurements (one measurement every ~ 12 minutes for the GC-FID and ~ 8 minutes for the CIMS) allows us to determine only the final product distribution (Table 3.1). The yields in Table 3.1 vary from those reported in Ng et al. (2008) due to refinements in the estimated CIMS sensitivity, but these changes do not significantly alter the conclusions drawn in our earlier work. Due to the computational intensity of estimating the dipole and polarizability of large molecules, we have assumed that the CIMS has the same sensitivity to all of the C_9 and C_{10} compounds.

The only species for which we see time dependent signals are the ROOR dimer compounds (CIMS m/z 332, 377, and 393), which reach peak signals 1-3 h after the

reaction is initiated, followed by a slow decay. This slow rise and decay is likely a result of the fact that these compounds have low vapor pressures and thus interact significantly with instrument tubing or condense into secondary organic aerosol ($\sim 10 \mu\text{g}/\text{m}^3$ of SOA forms rapidly in this experiment). For these compounds, the reported values are the peak mixing ratios seen during the experiment.

3.3.1 Nitrate yield

C_5 nitrooxycarbonyls, hydroxynitrates, and nitrooxyhydroperoxides, the major products of the isoprene- NO_3 reaction, are detected by the CIMS at m/z 230, 232, and 248, respectively. In addition, we see compounds appearing at m/z 216, 246, and 264, which are consistent with products resulting from the isomerization of the alkoxy (RO) radical originating from the δ -nitrooxyperoxy radical from (1,4) or (4,1) addition (the notation (x,y) indicates NO_3 addition to the x carbon and subsequent N_2O_5 addition to the y carbon) (Figure 3.2). Previous studies have shown that (1,4) additions are dominant in this system (Skov et al., 1992; Berndt and Böge, 1997; Suh et al., 2001). Isomerization also leads to a product at m/z 248, the same mass as the nitrooxyhydroperoxide. To estimate the ratio of these two isobaric species, we assume that the alkoxy radical yield from RO_2 - RO_2 reactions is identical for both the non-isomerized and isomerized nitrooxyperoxy radical (the branching ratio of RO_2 - RO_2 is discussed further in section 3.3.4). Finally, we see dimer ROOR products at m/z 332, 377, and 393 (further discussed in section 3.3.6). Summing the concentrations of these nitrates (and noting that the ROOR compounds at m/z 377 and 393 sequester two nitrates), we find a total organic nitrate concentration of ~ 100 ppb.

We express the nitrate yield with respect to both reacted nitrogen or carbon. For the nitrogen-based yield, we divide the nitrate concentration by the amount of NO_3 radical consumed, which is equivalent to the loss of N_2O_5 during this reaction. Lacking a quantitative measurement of N_2O_5 , we use the change in NO_2 concentration after the addition of isoprene (~ 125 ppb) as a proxy. Each conversion of N_2O_5 to NO_3 releases NO_2 , but the total change in NO_2 may be an overestimate of total NO_3 reacted because NO_2 can also be released in the formation of methyl vinyl ketone (MVK), methacrolein (MACR), 3-methylfuran (3-MF), and the C_5 hydroxycarbonyl (Figure 3.3), though in section 3.3.2 we discuss alternative formation pathways for these compounds. Subtracting these additional NO_2 sources to get a lower limit for NO_3 consumption leads to an NO_3 consumption range of 109–125 ppb and a corresponding nitrate yield of ~ 80 –90%.

This high yield suggests that the NO_3 radical reacts with isoprene predominantly, if not exclusively, via addition to a double bond. The CIMS does not see a detectable rise in HNO_3 , indicating that hydrogen abstraction is not a significant pathway for this reaction (our sensitivity to HNO_3 , however, is hampered by a large background – probably from impurities in the N_2O_5 or reaction of N_2O_5 with trace water). Assuming most of the 16.1 ppb of MVK, MACR, 3-MF, and the C_5 hydroxycarbonyl originates from nitrooxyperoxy radicals, we account for $\sim 100\%$ of the NO_3 reacted. Additionally, although our experimental design seeks to minimize reactions of NO_3 with species other than isoprene, our yield estimate should be considered a lower limit because there are also possible (likely small) losses of NO_3 from reaction with other radicals or first-generation products, or heterogeneously to the chamber walls or SOA.

The measured nitrate yield with respect to NO_3 is consistent with the substantial yields determined by other studies: $\sim 95\%$ (under NO-free conditions) (Berndt and Böge, 1997), $57 \pm 11\%$ (Perring et al., 2009), and $70 \pm 8\%$ (Rollins et al., 2009). Variance in yields with different experimental methods is not surprising because they depend on the relative concentrations of different radicals, as well as physical loss and mixing processes, which are unique to each work. Furthermore, the final product distribution is a strong function of the distribution of peroxy radical isomers: δ -nitrooxyperoxy radicals tend to maintain their nitrate functionality (with the exception of the possible formation of hydroxycarbonyl or 3-MF), while β -nitrooxyperoxy radicals, if they become nitrooxyalkoxy radicals, are likely to lose the nitrate to form MVK or MACR (Vereecken and Peeters, 2009). Berndt and Böge (1997) and Peeters et al. (2009) suggest that peroxy radical isomers formed from isoprene oxidation are continuously interconverting, so the distribution of isomers that defines the final product distribution may also be sensitive to specific experimental conditions.

To calculate the nitrate yield with respect to carbon, we divide the concentration of nitrates by the amount of isoprene reacted. Because a portion of the isoprene reacts immediately upon introduction into the chamber, the exact starting isoprene concentration is uncertain. Therefore, we assume that each of the products listed in Table 3.1 comes from one isoprene molecule, with the exception of the ROOR compounds (which comprise two isoprene molecules) and hydrogen peroxide (which comprises zero). This leads to an estimate of ~ 128 ppb of isoprene reacted, and a nitrate yield of $\sim 80\%$. As with the nitrogen-based yield, this result too is consistent with other studies: \sim

80% (Barnes et al., 1990), ~ 90% (Berndt and Böge, 1997), $70 \pm 8\%$ (Rollins et al., 2009), and $65 \pm 12\%$ (Perring et al., 2009).

That our CIMS-derived estimate of isoprene consumption is higher than our independent estimate of NO_3 consumption (by up to 20% depending on the sources of NO_2) suggests that our reported nitrate yields may be overestimated slightly, and should therefore be considered upper limits. The discrepancy between our estimates of isoprene and NO_3 consumption is likely attributable to the lack of an empirical calibration for the CIMS.

3.3.2 Hydroxyl radical (OH) formation

The CIMS detects the formation of products at m/z 185, 187, 203, and 201, which are indicative of compounds at MW 100, 102, 118, and 116, respectively. These compounds are analogous to those depicted in Figures 3.1 and 3.2, only with oxidation initiated by the hydroxyl radical (OH) instead of NO_3 (Surratt et al., 2010). Perring et al. (2009) report PTR-MS signals at m/z 101, 103, 119, and 117, which could be the protonated clusters of these compounds, though they attribute the latter three m/z to water clusters of other major product ions. Under the dry conditions of our experiment, however, we do not typically observe water clusters with, or significant fragmentation of, the product ions, so we are confident that the signals on the CIMS in fact represent hydroxy compounds. OH formation may also contribute to some or all of the MVK and MACR produced in our system, though it is likely most of the 3-MF comes from isoprene- NO_3 reactions because its yield in the isoprene-OH system is low (Ruppert and Becker, 2000; Paulot et al., 2009b).

We consider the following five possible routes to OH formation in our system: reactions of (i) O₃ and isoprene (Neeb and Moortgat, 1999), (ii) HO₂ and O₃ (Sinha et al., 1987), (iii) HO₂ and NO (Seeley et al., 1996), (iv) HO₂ and NO₃ (Mellouki et al., 1993), and (v) RO₂ and HO₂ (Hasson et al., 2004, 2005; Jenkin et al., 2007, 2008, 2010; Crowley and Dillon, 2008). Hypotheses (i) and (ii) are unlikely to occur. Not only is no O₃ detected during the experiment (limit of detection ~ 2 ppb), but there is no evidence in the CIMS data of significant organic acid or peroxide formation, which would result from the reaction of O₃ with isoprene (Hasson et al., 2001; Orzechowska and Paulson, 2005). Furthermore, for hypothesis (ii) to be feasible, HO₂-O₃ reactions ($k = 1.9 \times 10^{-15} \text{ cm}^3 \text{ molec}^{-1} \text{ s}^{-1}$, Sander et al., 2006) must be significantly faster than HO₂-HO₂ reactions ($k = 2.48 \times 10^{-12} \text{ cm}^3 \text{ molec}^{-1} \text{ s}^{-1}$ at 1 atm and 298K, Sander et al., 2006), which produce ppb levels of H₂O₂ in the system (Table 3.1). This would require O₃ to be more than three orders of magnitude more abundant than HO₂, i.e., at ppm levels, that cannot come from trace contamination of the chamber.

To examine the remaining hypotheses, we create a box model incorporating the major reactions in the system for developing a qualitative understanding of which processes may be important for the final product yield. Table 3.2 lists the parameters of this box model; for rate constants that have not been experimentally determined, we use estimates based on the literature, but caution that the actual rate constants may differ significantly. Initial conditions reflect the nominal concentration of reagents in the chamber: [isoprene] = 800 ppb, [N₂O₅] = 125 ppb, and [NO₂] = 50 ppb (the NO₂ likely results from decomposition of N₂O₅ prior to isoprene injection). In reality, though, the isoprene concentration is higher than 800 ppb during the reaction because of our injection

method. As discussed later, there are major uncertainties in the HO₂ sources and magnitudes, so for the purposes of assessing possible OH sources, we assume as an upper limit that the formation rate of HO₂ is the same as that of RO₂; the final concentration of peroxides (i.e., [ROOH] + 2 x [H₂O₂]) is ~ 23 ppb, much less than the ~ 109-128 ppb of RO₂ that is formed (section 3.3.1), suggesting that the formation of HO₂ is significantly less than that of RO₂.

The box model shows that the NO levels in the chamber are too low to sustain substantial OH formation via hypothesis (iii). The NO_x monitor measures < 1 ppb of NO throughout our experiment, and any NO that may exist prior to the experiment (or as a trace impurity in the N₂O₅) reacts quickly with NO₃ after N₂O₅ injection; the NO lifetime is ~ 1 s with the N₂O₅ loading. Although NO may be generated as a minor channel of the NO₂ + NO₃ reaction, the rapid reaction of NO and NO₃ limits the steady state concentration of NO to < ~ 4 ppt, so HO₂ + NO is unlikely to contribute to significantly to the 12-21 ppb of OH that is formed in the system. In the simulation, NO at its maximum concentration cannot compete with other radicals (RO₂, HO₂, NO₃, and NO₂) reacting with HO₂.

The box model also suggests that hypothesis (iv) is not feasible because of the substantial difference in the rates of the NO₃-isoprene and NO₃-HO₂ reactions, both of which are well established experimentally. Under the base conditions of the box model in Table 3.2, which significantly overestimates the prevalence of HO₂ and underestimates the concentration of isoprene, less than 1% of the NO₃ reacts with HO₂, while 94% reacts with isoprene and the rest with RO₂. Therefore, while there is significant uncertainty with the RO₂-HO₂, RO₂-RO₂, and RO₂-NO₃ rate constants, the frequency of the NO₃-

HO₂ reaction predicted by the model is quite insensitive to these rates. Even if we favor NO₃-HO₂ reactions by reducing the RO₂-HO₂ and RO₂-NO₃ rate constants by a factor of 100, we obtain ~ 5 ppb of OH formation; in contrast, lowering the isoprene-NO₃ rate constant leads to significantly more production of OH via NO₃-HO₂ (Figure 3.4). These simulations reflect the observations of Atkinson et al. (1988) during hydrocarbon-NO₃ kinetics studies that there is apparent OH formation when slower reacting hydrocarbons are studied. The reaction of isoprene with NO₃ is sufficiently fast under our experimental conditions, however, that such behavior should not occur.

We therefore conclude that formation of OH radicals most likely results from the reaction of RO₂ and HO₂ radicals. Quantifying the branching ratio of the RO₂-HO₂ reaction, however, is not trivial. There are four documented pathways for the RO₂-HO₂ reaction:



Channel (3.1a) can be quantified with CIMS measurements of peroxides. We neglect channel (3.1b), first because there is no evidence for ozone formation, and also because this channel is believed to proceed via a hydroperoxide intermediate that yields O₃ only if RO₂ is an acylperoxy radical (RC(O)OO) (Hasson et al., 2005). To quantify channel (3.1c), we can use the sum of OH products as a tracer, but MVK, MACR, and the C₅

hydroxycarbonyl can come from either OH or NO₃, which leads to uncertainty in this quantity. Similarly, the nitrooxycarbonyl can result directly from reaction (3.1d), indirectly from the RO formed in reaction (3.1c), or RO₂-RO₂. Because multiple pathways share common products, and lacking more knowledge about these individual pathways, we cannot unambiguously constrain the RO₂-HO₂ branching ratios with the available data.

Recognizing the uncertainties, we estimate the OH yield from RO₂-HO₂ but emphasize that our assumptions and results must be verified by further studies. We assume channel (3.1d) is negligible, as well as OH from RO₂-HO₂ reactions where the RO₂ originates from isoprene + OH (Paulot et al., 2009a), and ignore any RO₂-HO₂ reactions from the isomerized nitrooxy RO₂. We constrain the range of OH formation (channel 3.1c) to 9-20.5 ppb, with the upper limit being all the hydroxy products plus MVK and MACR, and the lower limit being the upper limit minus MVK, MACR, and the hydroxycarbonyl. We estimate channel (3.1a) by the concentration of the nitrooxyhydroperoxide at m/z 248, so obtain a range for (3.1c)/[(3.1a)+(3.1c)] of between 9/20.5 and 20.5/32.1, or 44-64%.

This high yield contrasts with the existing, albeit limited, literature on RO₂-HO₂ reaction channels. Thus far, significant OH yields (15-67%) have been found only for acylperoxy, methoxymethylperoxy (CH₃OCH₂O₂), and β-carbonylperoxy (RC(O)CH₂OO) radicals, while alkylperoxy and hydroxyalkylperoxy radicals have exhibited minimal yields (Hasson et al., 2004; Jenkin et al., 2007, 2008, 2010; Crowley and Dillon, 2008). Perhaps the presence of nitrooxy group or the additional double bond present in the RO₂ radicals in this study make the radical propagating channel more

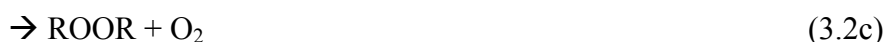
favoured than for the compounds previously studied. We also recognize that some entirely different mechanism unknown to us is responsible for the formation of OH.

3.3.3 RO_2 - RO_2 branching ratio

Using the data and assumptions described above, we derive a master equation for RO_2 - RO_2 reactions. An estimated 55 ppb of RO_2 passes through the channel forming $R'CHO$ and ROH , and 5 ppb becomes $ROOR$ (Table 3.1). The nitrooxycarbonyl yield in excess of the hydroxynitrate yield is assumed to arise from RO -forming channels of either RO_2 - HO_2 or RO_2 - RO_2 . Total RO formation is estimated to be 33.5-45 ppb, as calculated from the sum of the isomerized nitrates, 3-MF, and the excess hydroxynitrate (the upper limit includes MVK, MACR, and hydroxycarbonyl from isoprene- NO_3 reactions). Of this, 9-20.5 ppb comes from RO_2 - HO_2 , depending on the true provenance of MVK, MACR, and the hydroxycarbonyl.

Each pathway to RO (e.g., RO_2 - RO_2 , RO_2 - HO_2 , RO_2 - NO_3) has a different heat of reaction, which may affect the RO fate (Bernt and Böge, 1997; Atkinson, 2007). Lacking any specific knowledge about the dependence of RO fate on the reaction enthalpy, however, we assume that every RO behaves the same, regardless of source. We also neglect possible RO_2 - RO_2 reactions involving the hydroxyperoxy RO_2 .

Taking into account the uncertainties involving RO , we get between 13.5 (i.e., 33.5-20.5) and 36 (i.e., 45-9) ppb of RO coming from RO_2 - RO_2 , and between 73.5 and 96 ppb (i.e., between 55 + 5 + 13.5 and 55 + 5 + 36) of RO_2 undergoing RO_2 - RO_2 reactions. From this, we derive ranges for the RO_2 - RO_2 branching ratio:



where the branching ratios of (3.2a), (3.2b), and (3.2c) are 18-38%, 59-75%, and 7-10%, respectively.

To our knowledge, this is the first study analyzing the branching ratio of RO_2 - RO_2 reactions of isoprene nitrooxyperoxy radicals. For most peroxy radicals that have been studied, channel (3.2a) is typically more than 50%, while channel (3.2c) is generally considered negligible (Atkinson, 1997, and references therein). Ziemann (2002) proposes ROOR formation as the source of diacyl peroxides found in SOA from cycloalkene ozonolysis. Preliminary work in our laboratory has also detected ROOR compounds as products of RO_2 - RO_2 reactions from the NO_3 -initiated oxidation of 1,3-butadiene, as well as the OH-initiated oxidation of 1,3-butadiene and isoprene. There remain many uncertainties regarding the mechanism of RO_2 - RO_2 reactions (Dibble, 2008), so it is difficult to assess whether reported ROOR formation (or lack thereof) is a result of the particular radicals studied or the analytical techniques employed to study their reaction. It is possible that the larger peroxy radicals we have studied are more likely to form ROOR than smaller radicals because they have more vibrational modes with which to distribute collisional energy and prevent breaking apart upon collision with another RO_2 radical. This may be analogous to trends in organic nitrate (RONO_2) yields from RO_2 -NO reactions, which tend to increase with increasing RO_2 size (O'Brien et al., 1998; Arey et al., 2001; Matsunaga and Ziemann, 2009).

3.3.4 RO radical fate and HO₂ production

The fate of the alkoxy radical is important both for understanding the chamber studies and in nighttime chemistry as it leads to the production of HO₂. From the amount of excess hydroxycarbonyl formed, we estimate that 18 ppb of HO₂ forms from O₂ abstraction of RO (33.5-45 ppb; Section 3.3.3), or 40-54% of RO. This assumes that O₂ abstraction from RO is the sole source of excess nitrooxycarbonyl, and that direct formation from RO₂-HO₂ reactions (equation 3.1d) is negligible. This HO₂ estimate is somewhat lower than the total sum of HO₂ derived from peroxide measurements in our system (23 ppb, section 3.3.2). Additional HO₂ comes from O₂ abstraction from minor alkoxy radicals (the isomerized nitrooxyalkoxy and hydroxyalkoxy radicals), but it is not trivial to attempt an HO₂ balance because of the uncertainties in both the CIMS calibration and the sources and sinks of HO₂. HO₂ can result from the conversion of the nitrooxyalkoxy radical to a nitrooxycarbonyl, or MVK and MACR if the latter are from OH + isoprene; sinks of HO₂ include peroxide formation, RO₂-HO₂ derived alkoxy radicals that do not undergo abstraction, and from nitrooxycarbonyls formed directly from RO₂-HO₂ via channel (3.4c).

Because the δ -nitrooxyalkoxy radical, the dominant alkoxy radical in the system, can isomerize via a 1,5-H shift, the large HO₂ yield is somewhat surprising because isomerization reactions are typically faster than abstraction by O₂ (Atkinson, 2007). It is possible that the nitrooxy group limits isomerization when the δ -nitrooxyalkoxy radical is in a Z conformation. According to the structure-activity relationship of Kwok and Atkinson (1995), H-abstraction from a carbon with an attached nitrooxy group is an order

of magnitude slower than from a carbon with an attached methyl group. The nitrooxy group likely does not prevent isomerization – we see the analogous isomerized nitrates in experiments with 1,3-butadiene, for which the isomerization must abstract a hydrogen from the carbon α to the nitrooxy group – but more study is required to elucidate the effect of the NO_3 group on isomerization rate. It is also possible that O_2 abstractions are faster for the alkoxy radicals in this system.

While our HO_2 yield is higher than expected based on the alkoxy radical structure, it is lower than the value of 80% of RO_2 that has been used in modeling studies (Horowitz et al., 2007; Rollins et al., 2009). Therefore, models may overestimate the impact of isoprene- NO_3 reactions on nighttime HO_x chemistry in this respect.

3.3.5 Formation of dimer compounds

In Ng et al. (2008), we report the formation of ROOR dimer compounds at m/z 377 and 393. Further examination of the CIMS data reveals other isoprene dimer compounds. The most abundant of these, with a signal similar in magnitude to that of m/z 393, appears at m/z 332, which indicates a hydroxynitrate ROOR. One possible source for this compound is an RO_2 - RO_2 reaction where one RO_2 comes from NO_3 and the other from OH. The abundance of OH is much less than that of NO_3 , however, so it would be surprising if such a reaction would produce almost as much ROOR as the reaction between nitrooxyperoxy radicals. Alternatively, this compound may result from addition of an RO_2 radical to isoprene, creating a C_{10} alkyl (and subsequently alkyl peroxy) radical, which undergoes an RO_2 - RO_2 reaction to create the C_{10} hydroxynitrate ROOR (Figure 3.5). This mechanism for creating a C_{10} RO_2 radical is analogous to the

formation of bicyclic radicals by aromatic peroxy radicals (Atkinson and Arey, 2007). Small amounts of the corresponding nitrooxycarbonyl and nitrooxyhydroperoxide at m/z 330 and 348, respectively, are seen, as well as a compound at m/z 316 that can be a C_9 compound that results from isomerization of a C_{10} nitrooxyalkoxy radical; isomerization may also lead to a diol at m/z 348, the same mass as the hydroperoxide.

We do not know of any previous work that has examined RO_2 addition to alkenes under atmospheric conditions, though it has been reported in both gas-phase combustion (e.g., Osborn and Waddington, 1980; Stark and Waddington, 1995) and liquid-phase studies (e.g., van Sickle et al., 1965ab; Mayo, 1968; Simmons and van Sickle, 1973), producing both epoxides and polymeric peroxy radicals.

3.4 Implications

The observed high nitrate yields, in general agreement with previous results, support the modeling results of Horowitz et al. (2007) that isoprene- NO_3 reactions, while a minor sink of isoprene, are a substantial source of isoprene nitrates in the atmosphere. The formation and fate of these nitrates, in turn, significantly influences tropospheric NO_x and ozone.

Although we obtain similar nitrate yields relative to both reacted nitrogen and carbon, these two yields are fundamentally different quantities that coincidentally have similar magnitudes. Even in an ideal situation in which NO_3 reacts exclusively with isoprene (i.e., no reactions with RO_2 , HO_2 , walls, etc.), the nitrogen based yield (i.e., $[nitrates]/[NO_3 \text{ consumed}]$) is non-unity solely due to loss of the nitrate functionality by the initial isoprene- NO_3 adduct (Figure 3.2); in contrast, the carbon-based yield (i.e.,

[nitrates]/[isoprene reacted] or [nitrates]/[total carbon products]) is non-unity from both nitrate losses by the initial adduct and isoprene reactions with OH. For systems with extensive amounts of competing NO₃ sinks and/or OH formation, the nitrogen- and carbon-based yields may vary considerably. Thus, when applying experimental yields to atmospheric models, care must be taken to choose the appropriate value, as well as to consider the conditions under which those yields are obtained.

The large yield of products from reaction of OH with isoprene is potentially very important for nighttime chemistry, particularly because we propose that the source of OH is from RO₂-HO₂ reactions which likely dominate in the ambient environment. Recent field studies suggest that the radical propagating channels of RO₂-HO₂ reactions must be significant to explain observations (Thornton et al., 2002; Leileveld et al., 2008).

Previous studies of nighttime chemistry have considered only alkene ozonolysis and HO₂-NO, HO₂-O₃, and NO₃-HO₂ reactions as sources of OH (Bey et al., 1997, 2001ab; Harrison et al., 1998; Faloona et al., 2001; Gölz et al., 2001; Geyer et al., 2003b; Ren et al., 2003; Geyer and Stutz, 2004; Vaughan et al., 2006). While a missing OH source may explain instances where models underestimate field measurements of OH (Faloona et al., 2001; Ren et al., 2003), Geyer et al. (2003b) overpredict measurements by a factor of two without such a source. Clearly, there remain many unresolved issues surrounding the abundance of oxidants in the nighttime atmosphere.

While this study focuses on the first-generation products from the isoprene-NO₃ reaction, another nighttime source of OH in the atmosphere would be the further oxidation of the nitrooxyhydroperoxide, which can produce a dinitrooxyepoxide and OH (Paulot et al., 2009a). In another experiment described in detail in Ng et al. (2008), we

first add 179 ppb of isoprene to the chamber followed by three additions of N_2O_5 (~ 120, 50, and 210 ppb). After the first two additions, isoprene is completely consumed, so the third aliquot leads primarily to the formation of second-generation products; some second-generation products may be oxidized by this third addition, but the amount of N_2O_5 added is similar to the concentration of first generation products (which is roughly equal to the starting isoprene concentration), so such tertiary chemistry is likely to be minimal. After this third addition, the nitrooxyhydroperoxide signal drops ~ 8 ppb, while the signal for the dinitrooxyepoxide (at m/z 293) rises ~ 2.5 ppb. This indicates that the epoxide (and OH) yield from the NO_3 oxidation of the nitrooxyhydroperoxide is ~ 30%, compared to ~ 75% for OH oxidation of isoprene hydroxyhydroperoxides (Paulot et al., 2009a), although heterogeneous loss of epoxide to the acidic aerosol is also possible (Surratt et al., 2010). The yield in the NO_3 system is likely lower because the dominant first-generation peroxy radical is from the (1,4) addition of NO_3 . Therefore, to form an epoxide the second NO_3 must add to the 2-carbon, creating a secondary alkyl radical, whereas the more favored addition is likely to the 3-carbon creating a more stable tertiary alkyl radical (Figure 3.6). In the OH system, (1,2) and (4,3) additions in the first oxidation step are most common (Paulot et al., 2009b), which means that the epoxide-forming channel involves a second OH addition to the more favored 4- or 1- carbon, respectively.

As demonstrated by Ng et al. (2008), while ROOR compounds are minor products of RO_2 - RO_2 reactions, they may be important in the atmosphere because they present a means of significantly increasing the mass of a molecule, thereby reducing its volatility and increasing its potential to form SOA. Currently, field measurements of SOA burdens

often exceed those predicted by models (de Gouw et al., 2005; Heald et al., 2005; Johnson et al., 2006; Volkamer et al., 2006; Simpson et al., 2007), a discrepancy that may be explained by SOA formation pathways, such as ROOR, that are not included in models. In this work, we see evidence of an additional ROOR formation pathway, the RO₂ addition to alkenes, that may be relevant to SOA formation. As SOA itself is a minor product of hydrocarbon oxidation (Donahue et al., 2009), pathways that are negligible in the context of gas-phase oxidation mechanisms may in fact be important if they represent efficient pathways to forming SOA.

The formation of ROOR compounds in the atmosphere, and the importance of RO₂-RO₂ reactions in general, is difficult to predict because of the large uncertainties in the rates of all the relevant competing pathways (RO₂-RO₂, RO₂-NO₃, RO₂-NO, RO₂-HO₂, RO₂-alkene) as well as the large variation in ambient mixing ratios of the relevant species. It is clear, though, that RO₂-RO₂ reactions are most favored when the concentration of hydrocarbon is greater than that of oxidant. For the case of isoprene-NO₃ reactions, this most likely would occur in the early evening, as OH concentrations drop and NO₃ concentrations are still low, though during this time NO concentrations may still be high enough to react with a significant amount of RO₂.

Situations favoring nighttime RO₂-RO₂ (or RO₂-alkene) reactions may be more prevalent for monoterpenes and sesquiterpenes, which, unlike isoprene, may be emitted at night (Sakulyanontvittaya et al., 2008). Many of these compounds have exhibited high SOA yields in laboratory studies, though there are still many uncertainties in the SOA formation mechanism (Griffin et al., 1999; Hallquist et al., 1999; Spittler et al., 2006; Fry et al., 2009). Based on our experience with isoprene, the role of monoterpene and

sesquiterpene RO₂-RO₂ reactions in nighttime SOA formation is worthy of further study, particularly because the nitrooxy group is electron withdrawing, and presence of electron withdrawing groups has been shown to significantly increase RO₂-RO₂ reaction rates (Lightfoot et al., 1992). As noted by other investigators (e.g., Brown et al., 2009; Fry et al., 2009), SOA formed from the reaction of biogenic compounds with NO₃ – an anthropogenic oxidant – is consistent with the common finding that while SOA is largely composed of biogenic carbon (Bench et al., 2007; Schichtel et al., 2008), its concentrations are correlated with anthropogenic emissions (de Gouw et al., 2005, 2008; Quinn et al., 2006; Sullivan et al., 2006; Weber et al., 2007).

Most of the RO₂ formed from isoprene-NO₃ reactions are primary radicals, however, whereas a significant amount of the RO₂ derived from monoterpenes are likely to be secondary or tertiary. Primary RO₂ tend to undergo significantly faster RO₂-RO₂ reactions than secondary or tertiary RO₂ (Lightfoot et al., 1992). Reactivity trends are less certain for RO₂-NO, RO₂-NO₃, and RO₂-HO₂ reactions, but the variation in the available data is less pronounced than for RO₂-RO₂ (Lightfoot et al., 1992; Lesclaux, 1997; Wallington et al., 1997; Atkinson et al., 2006; Vaughan et al., 2006). So while monoterpenes and sesquiterpenes are generally more reactive with NO₃ than isoprene (i.e., have higher RO₂ formation rates) (Atkinson and Arey, 2003), RO₂-RO₂ reactions for these compounds may be less competitive than for isoprene under the same conditions because of the significantly lower RO₂-RO₂ rate constants compared to competing reactions.

Although we have gained insights into the isoprene-NO₃ system in this work, chamber studies such as those we report here have limitations. There currently exists no

stable precursor of NO_3 suitable for chamber studies, so chemical transformations occur the instant the NO_3 precursor and hydrocarbon meet; for isoprene, the chemistry occurs on a much faster timescale than the mixing. Because of our experimental conditions, we are able only to do an end product analysis of our experiments, and are unable to perform kinetic modeling, which could provide deeper insights into the system. Furthermore, while we can constrain RO_2 reaction pathways in chamber studies of OH oxidation (i.e., RO_2+NO for high NO_x conditions and RO_2+HO_2 for low NO_x conditions), this is currently not feasible for NO_3 chamber studies. Also, while the CIMS can isolate oxidation products with greater specificity than other techniques, the lack of commercial or easily synthesizable standards leads to uncertainties in product quantification.

Up to now, most studies relating to hydrocarbon oxidation mechanisms and kinetics have focused on ozone or the OH radical; application of the techniques employed in those studies to NO_3 oxidation kinetics and mechanisms offers promise to significantly advance our understanding of nighttime atmospheric chemistry, but will require overcoming challenges such as reagent synthesis (including isomeric specificity), finding suitable radical precursors, and limiting secondary and competing reactions. Many of our results (e.g., OH yield from $\text{RO}_2\text{-HO}_2$, RO yield from $\text{RO}_2\text{-RO}_2$, HO_2 formation from RO, ROOR formation, $\text{RO}_2\text{-HO}_2$ reaction rates) differ from those suggested by previous work on different – mostly small alkylperoxy, acylperoxy, or hydroxyalkylperoxy – systems. More studies focused on nitroxy and allylic peroxy radicals, as well as larger peroxy radicals, are warranted.

Acknowledgments

This research was funded by the U.S. Department of Energy Biological and Environmental Research Program DE-FG02-05ER63983 and by the U.S. Environmental Protection Agency STAR agreement RD-833749. Also, this material is based upon work supported by the National Science Foundation (NSF) under grant ATM-0432377 and an NSF Graduate Research Fellowship (AJK). The authors would like to thank C. D. Vecitis, J. Cheng, M. R. Hoffmann, K. Takematsu, and M. Okumura for experimental assistance, and J. D. Crouse, N. H. Donahue, N. C. Eddingsaas, F. Paulot, and H. O. T. Pye for helpful discussions.

References

Arey, J., Aschmann, S. M., Kwok, E. S. C., and Atkinson, R.: Alkyl nitrate, hydroxyalkyl nitrate, and hydroxycarbonyl formation from the NO_x-air photooxidations of C-5-C-8 n-alkanes, *Journal of Physical Chemistry A*, 105, 1020-1027, 2001.

Atkinson, R., Aschmann, S. M., and Pitts, J. N.: Rate constants for the gas-phase reactions of the NO₃ radical with a series of organic compounds at 296 +/- 2K, *Journal of Physical Chemistry*, 92, 3454-3457, 1988.

Atkinson, R.: Gas-phase tropospheric chemistry of volatile organic compounds .1. Alkanes and alkenes, *Journal of Physical and Chemical Reference Data*, 26, 215-290, 1997.

Atkinson, R., Baulch, D. L., Cox, R. A., Crowley, J. N., Hampson, R. F., Hynes, R. G., Jenkin, M. E., Rossi, M. J., and Troe, J.: Evaluated kinetic and photochemical data for

atmospheric chemistry: Volume II - gas phase reactions of organic species, *Atmospheric Chemistry and Physics*, 6, 3625-4055, 2006.

Atkinson, R.: Rate constants for the atmospheric reactions of alkoxy radicals: An updated estimation method, *Atmospheric Environment*, 41, 8468-8485, 10.1016/j.atmosenv.2007.07.002, 2007.

Atkinson, R., and Arey, J.: Mechanisms of the gas-phase reactions of aromatic hydrocarbons and PAHs with OH and NO₃ radicals, *Polycyclic Aromatic Compounds*, 27, 15-40, 10.1080/10406630601134243, 2007.

Barnes, I., Bastian, V., Becker, K. H., and Tong, Z.: Kinetics and products of the reactions of NO₃ with monoalkenes, dialkenes, and monoterpenes, *Journal of Physical Chemistry*, 94, 2413-2419, 1990.

Bench, G., Fallon, S., Schichtel, B., Malm, W., and McDade, C.: Relative contributions of fossil and contemporary carbon sources to PM 2.5 aerosols at nine Interagency Monitoring for Protection of Visual Environments (IMPROVE) network sites, *Journal of Geophysical Research-Atmospheres*, 112, D10205, 10.1029/2006jd007708, 2007.

Berndt, T., and Boge, O.: Gas-phase reaction of NO₃ radicals with isoprene: A kinetic and mechanistic study, *International Journal of Chemical Kinetics*, 29, 755-765, 1997.

Bey, I., Aumont, B., and Toupance, G.: The nighttime production of OH radicals in the continental troposphere, *Geophysical Research Letters*, 24, 1067-1070, 1997.

Bey, I., Aumont, B., and Toupance, G.: A modeling study of the nighttime radical chemistry in the lower continental troposphere 2. Origin and evolution of HOx, *Journal of Geophysical Research-Atmospheres*, 106, 9991-10001, 2001.

Biggs, P., Canosamas, C. E., Fracheboud, J. M., Shallcross, D. E., and Wayne, R. P.: Investigation into the kinetics and mechanism of the reaction of NO₃ with CH₃O₂ at 298 K and 2.5 Torr - a potential source of OH in the nighttime troposphere, *Journal of the Chemical Society-Faraday Transactions*, 90, 1205-1210, 1994.

Brown, S. S., Osthoff, H. D., Stark, H., Dube, W. P., Ryerson, T. B., Warneke, C., de Gouw, J. A., Wollny, A. G., Parrish, D. D., Fehsenfeld, F. C., and Ravishankara, A. R.: Aircraft observations of daytime NO₃ and N₂O₅ and their implications for tropospheric chemistry, *Journal of Photochemistry and Photobiology A-Chemistry*, 176, 270-278, 10.1016/j.jphotochem.2005.10.004, 2005.

Brown, S. S., Ryerson, T. B., Wollny, A. G., Brock, C. A., Peltier, R., Sullivan, A. P., Weber, R. J., Dube, W. P., Trainer, M., Meagher, J. F., Fehsenfeld, F. C., and Ravishankara, A. R.: Variability in nocturnal nitrogen oxide processing and its role in regional air quality, *Science*, 311, 67-70, 10.1126/science.1120120, 2006.

Brown, S. S., Degouw, J. A., Warneke, C., Ryerson, T. B., Dube, W. P., Atlas, E., Weber, R. J., Peltier, R. E., Neuman, J. A., Roberts, J. M., Swanson, A., Flocke, F., McKeen, S. A., Brioude, J., Sommariva, R., Trainer, M., Fehsenfeld, F. C., and Ravishankara, A. R.: Nocturnal isoprene oxidation over the Northeast United States in summer and its impact on reactive nitrogen partitioning and secondary organic aerosol, *Atmospheric Chemistry and Physics*, 9, 3027-3042, 2009.

Canosa-Mas, C. E., King, M. D., Lopez, R., Percival, C. J., Wayne, R. P., Shallcross, D. E., Pyle, J. A., and Daele, V.: Is the reaction between $\text{CH}_3\text{C}(\text{O})\text{O}_2$ and NO_3 important in the night-time troposphere?, *Journal of the Chemical Society-Faraday Transactions*, 92, 2211-2222, 1996.

Carlton, A. G., Wiedinmyer, C., and Kroll, J. H.: A review of Secondary Organic Aerosol (SOA) formation from isoprene, *Atmospheric Chemistry and Physics*, 9, 4987-5005, 2009.

Carslaw, N., Carpenter, L. J., Plane, J. M. C., Allan, B. J., Burgess, R. A., Clemitshaw, K. C., Coe, H., and Penkett, S. A.: Simultaneous observations of nitrate and peroxy radicals in the marine boundary layer, *Journal of Geophysical Research-Atmospheres*, 102, 18917-18933, 1997.

Chameides, W. L., Lindsay, R. W., Richardson, J., and Kiang, C. S.: The role of biogenic hydrocarbons in urban photochemical smog - Atlanta as a case study, *Science*, 241, 1473-1475, 1988.

Claeys, M., Graham, B., Vas, G., Wang, W., Vermeylen, R., Pashynska, V., Cafmeyer, J., Guyon, P., Andreae, M. O., Artaxo, P., and Maenhaut, W.: Formation of secondary organic aerosols through photooxidation of isoprene, *Science*, 303, 1173-1176, 2004.

Cocker, D. R., Flagan, R. C., and Seinfeld, J. H.: State-of-the-art chamber facility for studying atmospheric aerosol chemistry, *Environmental Science & Technology*, 35, 2594-2601, 10.1021/es0019169, 2001.

Crouse, J. D., McKinney, K. A., Kwan, A. J., and Wennberg, P. O.: Measurement of gas-phase hydroperoxides by chemical ionization mass spectrometry, *Analytical Chemistry*, 78, 6726-6732, 10.1021/ac0604235, 2006.

Daele, V., Laverdet, G., Lebras, G., and Poulet, G.: Kinetics of the reactions $\text{CH}_3\text{O}+\text{NO}$, $\text{CH}_3\text{O}+\text{NO}_3$, and $\text{CH}_3\text{O}_2+\text{NO}_3$, *Journal of Physical Chemistry*, 99, 1470-1477, 1995.

Davidson, J. A., Viggiano, A. A., Howard, C. J., Dotan, I., Fehsenfeld, F. C., Albritton, D. L., and Ferguson, E. E.: Rate constants for reactions of O_2^+ , NO_2^+ , NO^+ , H_3O^+ , CO_3^- , NO_2^- and halide ions with N_2O_5 AT 300 K, *Journal of Chemical Physics*, 68, 2085-2087, 1978.

de Gouw, J. A., Middlebrook, A. M., Warneke, C., Goldan, P. D., Kuster, W. C., Roberts, J. M., Fehsenfeld, F. C., Worsnop, D. R., Canagaratna, M. R., Pszenny, A. A. P., Keene, W. C., Marchewka, M., Bertman, S. B., and Bates, T. S.: Budget of organic carbon in a

polluted atmosphere: Results from the New England Air Quality Study in 2002, *Journal of Geophysical Research-Atmospheres*, 110, D16305, 10.1029/2004jd005623, 2005.

de Gouw, J. A., Brock, C. A., Atlas, E. L., Bates, T. S., Fehsenfeld, F. C., Goldan, P. D., Holloway, J. S., Kuster, W. C., Lerner, B. M., Matthew, B. M., Middlebrook, A. M., Onasch, T. B., Peltier, R. E., Quinn, P. K., Senff, C. J., Stohl, A., Sullivan, A. P., Trainer, M., Warneke, C., Weber, R. J., and Williams, E. J.: Sources of particulate matter in the northeastern United States in summer: 1. Direct emissions and secondary formation of organic matter in urban plumes, *Journal of Geophysical Research-Atmospheres*, 113, D08301, 10.1029/2007jd009243, 2008.

Dibble, T. S.: Failures and limitations of quantum chemistry for two key problems in the atmospheric chemistry of peroxy radicals, *Atmospheric Environment*, 42, 5837-5848, 10.1016/j.atmosenv.2007.11.005, 2008.

Dillon, T. J., and Crowley, J. N.: Direct detection of OH formation in the reactions of HO₂ with CH₃C(O)O₂ and other substituted peroxy radicals, *Atmospheric Chemistry and Physics*, 8, 4877-4889, 2008.

Donahue, N. M., Robinson, A. L., and Pandis, S. N.: Atmospheric organic particulate matter: From smoke to secondary organic aerosol, *Atmospheric Environment*, 43, 94-106, 10.1016/j.atmosenv.2008.09.055, 2009.

Faloona, I., Tan, D., Brune, W., Hurst, J., Barket, D., Couch, T. L., Shepson, P., Apel, E., Riemer, D., Thornberry, T., Carroll, M. A., Sillman, S., Keeler, G. J., Sagady, J., Hooper, D., and Paterson, K.: Nighttime observations of anomalously high levels of hydroxyl radicals above a deciduous forest canopy, *Journal of Geophysical Research-Atmospheres*, 106, 24315-24333, 2001.

Fan, J. W., and Zhang, R. Y.: Atmospheric Oxidation Mechanism of Isoprene, *Environmental Chemistry*, 1, 140-149, 10.1071/en04045, 2004.

Fiore, A. M., Horowitz, L. W., Purves, D. W., Levy, H., Evans, M. J., Wang, Y. X., Li, Q. B., and Yantosca, R. M.: Evaluating the contribution of changes in isoprene emissions to surface ozone trends over the eastern United States, *Journal of Geophysical Research-Atmospheres*, 110, D12303, 10.1029/2004jd005485, 2005.

Forkel, R., Klemm, O., Graus, M., Rappengluck, B., Stockwell, W. R., Grabmer, W., Held, A., Hansel, A., and Steinbrecher, R.: Trace gas exchange and gas phase chemistry in a Norway spruce forest: A study with a coupled 1-dimensional canopy atmospheric chemistry emission model, *Atmospheric Environment*, 40, S28-S42, 10.1016/j.atmosenv.2005.11.070, 2006.

Francisco-Marquez, M., Alvarez-Idaboy, J. R., Galano, A., and Vivier-Bunge, A.: A possible mechanism for furan formation in the tropospheric oxidation of dienes, *Environmental Science & Technology*, 39, 8797-8802, 10.1021/es0500714, 2005.

Fry, J. L., Kiendler-Scharr, A., Rollins, A. W., Wooldridge, P. J., Brown, S. S., Fuchs, H., Dube, W., Mensah, A., dal Maso, M., Tillmann, R., Dorn, H. P., Brauers, T., and Cohen, R. C.: Organic nitrate and secondary organic aerosol yield from NO₃ oxidation of beta-pinene evaluated using a gas-phase kinetics/aerosol partitioning model, *Atmospheric Chemistry and Physics*, 9, 1431-1449, 2009.

Fuentes, J. D., Wang, D., Bowling, D. R., Potosnak, M., Monson, R. K., Goliff, W. S., and Stockwell, W. R.: Biogenic hydrocarbon chemistry within and above a mixed deciduous forest, *Journal of Atmospheric Chemistry*, 56, 165-185, 10.1007/s10874-006-9048-4, 2007.

Garden, A. L., Paulot, F., Crouse, J. D., Maxwell-Cameron, I. J., Wennberg, P. O., and Kjaergaard, H. G.: Calculation of conformationally weighted dipole moments useful in ion-molecule collision rate estimates, *Chem. Phys. Lett.*, 474, 45-50, 10.1016/j.cplett.2009.04.038, 2009.

Geyer, A., Alicke, B., Ackermann, R., Martinez, M., Harder, H., Brune, W., di Carlo, P., Williams, E., Jobson, T., Hall, S., Shetter, R., and Stutz, J.: Direct observations of daytime NO₃: Implications for urban boundary layer chemistry, *Journal of Geophysical Research-Atmospheres*, 108, 4368, 10.1029/2002jd002967, 2003a.

Geyer, A., Bachmann, K., Hofzumahaus, A., Holland, F., Konrad, S., Klupfel, T., Patz, H. W., Perner, D., Mihelcic, D., Schafer, H. J., Volz-Thomas, A., and Platt, U.: Nighttime formation of peroxy and hydroxyl radicals during the BERLIOZ campaign: Observations

and modeling studies, *Journal of Geophysical Research-Atmospheres*, 108, 8249, 10.1029/2001jd000656, 2003b.

Geyer, A., and Stutz, J.: Vertical profiles of NO_3 , N_2O_5 , O_3 , and NO_x in the nocturnal boundary layer: 2. Model studies on the altitude dependence of composition and chemistry, *Journal of Geophysical Research-Atmospheres*, 109, D12307, 10.1029/2003jd004211, 2004.

Gölz, C., Senzig, J., and Platt, U.: NO_3 -initiated oxidation of biogenic hydrocarbons, *Chemosphere - Global Change Science*, 3, 339-352, 2001.

Griffin, R. J., Cocker, D. R., Flagan, R. C., and Seinfeld, J. H.: Organic aerosol formation from the oxidation of biogenic hydrocarbons, *Journal of Geophysical Research-Atmospheres*, 104, 3555-3567, 1999.

Guenther, A., Karl, T., Harley, P., Wiedinmyer, C., Palmer, P. I., and Geron, C.: Estimates of global terrestrial isoprene emissions using MEGAN (Model of Emissions of Gases and Aerosols from Nature), *Atmospheric Chemistry and Physics*, 6, 3181-3210, 2006.

Hallquist, M., Wangberg, I., Ljungstrom, E., Barnes, I., and Becker, K. H.: Aerosol and product yields from NO_3 radical-initiated oxidation of selected monoterpenes, *Environmental Science & Technology*, 33, 553-559, 1999.

Harley, P., Vasconcellos, P., Vierling, L., Pinheiro, C. C. D., Greenberg, J., Guenther, A., Klinger, L., De Almeida, S. S., Neill, D., Baker, T., Phillips, O., and Malhi, Y.: Variation in potential for isoprene emissions among Neotropical forest sites, *Global Change Biology*, 10, 630-650, 10.1111/j.1529-8817.2003.00760.x, 2004.

Harrison, R. M., Shi, J. P., and Grenfell, J. L.: Novel nighttime free radical chemistry in severe nitrogen dioxide pollution episodes, *Atmospheric Environment*, 32, 2769-2774, 1998.

Hasson, A. S., Ho, A. W., Kuwata, K. T., and Paulson, S. E.: Production of stabilized Criegee intermediates and peroxides in the gas phase ozonolysis of alkenes 2. Asymmetric and biogenic alkenes, *Journal of Geophysical Research-Atmospheres*, 106, 34143-34153, 2001.

Hasson, A. S., Tyndall, G. S., and Orlando, J. J.: A product yield study of the reaction of HO₂ radicals with ethyl peroxy (C₂H₅O₂), acetyl peroxy (CH₃C(O)O₂), and acetyl peroxy (CH₃C(O)CH₂O₂) radicals, *Journal of Physical Chemistry A*, 108, 5979-5989, 10.1021/jp048873t, 2004.

Hasson, A. S., Kuwata, K. T., Arroyo, M. C., and Petersen, E. B.: Theoretical studies of the reaction of hydroperoxy radicals (HO₂) with ethyl peroxy (CH₃CH₂O₂), acetyl peroxy (CH₃C(O)O₂) and acetyl peroxy (CH₃C(O)CH₂O₂) radicals, *Journal of Photochemistry and Photobiology A-Chemistry*, 176, 218-230, 10.1016/j.jphotochem.2005.08.012, 2005.

Heald, C. L., Jacob, D. J., Park, R. J., Russell, L. M., Huebert, B. J., Seinfeld, J. H., Liao, H., and Weber, R. J.: A large organic aerosol source in the free troposphere missing from current models, *Geophysical Research Letters*, 32, L18809, 10.1029/2005gl023831, 2005.

Heintz, F., Platt, U., Flentje, H., and Dubois, R.: Long-term observation of nitrate radicals at the tor station, Kap Arkona (Rugen), *Journal of Geophysical Research-Atmospheres*, 101, 22891-22910, 1996.

Horowitz, L. W., Liang, J. Y., Gardner, G. M., and Jacob, D. J.: Export of reactive nitrogen from North America during summertime: Sensitivity to hydrocarbon chemistry, *Journal of Geophysical Research-Atmospheres*, 103, 13451-13476, 1998.

Horowitz, L. W., Fiore, A. M., Milly, G. P., Cohen, R. C., Perring, A., Wooldridge, P. J., Hess, P. G., Emmons, L. K., and Lamarque, J. F.: Observational constraints on the chemistry of isoprene nitrates over the eastern United States, *Journal of Geophysical Research-Atmospheres*, 112, D12s08, 10.1029/2006jd007747, 2007.

Jay, K., and Stieglitz, L.: The gas-phase addition of NO_x to olefins, *Chemosphere*, 19, 1939-1950, 1989.

Jenkin, M. E., Hurley, M. D., and Wallington, T. J.: Investigation of the radical product channel of the $\text{CH}_3\text{C}(\text{O})\text{O}_2 + \text{HO}_2$ reaction in the gas phase, *Physical Chemistry Chemical Physics*, 9, 3149-3162, 10.1039/b702757e, 2007.

Jenkin, M. E., Hurley, M. D., and Wallington, T. J.: Investigation of the radical product channel of the $\text{CH}_3\text{C}(\text{O})\text{CH}_2\text{O}_2 + \text{HO}_2$ reaction in the gas phase, *Physical Chemistry Chemical Physics*, 10, 4274-4280, 10.1039/b802898b, 2008.

Jenkin, M. E., Hurley, M. A., and Wallington, T. J.: Investigation of the Radical Product Channel of the $\text{CH}_3\text{OCH}_2\text{O}_2 + \text{HO}_2$ Reaction in the Gas Phase, *Journal of Physical Chemistry A*, 114, 408-416, 10.1021/jp908158w, 2010.

Johnson, D., Jenkin, M. E., Wirtz, K., and Martin-Reviejo, M.: Simulating the formation of secondary organic aerosol from the photooxidation of aromatic hydrocarbons, *Environmental Chemistry*, 2, 35-48, 10.1071/en04079, 2005.

Keywood, M. D., Varutbangkul, V., Bahreini, R., Flagan, R. C., and Seinfeld, J. H.: Secondary organic aerosol formation from the ozonolysis of cycloalkenes and related compounds, *Environmental Science & Technology*, 38, 4157-4164, 10.1021/es.035363o, 2004.

Kroll, J. H., Ng, N. L., Murphy, S. M., Flagan, R. C., and Seinfeld, J. H.: Secondary organic aerosol formation from isoprene photooxidation under high- NO_x conditions, *Geophysical Research Letters*, 32, L18808, 10.1029/2005gl023637, 2005.

Kroll, J. H., Ng, N. L., Murphy, S. M., Flagan, R. C., and Seinfeld, J. H.: Secondary organic aerosol formation from isoprene photooxidation, *Environmental Science & Technology*, 40, 1869-1877, 10.1021/es0524301, 2006.

Kwok, E. S. C., and Atkinson, R.: Estimation of hydroxyl radical reaction rate constants for gas-phase organic compounds using a structure-activity relationship - an update, *Atmospheric Environment*, 29, 1685-1695, 1995.

Kwok, E. S. C., Aschmann, S. M., Arey, J., and Atkinson, R.: Product formation from the reaction of the NO₃ radical with isoprene and rate constants for the reactions of methacrolein and methyl vinyl ketone with the NO₃ radical, *International Journal of Chemical Kinetics*, 28, 925-934, 1996.

Lelieveld, J., Butler, T. M., Crowley, J. N., Dillon, T. J., Fischer, H., Ganzeveld, L., Harder, H., Lawrence, M. G., Martinez, M., Taraborrelli, D., and Williams, J.: Atmospheric oxidation capacity sustained by a tropical forest, *Nature*, 452, 737-740, 10.1038/nature06870, 2008.

Lesclaux, R.: Combination of Peroxyl Radicals in the Gas Phase, in: *Peroxyl Radicals*, edited by: Alfassi, Z., Wiley, 81-112, 1997.

Lightfoot, P. D., Cox, R. A., Crowley, J. N., Destriau, M., Hayman, G. D., Jenkin, M. E., Moortgat, G. K., and Zabel, F.: Organic peroxy radicals - kinetics, spectroscopy and tropospheric chemistry, *Atmospheric Environment Part A-General Topics*, 26, 1805-1961, 1992.

Matsunaga, A., and Ziemann, P. J.: Yields of beta-Hydroxynitrates and Dihydroxynitrates in Aerosol Formed from OH Radical-Initiated Reactions of Linear Alkenes in the

Presence of NO_x, *Journal of Physical Chemistry A*, 113, 599-606, 10.1021/jp807764d, 2009.

Mayo, F. R.: Free radical autoxidations of hydrocarbons, *Accounts of Chemical Research*, 1, 193-201, 1968.

Mellouki, A., Talukdar, R. K., Bopegedera, A., and Howard, C. J.: Study of the kinetics of the reactions of NO₃ with HO₂ and OH, *International Journal of Chemical Kinetics*, 25, 25-39, 1993.

Neeb, P., and Moortgat, G. K.: Formation of OH radicals in the gas-phase reaction of propene, isobutene, and isoprene with O₃: Yields and mechanistic implications, *Journal of Physical Chemistry A*, 103, 9003-9012, 1999.

Ng, N. L., Kwan, A. J., Surratt, J. D., Chan, A. W. H., Chhabra, P. S., Sorooshian, A., Pye, H. O. T., Crouse, J. D., Wennberg, P. O., Flagan, R. C., and Seinfeld, J. H.: Secondary organic aerosol (SOA) formation from reaction of isoprene with nitrate radicals (NO₃), *Atmospheric Chemistry and Physics*, 8, 4117-4140, 2008.

O'Brien, J. M., Czuba, E., Hastie, D. R., Francisco, J. S., and Shepson, P. B.: Determination of the hydroxy nitrate yields from the reaction of C-2-C-6 alkenes with OH in the presence of NO, *Journal of Physical Chemistry A*, 102, 8903-8908, 1998.

Orzechowska, G. E., and Paulson, S. E.: Photochemical sources of organic acids. 1. Reaction of ozone with isoprene, propene, and 2-butenes under dry and humid conditions using SPME, *Journal of Physical Chemistry A*, 109, 5358-5365, 10.1021/jp050166s, 2005.

Osborne, D. A., and Waddington, D. J.: Reactions of oxygenated radicals in the gas phase: 7. Reactions of methylperoxyl radicals and alkenes, *Journal of the Chemical Society-Perkin Transactions 2*, 925-930, 1980.

Paulot, F., Crouse, J. D., Kjaergaard, H. G., Kroll, J. H., Seinfeld, J. H., and Wennberg, P. O.: Isoprene photooxidation: new insights into the production of acids and organic nitrates, *Atmospheric Chemistry and Physics*, 9, 1479-1501, 2009a.

Paulot, F., Crouse, J. D., Kjaergaard, H. G., Kurten, A., St Clair, J. M., Seinfeld, J. H., and Wennberg, P. O.: Unexpected Epoxide Formation in the Gas-Phase Photooxidation of Isoprene, *Science*, 325, 730-733, 10.1126/science.1172910, 2009b.

Peeters, J., Nguyen, T. L., and Vereecken, L.: HOx radical regeneration in the oxidation of isoprene, *Physical Chemistry Chemical Physics*, 11, 5935-5939, 10.1039/b908511d, 2009.

Penkett, S. A., Burgess, R. A., Coe, H., Coll, I., Hov, O., Lindskog, A., Schmidbauer, N., Solberg, S., Roemer, M., Thijsse, T., Beck, J., and Reeves, C. E.: Evidence for large average concentrations of the nitrate radical (NO₃) in Western Europe from the HANSA

hydrocarbon database, *Atmospheric Environment*, 41, 3465-3478,

10.1016/j.atmosenv.2006.11.055, 2007.

Perring, A. E., Wisthaler, A., Graus, M., Wooldridge, P. J., Lockwood, A. L., Mielke, L. H., Shepson, P. B., Hansel, A., and Cohen, R. C.: A product study of the isoprene+NO₃ reaction, *Atmospheric Chemistry and Physics*, 9, 4945-4956, 2009.

Platt, U., Perner, D., Schroder, J., Kessler, C., and Toennissen, A.: The diurnal variation of NO₃, *Journal of Geophysical Research-Oceans and Atmospheres*, 86, 1965-1970, 1981.

Platt, U., and Janssen, C.: Observation and role of the free radicals NO₃, ClO, BrO and IO in the troposphere, *Faraday Discussions*, 100, 175-198, 1995.

Quinn, P. K., Bates, T. S., Coffman, D., Onasch, T. B., Worsnop, D., Baynard, T., de Gouw, J. A., Goldan, P. D., Kuster, W. C., Williams, E., Roberts, J. M., Lerner, B., Stohl, A., Pettersson, A., and Lovejoy, E. R.: Impacts of sources and aging on submicrometer aerosol properties in the marine boundary layer across the Gulf of Maine, *J. Geophys. Res.*, 111, D23S36, 10.1029/2006jd007582, 2006.

Ren, X. R., Harder, H., Martinez, M., Leshner, R. L., Oligier, A., Shirley, T., Adams, J., Simpas, J. B., and Brune, W. H.: HO_x concentrations and OH reactivity observations in New York City during PMTACS-NY2001, *Atmospheric Environment*, 37, 3627-3637, 10.1016/s1352-2310(03)00460-6, 2003.

Roberts, J. M., Williams, J., Baumann, K., Buhr, M. P., Goldan, P. D., Holloway, J., Hubler, G., Kuster, W. C., McKeen, S. A., Ryerson, T. B., Trainer, M., Williams, E. J., Fehsenfeld, F. C., Bertman, S. B., Nouaime, G., Seaver, C., Grodzinsky, G., Rodgers, M., and Young, V. L.: Measurements of PAN, PPN, and MPAN made during the 1994 and 1995 Nashville Intensives of the Southern Oxidant Study: Implications for regional ozone production from biogenic hydrocarbons, *Journal of Geophysical Research-Atmospheres*, 103, 22473-22490, 1998.

Rollins, A. W., Kiendler-Scharr, A., Fry, J. L., Brauers, T., Brown, S. S., Dorn, H. P., Dube, W. P., Fuchs, H., Mensah, A., Mentel, T. F., Rohrer, F., Tillmann, R., Wegener, R., Wooldridge, P. J., and Cohen, R. C.: Isoprene oxidation by nitrate radical: alkyl nitrate and secondary organic aerosol yields, *Atmospheric Chemistry and Physics*, 9, 6685-6703, 2009.

Ruppert, L., and Becker, K. H.: A product study of the OH radical-initiated oxidation of isoprene: formation of C-5-unsaturated diols, *Atmospheric Environment*, 34, 1529-1542, 2000.

Sakulyanontvittaya, T., Duhl, T., Wiedinmyer, C., Helmig, D., Matsunaga, S., Potosnak, M., Milford, J., and Guenther, A.: Monoterpene and sesquiterpene emission estimates for the United States, *Environmental Science & Technology*, 42, 1623-1629, 10.1021/es702274e, 2008.

Chemical Kinetics and Photochemical Data for Use in Atmospheric Studies: Evaluation Number 15: jpldataeval.jpl.nasa.gov, 2006.

Schichtel, B. A., Malm, W. C., Bench, G., Fallon, S., McDade, C. E., Chow, J. C., and Watson, J. G.: Fossil and contemporary fine particulate carbon fractions at 12 rural and urban sites in the United States, *Journal of Geophysical Research-Atmospheres*, 113, D02311, [10.1029/2007jd008605](https://doi.org/10.1029/2007jd008605), 2008.

Seeley, J. V., Meads, R. F., Elrod, M. J., and Molina, M. J.: Temperature and pressure dependence of the rate constant for the HO₂+NO reaction, *Journal of Physical Chemistry*, 100, 4026-4031, 1996.

Sharkey, T. D., Singaas, E. L., Vanderveer, P. J., and Geron, C.: Field measurements of isoprene emission from trees in response to temperature and light, *Tree Physiology*, 16, 649-654, 1996.

Simmons, K. E., and van Sickle, D. E.: Addition abstraction competition of acylperoxy radicals reacting with alkenes - cooxidation of cyclohexene and valeraldehyde, *Journal of the American Chemical Society*, 95, 7759-7763, 1973.

Simpson, D., Yttri, K. E., Klimont, Z., Kupiainen, K., Caseiro, A., Gelencser, A., Pio, C., Puxbaum, H., and Legrand, M.: Modeling carbonaceous aerosol over Europe: Analysis of the CARBOSOL and EMEP EC/OC campaigns, *Journal of Geophysical Research-Atmospheres*, 112, D23s14, [10.1029/2006jd008158](https://doi.org/10.1029/2006jd008158), 2007.

Sinha, A., Lovejoy, E. R., and Howard, C. J.: Kinetic study of the reaction of HO₂ with ozone, *Journal of Chemical Physics*, 87, 2122-2128, 1987.

Skov, H., Hjorth, J., Lohse, C., Jensen, N. R., and Restelli, G.: Products and mechanisms of the reactions of the nitrate radical (NO₃) with isoprene, 1,3-butadiene and 2,3-dimethyl-1,3-butadiene in air, *Atmospheric Environment Part A-General Topics*, 26, 2771-2783, 1992.

Smith, N., Plane, J. M. C., Nien, C. F., and Solomon, P. A.: Nighttime radical chemistry in the San Joaquin Valley, *Atmospheric Environment*, 29, 2887-2897, 1995.

Spittler, M., Barnes, I., Bejan, I., Brockmann, K. J., Benter, T., and Wirtz, K.: Reactions of NO₃ radicals with limonene and alpha-pinene: Product and SOA formation, *Atmospheric Environment*, 40, S116-S127, 10.1016/j.atmosenv.2005.09.093, 2006.

Stark, M. S., and Waddington, D. J.: Oxidation of propene in the gas-phase, *International Journal of Chemical Kinetics*, 27, 123-151, 1995.

Starn, T. K., Shepson, P. B., Bertman, S. B., Riemer, D. D., Zika, R. G., and Olszyna, K.: Nighttime isoprene chemistry at an urban-impacted forest site, *Journal of Geophysical Research-Atmospheres*, 103, 22437-22447, 1998.

Steinbacher, M., Dommen, J., Ordonez, C., Reimann, S., Gruebler, F., Staehelin, J., Andreani-Aksoyoglu, S., and Prevot, A. S. H.: Volatile organic compounds in the Po

Basin. part B: Biogenic VOCs, *Journal of Atmospheric Chemistry*, 51, 293-315, 10.1007/s10874-005-3577-0, 2005.

Stroud, C. A., Roberts, J. M., Williams, E. J., Hereid, D., Angevine, W. M., Fehsenfeld, F. C., Wisthaler, A., Hansel, A., Martinez-Harder, M., Harder, H., Brune, W. H., Hoenninger, G., Stutz, J., and White, A. B.: Nighttime isoprene trends at an urban forested site during the 1999 Southern Oxidant Study, *Journal of Geophysical Research-Atmospheres*, 107, 4291, 10.1029/2001jd000959, 2002.

Su, T., and Chesnavich, W. J.: Parameterization of the ion-polar molecule collision rate constant by trajectory calculations, *Journal of Chemical Physics*, 76, 5183-5185, 1982.

Suh, I., Lei, W. F., and Zhang, R. Y.: Experimental and theoretical studies of isoprene reaction with NO₃, *Journal of Physical Chemistry A*, 105, 6471-6478, 10.1021/jp0105950, 2001.

Sullivan, A. P., Peltier, R. E., Brock, C. A., de Gouw, J. A., Holloway, J. S., Warneke, C., Wollny, A. G., and Weber, R. J.: Airborne measurements of carbonaceous aerosol soluble in water over northeastern United States: Method development and an investigation into water-soluble organic carbon sources, *Journal of Geophysical Research-Atmospheres*, 111, D23s46, 10.1029/2006jd007072, 2006.

Surratt, J. D., Murphy, S. M., Kroll, J. H., Ng, N. L., Hildebrandt, L., Sorooshian, A., Szmigielski, R., Vermeylen, R., Maenhaut, W., Claeys, M., Flagan, R. C., and Seinfeld,

J. H.: Chemical composition of secondary organic aerosol formed from the photooxidation of isoprene, *Journal of Physical Chemistry A*, 110, 9665-9690, 10.1021/jp061734m, 2006.

Surratt, J. D., Chan, A. W. H., Eddingsaas, N. C., Chan, M. N., Loza, C. L., Kwan, A. J., Hersey, S. P., Flagan, R. C., Wennberg, P. O., and Seinfeld, J. H.: Reactive intermediates revealed in secondary organic aerosol formation from isoprene, *Proceedings of the National Academy of Sciences of the United States of America*, 107, 6640-6645, 10.1073/pnas.0911114107, 2010.

Thornton, J. A., Wooldridge, P. J., Cohen, R. C., Martinez, M., Harder, H., Brune, W. H., Williams, E. J., Roberts, J. M., Fehsenfeld, F. C., Hall, S. R., Shetter, R. E., Wert, B. P., and Fried, A.: Ozone production rates as a function of NO_x abundances and HO_x production rates in the Nashville urban plume, *Journal of Geophysical Research-Atmospheres*, 107, 4146, 10.1029/2001jd000932, 2002.

van Sickle, D. E., Mayo, F. R., and Arluck, R. M.: Liquid-phase oxidations of cyclic alkenes, *Journal of the American Chemical Society*, 87, 4824-4832, 1965a.

van Sickle, D. E., Mayo, F. R., and Arluck, R. M.: Liquid-phase oxidation of cyclopentene, *Journal of the American Chemical Society*, 87, 4832-4837, 1965b.

Vaughan, S., Canosa-Mas, C. E., Pfrang, C., Shallcross, D. E., Watson, L., and Wayne, R. P.: Kinetic studies of reactions of the nitrate radical (NO₃) with peroxy radicals

(RO₂): an indirect source of OH at night?, *Physical Chemistry Chemical Physics*, 8, 3749-3760, 10.1039/b605569a, 2006.

Vereecken, L., and Peeters, J.: Decomposition of substituted alkoxy radicals-part I: a generalized structure-activity relationship for reaction barrier heights, *Physical Chemistry Chemical Physics*, 11, 9062-9074, 10.1039/b909712k, 2009.

Volkamer, R., Jimenez, J. L., San Martini, F., Dzepina, K., Zhang, Q., Salcedo, D., Molina, L. T., Worsnop, D. R., and Molina, M. J.: Secondary organic aerosol formation from anthropogenic air pollution: Rapid and higher than expected, *Geophysical Research Letters*, 33, L17811, 10.1029/2006gl026899, 2006.

von Friedeburg, C., Wagner, T., Geyer, A., Kaiser, N., Vogel, B., Vogel, H., and Platt, U.: Derivation of tropospheric NO₃ profiles using off-axis differential optical absorption spectroscopy measurements during sunrise and comparison with simulations, *Journal of Geophysical Research-Atmospheres*, 107, 4168, 10.1029/2001jd000481, 2002.

von Kuhlmann, R., Lawrence, M. G., Poschl, U., and Crutzen, P. J.: Sensitivities in global scale modeling of isoprene, *Atmospheric Chemistry and Physics*, 4, 1-17, 2004.

Wallington, T. J., Nielsen, O. J., and Sehested, J.: Reactions of Organic Peroxy Radicals in the Gas Phase, in: *Peroxy Radicals*, edited by: Alfassi, Z., Wiley, 113-172, 1997.

Warneke, C., de Gouw, J. A., Goldan, P. D., Kuster, W. C., Williams, E. J., Lerner, B. M., Jakoubek, R., Brown, S. S., Stark, H., Aldener, M., Ravishankara, A. R., Roberts, J. M., Marchewka, M., Bertman, S., Sueper, D. T., McKeen, S. A., Meagher, J. F., and Fehsenfeld, F. C.: Comparison of daytime and nighttime oxidation of biogenic and anthropogenic VOCs along the New England coast in summer during New England Air Quality Study 2002, *Journal of Geophysical Research-Atmospheres*, 109, D10309, 10.1029/2003jd004424, 2004.

Wayne, R. P., Barnes, I., Biggs, P., Burrows, J. P., Canosamas, C. E., Hjorth, J., Lebras, G., Moortgat, G. K., Perner, D., Poulet, G., Restelli, G., and Sidebottom, H.: The nitrate radical - physics, chemistry, and the atmosphere, *Atmospheric Environment Part A-General Topics*, 25, 1-203, 1991.

Weber, R. J., Sullivan, A. P., Peltier, R. E., Russell, A., Yan, B., Zheng, M., de Gouw, J., Warneke, C., Brock, C., Holloway, J. S., Atlas, E. L., and Edgerton, E.: A study of secondary organic aerosol formation in the anthropogenic-influenced southeastern United States, *Journal of Geophysical Research-Atmospheres*, 112, D13302, 10.1029/2007jd008408, 2007.

Williams, J., Roberts, J. M., Fehsenfeld, F. C., Bertman, S. B., Buhr, M. P., Goldan, P. D., Hubler, G., Kuster, W. C., Ryerson, T. B., Trainer, M., and Young, V.: Regional ozone from biogenic hydrocarbons deduced from airborne measurements of PAN, PPN, and MPAN, *Geophysical Research Letters*, 24, 1099-1102, 1997.

Zhang, D., and Zhang, R. Y.: Unimolecular decomposition of nitrooxyalkyl radicals from NO₃-isoprene reaction, *Journal of Chemical Physics*, 116, 9721-9728, 10.1063/1.1476695, 2002.

Compound	Method	m/z (CIMS)	final concentration (ppb)
C4 compounds			
MACR	GC-FID	-----	3
MVK	GC-FID	-----	6
C4 hydroxy carbonyl	CIMS	171	< 0.5
C5 Nitrates			
C5 nitrooxycarbonyl	CIMS	230	45.7
C5 hydroxynitrate	CIMS	232	27.5
C5 nitrooxy hydroperoxide	CIMS	248	11.6
C5 Isomerized Nitrates			
C5 nitrooxy hydroxy carbonyl	CIMS	246	5.5
C5 nitrooxy diol	CIMS	248	3.0
C5 nitrooxy hydroxy hydroperoxide	CIMS	264	2.1
C4 nitrooxy carbonyl	CIMS	216	0.6
C5 Hydroxy compounds			
C5 hydroxy carbonyl	CIMS	185	2.6
C5 diol	CIMS	187	2.3
C5 hydroxy hydroperoxide	CIMS	203	4.2
C5 Isomerized hydroxy compounds			
C5 dihydroxy carbonyl	CIMS	201	1.5
C5 triol	CIMS	203	1.3
C5 dihydroxy hydroperoxide	CIMS	219	< 0.5
Dimer compounds			
dinitrooxy ROOR	CIMS	377	1.4
isomerized dinitrooxy ROOR	CIMS	393	0.9
nitrooxy carbonyl ROOR	CIMS	330	< 0.5
hydroxy nitrate ROOR	CIMS	332	0.9
nitrooxy hydroperoxide ROOR	CIMS	348	< 0.5
C9 nitrooxy ROOR carbonyl	CIMS	316	< 0.5
Other			
3-MF	GC-FID	-----	4.5
hydroxyacetone	CIMS	159	0.5
hydrogen peroxide	CIMS	119	2.4
glycolaldehyde	CIMS	145	0.9

Table 3.1: Products detected by GC-FID and CIMS. Products with small but non-zero signals are noted as < 0.5 ppb.

No.	Reaction	Rate constant	Source
1	$\text{NO}_3 + \text{isoprene} \rightarrow \text{RO}_2 + \text{HO}_2$	6.6E-13	Atkinson, 1997
2	$\text{RO}_2 + \text{RO}_2 \rightarrow \text{products}$	1.0E-13	Atkinson et al., 2006, and references therein
3	$\text{RO}_2 + \text{NO}_3 \rightarrow \text{products}$	3.0E-12	Biggs et al., 1994; Daele et al., 1995; Canosa-Mas et al., 1996; Vaughan et al., 2006
4	$\text{RO}_2 + \text{HO}_2 \rightarrow \text{products}$	2.2E-11	Atkinson et al., 2006, and references therein
5	$\text{NO}_3 + \text{HO}_2 \rightarrow \text{OH} + \text{NO}_2 + \text{O}_2$	3.5E-12	Sander et al., 2006, and references therein
6	$\text{NO}_2 + \text{NO}_3 \rightarrow \text{N}_2\text{O}_5$	6.7E-12	Sander et al., 2006, and references therein
7	$\text{N}_2\text{O}_5 \rightarrow \text{NO}_2 + \text{NO}_3$	2.2E-01	Sander et al., 2006, and references therein
8	$\text{HO}_2 + \text{HO}_2 \rightarrow \text{H}_2\text{O}_2$	2.5E-12	Sander et al., 2006, and references therein
9	$\text{HO}_2 + \text{NO}_2 \rightarrow \text{HO}_2\text{NO}_2$	2.8E-12	Sander et al., 2006, and references therein
10	$\text{HO}_2\text{NO}_2 \rightarrow \text{HO}_2 + \text{NO}_2$	1.7E-01	Sander et al., 2006, and references therein
11	$\text{NO}_3 + \text{NO}_2 \rightarrow \text{NO} + \text{NO}_2 + \text{O}_2$	6.6E-16	Sander et al., 2006, and references therein
12	$\text{NO}_3 + \text{NO} \rightarrow 2\text{NO}_2$	2.6E-11	Sander et al., 2006, and references therein
13	$\text{HO}_2 + \text{NO} \rightarrow \text{NO}_2 + \text{OH}$	8.1E-12	Sander et al., 2006, and references therein

Table 3.2: Reactions considered for assessment of OH sources in isoprene- NO_3 system. All rate constant units are $\text{cm}^3 \text{molec}^{-1} \text{s}^{-1}$, except k_7 and k_{10} , which are s^{-1} . Rates of reactions involving RO_2 are based on an approximation of values found in the literature. HO_2 yield in reaction 1 is an upper limit to facilitate model analysis.

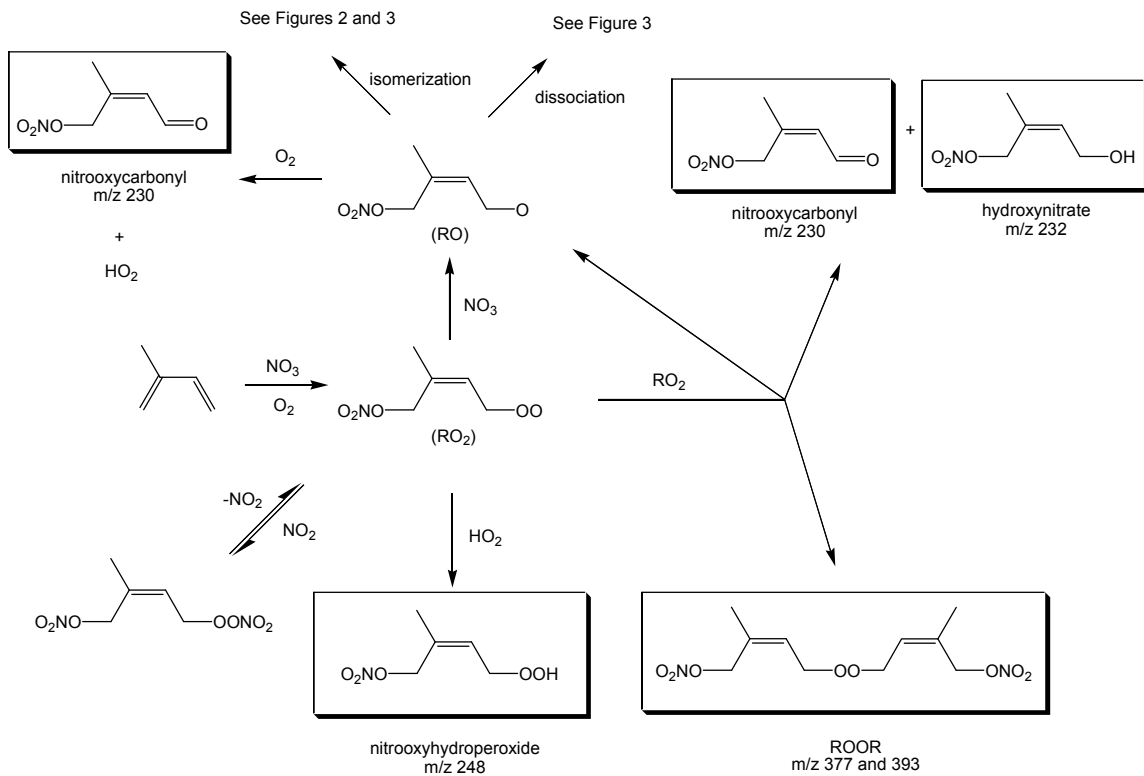


Figure 3.1. Generalized reaction mechanism in the isoprene-NO₃ system. Boxed compounds are detected by CIMS instrument at the indicated m/z values.

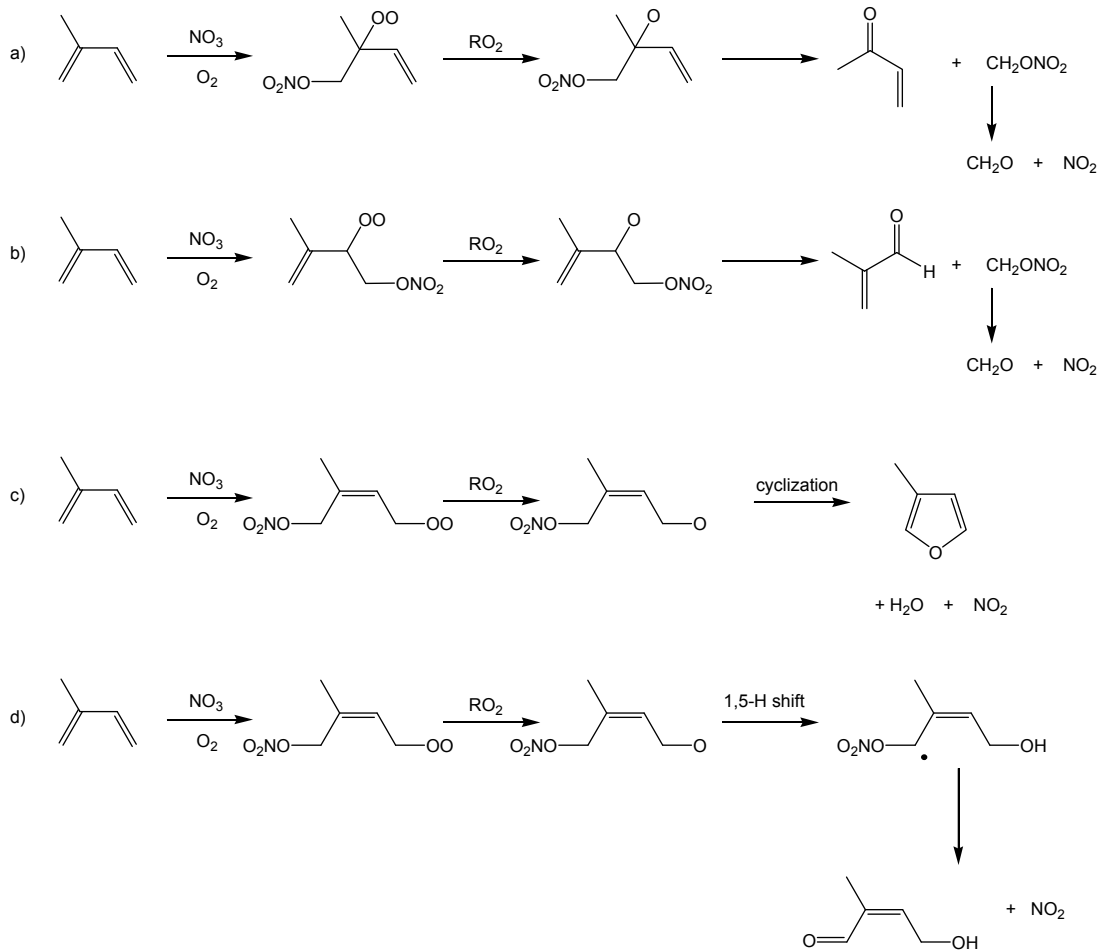


Figure 3.3. Formation mechanism of methyl vinyl ketone (a), methacrolein (b), 3-methylfuran (c), and hydroxycarbonyl (d), leading to release of NO_2 . The exact mechanism of 3-methylfuran formation is still unknown (Francisco-Márquez et al., 2005).

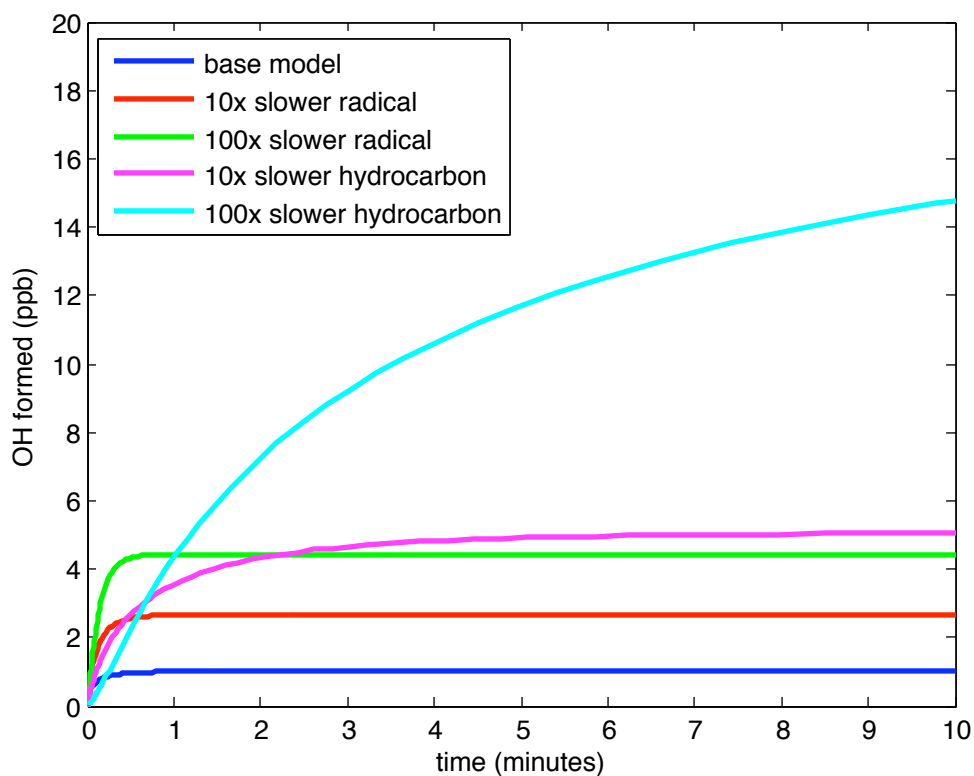


Figure 3.4. Box model simulations for OH production in isoprene-NO₃ system. Blue: base case described in Table 2; Red: RO₂-HO₂ and RO₂-NO₃ rate constants reduced by factor of 10; Green: RO₂-HO₂ and RO₂-NO₃ rate constants reduced by factor of 100; Pink: isoprene-NO₃ rate constant reduced by factor of 100; Light Blue: isoprene-NO₃ rate constant reduced by factor of 100. Initial conditions: 150 ppb N₂O₅, 800 ppb isoprene, 50 ppb NO₂.

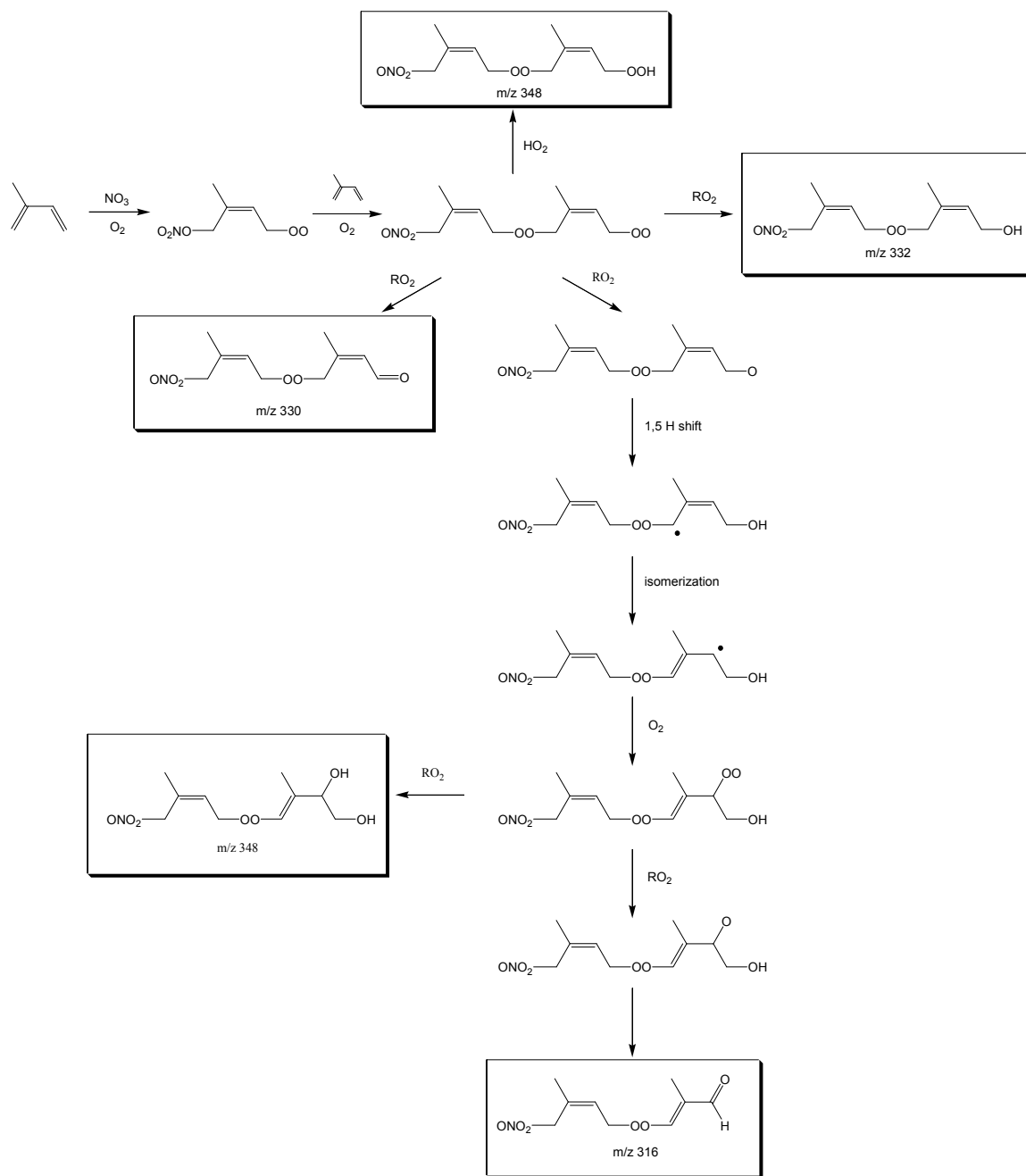


Figure 3.5. Proposed formation mechanisms of products detected by CIMS at m/z 316, 330, 332, and 348. Other isomers are possible.

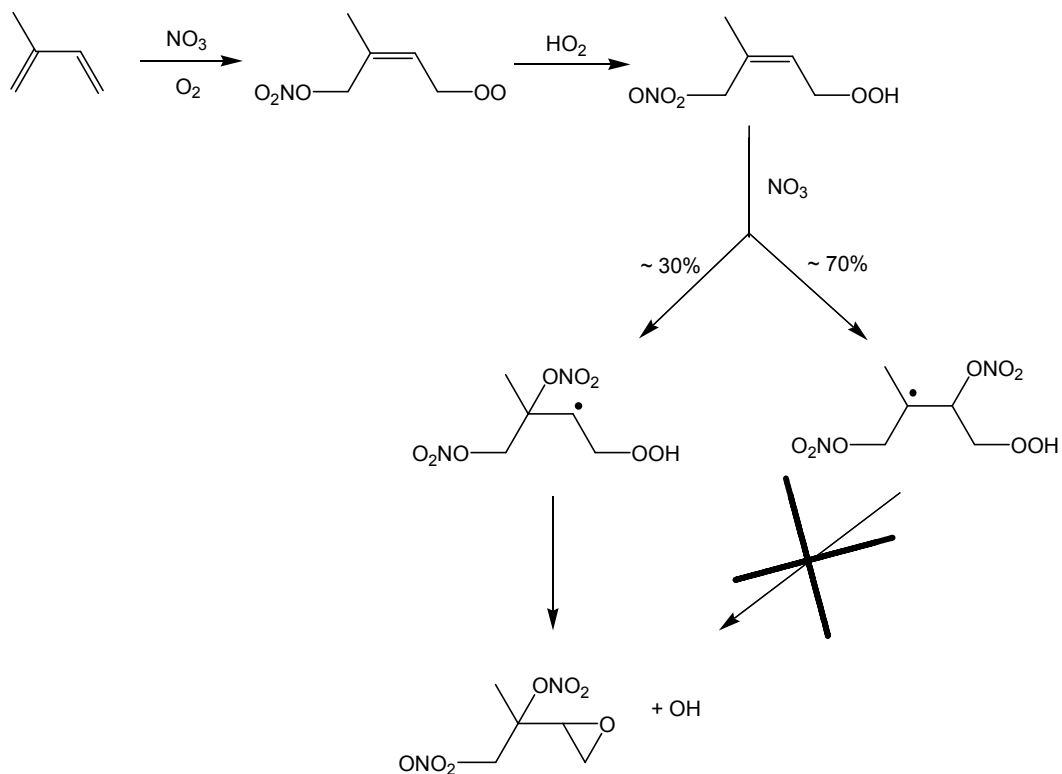


Figure 3.6. Formation mechanism of dinitrooxyepoxide and hydroxyl radical from oxidation of nitrooxyhydroperoxide.

Chapter 4

The potential flux of oxygenated volatile organic compounds from organic aerosol oxidation³

³ Adapted from Kwan, A. J., Crouse, J. D., Clarke, A. D., Shinozuka, Y., Anderson, B. E., Crawford, J. H., Avery, M. A., McNaughton, C. S., Brune, W. H., Singh, H. B., and Wennberg, P. O.: On the flux of oxygenated volatile organic compounds from organic aerosol oxidation, *Geophysical Research Letters*, 33, L15815, 10.1029/2006gl026144, 2006.

Abstract

Previous laboratory and field studies suggest that oxidation of organic aerosols can be a source of oxygenated volatile organic compounds (OVOC). Using measurements of atmospheric oxidants and aerosol size distributions performed on the NASA DC-8 during the INTEX-NA campaign, we estimate the potential magnitude of the continental summertime OVOC flux from organic aerosol oxidation by OH to be as large as 70 pptv C/day in the free troposphere. Contributions from O₃, H₂O₂, and photolysis may increase this estimate. These processes may provide a large, diffuse source of OVOC that has not been included in current atmospheric models, and thus have a significant impact on our understanding of organic aerosol, OVOC, PAN, and HOx chemistry.

4.1 Introduction

Oxygenated volatile organic compounds (OVOC) comprise a large number of the species whose transport to the remote troposphere can impact radical budgets and sequester NO_x in the form of nitrates (Singh et al., 1995; Wennberg et al., 1998; Muller and Brasseur, 1999). In addition, they play a role in the formation of organic aerosols (OA) (Kanakidou et al., 2005, and references therein). Field campaigns have noted large concentrations of OVOC throughout the troposphere, but their budgets are poorly understood (Singh et al., 2001, 2004; Wisthaler et al., 2002).

Ellison et al. (1999) suggest that oxidation of OA may provide an OVOC source to the remote troposphere. Field campaigns have established the ubiquity of OA throughout the troposphere (Murphy et al., 1998; Kanakidou et al., 2005). Most aerosols

contain both organic and inorganic components, though significantly, the organic fraction tends to be found on aerosol surfaces (Tervahattu et al., 2002ab, 2005, and references therein).

Laboratory studies have demonstrated that organic surfaces can be oxidized by OH and O₃ (Rudich, 2003, and references therein; Thornberry and Abbatt, 2004; Molina et al., 2004). Several of these studies have shown volatilization of OVOC resulting from organic surface oxidation. Molina et al. (2004), for example, report the full volatilization of a C₁₈ alkane monolayer following heterogeneous loss of 2-3 OH radicals to the surface, with many (though not exclusively) OVOC products. Evidence for such chemistry in the ambient environment include the demonstration by Grannas et al. (2004) that photooxidation of snow phase organic matter may explain the daytime flux of lightweight OVOC from snowpack to the boundary layer, and field observations that atmospheric OA becomes more oxidized with greater ozone exposure and/or age (Gogou et al., 1996; de Gouw et al., 2005; Quinn et al., 2005; McFiggans et al., 2005).

Here, we use data collected on the NASA DC-8 during the INTEX-NA campaign over North America in the summer of 2004 to place constraints on OA oxidation's potential contribution to continental summertime OVOC budgets.

4.2 Method

Aerosol size distributions for particles 10 nm to 3 μm in diameter were measured on the DC-8 using a differential mobility analyzer (DMA) and an optical particle counter (OPC) (Clarke et al., 2004). Comparison of the DMA and OPC data to measurements of larger and ultrafine particles indicates that these instruments generally capture >90% of

the total aerosol surface area except in a few select plumes. The aerosol size is quantified in conditions that are often dryer than the ambient atmosphere, so the aerosols may lose water (and thus mass) prior to measurement. Correcting for this effect is non-trivial, particularly for submicron particles, so we neglect it in our calculations. We believe this may lead to an underestimate of the total ambient surface area of less than 30%. OH measurements were made by laser induced fluorescence (Faloona et al., 2004), ozone by chemiluminescence (Avery et al., 2006), and H₂O₂ by chemical ionization mass spectrometry (Crouse et al., 2006).

The collision rate of an oxidant with aerosol along the flight track was estimated using 1-minute averages of the aerosol surface area and oxidant mixing ratios:

$$\text{collisions} = \frac{1}{4} \times (8RT/\pi M)^{1/2} \times S \times [O_x] \times f(D)$$

where the factor of 1/4 converts aerosol surface area to cross sectional area, $(8RT/\pi M)^{1/2}$ is the thermal speed of the oxidant (R is the universal gas constant, T is temperature, M is the oxidant molar mass), S the aerosol surface area, [O_x] the concentration of oxidant (converted to a 24-hour average in the case of OH), and f(D) the correction applied due to gas-phase diffusion limitations to large particles (for OH only) (Fuchs and Sutugin, 1971).

For each point along the DC-8 flight track, we obtain a 24-hour average [OH] by scaling the observed [OH] by the ratio of the diurnally-averaged to instantaneous [OH] calculated from a highly constrained box model (NASA LaRC photochemical box model (Crawford et al., 1999)). Cloud effects on actinic flux, which affect [OH], are assumed to

be constant throughout the day, though they are generally transient. We expect that our large dataset sufficiently captures the variability of cloud effects such that they will not significantly bias our estimate.

Following the studies of Bertram et al. (2001) and Molina et al. (2004) we assume that each OH collision is reactive ($\gamma=1$) and volatilizes 6 organic carbons. Although the alkane used in the Molina et al. (2004) study is not representative of all OA surfaces, long chain fatty acids may comprise a significant fraction (Tervahattu et al., 2002ab, 2005). These parameters represent by far the largest uncertainties in our analysis. Because our assumptions imply a unity accommodation coefficient ($\alpha=1$), we account for diffusion limitations in calculating the OH collision rate.

Estimating the OVOC flux from aerosol collisions with O_3 and H_2O_2 is significantly more difficult. While OH is highly reactive with many classes of organic compounds, O_3 reactivity and product yield are very substrate dependent (Rudich, 2003; Thornberry and Abbatt, 2004). Also, unlike for OH (Molina et al., 2004), O_3 reactivity with solid organic surfaces may depend on relative humidity (Poschl et al., 2001). For H_2O_2 , we found no experimental studies allowing us to constrain γ or the product yield. For these oxidants, though, estimating the collision rate with aerosols is a first step for assessing their potential contributions to OVOC flux. We expect that the accommodation coefficients for these two oxidants are significantly less than unity – Berkowitz et al. (2001), for example, estimate $\alpha_{O_3} \sim 10^{-3}$ – and thus do not consider diffusion limitations for their collision rates.

4.3 Results and Discussion

Calculated 24-hour average collision rates are plotted as a function of elevation in Figure 4.1. For OH (Figure 4.1a) and O₃ (Figure 4.1b), most of the variability is driven by the (dry) aerosol surface area, whose elevation bin means range from ~10 μm²/cc in the upper troposphere to ~150 μm²/cc in the lowest elevation bin. For OH, we estimate the upper tropospheric collision rate to be ~1x10³ collisions/cc/sec. Our assumption of carbon volatilization from Molina et al. (2004) thus yields an estimated OVOC source of ~70 pptv C/day in the upper troposphere. A significantly larger source would exist in the lower troposphere (~500 pptv C/day in the lowest 2 km), but the contribution of this mechanism to OVOC concentrations will be less significant because of the much larger OVOC sources from gas phase oxidation of larger hydrocarbons in this region.

Assuming a product yield for O₃ similar to that of OH, the ratio of OH to O₃ collisions gives a value of $\gamma_{O_3} \sim 10^{-6}$ necessary for the OVOC flux from O₃ to equal that from OH. Achieving this value would require only ~0.1% surface coverage by typical alkene liquids ($\gamma \sim 10^{-3}$) (de Gouw and Lovejoy, 1998; Rudich, 2003). Thus, it is plausible that for certain aerosols reaction with O₃ can be a significant oxidation mechanism. This is particularly true in the lower troposphere, where most primary (i.e., more unsaturated) OA is expected to reside. For H₂O₂ (Figure 1c), the equivalent $\gamma_{H_2O_2}$ ranges from ~10⁻⁵ in the lower troposphere to ~10⁻² in the upper troposphere, so H₂O₂'s contribution to OVOC flux is likely confined to the lower troposphere or in cloud. Because of clouds' high aerosol surface area, increased actinic flux, and potential for aqueous phase chemistry, aerosol oxidation in clouds may warrant particular attention.

Photolysis can, in principle, also lead to the decomposition of OA (Kieber et al., 1990). To be competitive with the OH chemistry, however, photolysis rates would have

to be relatively fast ($J \sim 10^{-6}$), as it is likely less efficient at degrading organic molecules in the condensed phase than in the gas phase: caging effects can stabilize the intermediates and aid their recombination or polymerization so that they remain in the bulk phase.

4.4 Implications

A dispersed and previously unconsidered source of OVOC from aerosol oxidation may have important implications for tropospheric photochemistry. For example, measurements of acetaldehyde (CH_3CHO) have routinely exceeded model predictions (Singh et al., 2001, 2004; Wisthaler et al., 2002); this was also true during INTEX-NA (Figure 4.2a). For each acetaldehyde measurement, we divide the difference between measured and box model-predicted mixing ratios by the photochemical lifetime to estimate the flux necessary to reconcile the difference. We find that a source of ~ 90 pptv/day (~ 180 pptv C/day) is required to sustain the observed acetaldehyde concentrations in the upper troposphere. INTEX-NA also marked the first extensive airborne measurements of peroxyacetic acid ($\text{CH}_3\text{C}(\text{O})\text{OOH}$, PAA), which significantly exceeded model-predicted values in the upper troposphere as well (Figure 4.2b); a similar analysis for PAA yields an estimated missing source of ~ 20 -200 pptv C/day (Crouse et al., in preparation). Even considering only acetaldehyde, oxidation by OH alone is likely too small to explain the upper tropospheric discrepancies between OVOC measurements and models; other oxidation mechanisms or alternative explanations should be explored.

A significant flux of OVOC from aerosol would have consequent impacts on HO_x and peroxyacyl nitrates. In fact, if the observations and our understanding of the subsequent chemistry of acetaldehyde are correct, peroxyacetyl nitrate (PAN) formation

is very fast in the upper troposphere. Observations of PAN are not, however, consistent with those of acetaldehyde, based on current understanding of the chemistry that links these compounds (Staudt et al., 2003).

A large OVOC flux from aerosol is also incompatible with current OA budgets. The IPCC (2001) estimate of OA flux is ~ 150 Tg “organic matter”/year, or ~ 100 Tg C/year. If our estimated OA oxidation rate from OH were representative of the entire atmosphere, the global flux of organic carbon from aerosol would be as large as ~ 150 Tg C/yr (integrating with bin median collision rates, ~ 100 TgC/yr; interquartile range, ~ 50 – 200 Tg C/yr). This is clearly an upper limit due to the assumptions of unity γ and that the continental summertime conditions of INTEX-NA are representative. Nonetheless, even a fraction of this large flux would imply that oxidation may need to be included in models, which currently consider only wet depositional loss. From our carbon flux (and assuming an aerosol density of 1 g/cc and an organic carbon fraction of 0.5), we estimate the median lifetime of aerosol organic carbon to be ~ 10 days; thus, oxidation may be an important sink, particularly in the upper troposphere and regions with minimal precipitation.

Consideration of an additional significant sink would dramatically increase top-down estimates of OA flux based on aerosol measurements and inferences about loss processes. Bottom-up estimates, deduced from emission inventories and secondary organic aerosol (SOA) yields for precursor gases, may also be too low: Holzinger et al. (2005), for example, demonstrate that many biogenic SOA precursors are too short-lived to have been previously measured, and thus have been omitted from emission inventories. Furthermore, because of the diversity of SOA precursor gases, the photochemistry and

SOA yield of only a few model compounds have been extensively studied. Even for relatively well studied compounds, such as isoprene, estimates of SOA yields are undergoing significant revision upwards (Limbeck et al, 2003; Claeys et al., 2004ab; Kanakidou et al., 2005; Kroll et al., 2005). In addition, our understanding of other aspects of OA chemistry is poor. For example, Heald et al. (2005), considering only wet depositional loss, underpredict OA mass in the free troposphere 1-2 orders of magnitude, which they cannot attribute merely to OA flux underestimates.

4.5 Conclusions and recommendations

Our estimate of the OVOC source and its atmospheric impact are highly uncertain due to the complexity of the processes involved and the paucity of laboratory and field data for quantifying key parameters. Continued identification of OA constituents and study of oxidant interactions with a wider range of substrates is necessary to better constrain OVOC flux from atmospheric aerosols. Of particular concern is that much of the OA in the atmosphere may actually consist of highly oxidized humic like substances (HULIS) (Limbeck et al., 2003; Claeys et al., 2004a); whether HULIS can be volatilized in a similar fashion as the aliphatic compounds studied in the laboratory must be investigated. De Gouw and Lovejoy (1998) find that ozone reacts with liquid aldehydes and ketones ($\gamma \sim 10^{-4}$), but do not determine if any gas phase products form. An additional difficulty in applying laboratory studies is that they have utilized reaction parameters, such as low pressures and $[O_2]$, and high $[O_3]$ and $[OH]$, that are not representative of the real atmosphere. Moise and Rudich (2000) find, for example, that γ_{O_3} drops when O_2 instead of He is used as a carrier gas in their

experiments; also, Molina et al. (2004) propose that the carbon volatilization in their experiments would be reduced at atmospheric $[O_2]$. Laboratory studies on OA particles, rather than surface coatings on glassware, show that γ_{O_3} is also a function of aerosol size due to diffusion limitations in the bulk (Smith et al., 2002; Morris et al., 2002), which should be further investigated. Other oxidants, such as NO_3 , may also play an important role in aerosol oxidation. Finally, our analysis assumes that all aerosols are completely covered with organic films; accurate parameterizations of surface coverage are impossible without more field studies of aerosol surface coatings.

Acknowledgments

We thank Jonathan Abbatt (U. Toronto) for reviewing a draft of this manuscript, Steven Howell (U. Hawaii) for helpful discussions, Clyde Brown (NASA LaRC) for preparing merged data files, and the NASA Tropospheric Chemistry Program office for support of the INTEX-NA campaign. This material is based upon work supported under an NSF Graduate Research Fellowship (AJK) and EPA STAR Fellowship (JDC).

References

- Ammann, M., Poschl, U., and Rudich, Y.: Effects of reversible adsorption and Langmuir-Hinshelwood surface reactions on gas uptake by atmospheric particles, *Physical Chemistry Chemical Physics*, 5, 351-356, 10.1039/b208708a, 2003.
- Berkowitz, C. M., Zaveri, R. A., Bian, X. D., Zhong, S. Y., Disselkamp, R. S., Laulainen, N. S., and Chapman, E. G.: Aircraft observations of aerosols, O_3 and NO_y in a nighttime urban plume, *Atmospheric Environment*, 35, 2395-2404, 2001.

Bertram, A. K., Ivanov, A. V., Hunter, M., Molina, L. T., and Molina, M. J.: The reaction probability of OH on organic surfaces of tropospheric interest, *Journal of Physical Chemistry A*, 105, 9415-9421, 10.1021/jp0114034, 2001.

Claeys, M., Graham, B., Vas, G., Wang, W., Vermeylen, R., Pashynska, V., Cafmeyer, J., Guyon, P., Andreae, M. O., Artaxo, P., and Maenhaut, W.: Formation of secondary organic aerosols through photooxidation of isoprene, *Science*, 303, 1173-1176, 2004a.

Claeys, M., Wang, W., Ion, A. C., Kourtchev, I., Gelencser, A., and Maenhaut, W.: Formation of secondary organic aerosols from isoprene and its gas-phase oxidation products through reaction with hydrogen peroxide, *Atmospheric Environment*, 38, 4093-4098, 10.1016/j.atmosenv.2004.06.001, 2004b.

Clarke, A. D., Shinozuka, Y., Kapustin, V. N., Howell, S., Huebert, B., Doherty, S., Anderson, T., Covert, D., Anderson, J., Hua, X., Moore, K. G., McNaughton, C., Carmichael, G., and Weber, R.: Size distributions and mixtures of dust and black carbon aerosol in Asian outflow: Physiochemistry and optical properties, *Journal of Geophysical Research-Atmospheres*, 109, D15s09, 10.1029/2003jd004378, 2004.

Crawford, J., Davis, D., Olson, J., Chen, G., Liu, S., Gregory, G., Barrick, J., Sachse, G., Sandholm, S., Heikes, B., Singh, H., and Blake, D.: Assessment of upper tropospheric HOx sources over the tropical Pacific based on NASA GTE/PEM data: Net effect on HOx and other photochemical parameters, *Journal of Geophysical Research-Atmospheres*, 104, 16255-16273, 1999.

de Gouw, J. A., and Lovejoy, E. R.: Reactive uptake of ozone by liquid organic compounds, *Geophysical Research Letters*, 25, 931-934, 1998.

de Gouw, J. A., Middlebrook, A. M., Warneke, C., Goldan, P. D., Kuster, W. C., Roberts, J. M., Fehsenfeld, F. C., Worsnop, D. R., Canagaratna, M. R., Pszenny, A. A. P., Keene, W. C., Marchewka, M., Bertman, S. B., and Bates, T. S.: Budget of organic carbon in a polluted atmosphere: Results from the New England Air Quality Study in 2002, *Journal of Geophysical Research-Atmospheres*, 110, D16305, 10.1029/2004jd005623, 2005.

Ellison, G. B., Tuck, A. F., and Vaida, V.: Atmospheric processing of organic aerosols, *Journal of Geophysical Research-Atmospheres*, 104, 11633-11641, 1999.

Faloona, I. C., Tan, D., Leshner, R. L., Hazen, N. L., Frame, C. L., Simpas, J. B., Harder, H., Martinez, M., Di Carlo, P., Ren, X. R., and Brune, W. H.: A laser-induced fluorescence instrument for detecting tropospheric OH and HO₂: Characteristics and calibration, *Journal of Atmospheric Chemistry*, 47, 139-167, 2004.

Fuchs, N. A., and Sutugin, A. G.: Highly-dispersed aerosols, in: *Topics in Current Aerosol Research, Part 2*, edited by: Hidy, G. M., and Block, J. R., Elsevier, New York, 1971.

Gogou, A., Stephanou, E. G., Stratigakis, N., Grimalt, J. O., Simo, R., Aceves, M., and Albaiges, J.: Differences in lipid and organic salt constituents of aerosols from eastern

and western Mediterranean coastal cities, *Atmospheric Environment*, 28, 1301-1310, 1994.

Grannas, A. M., Shepson, P. B., and Filley, T. R.: Photochemistry and nature of organic matter in Arctic and Antarctic snow, *Global Biogeochemical Cycles*, 18, Gb1006, 10.1029/2003gb002133, 2004.

Heald, C. L., Jacob, D. J., Park, R. J., Russell, L. M., Huebert, B. J., Seinfeld, J. H., Liao, H., and Weber, R. J.: A large organic aerosol source in the free troposphere missing from current models, *Geophysical Research Letters*, 32, L18809, 10.1029/2005gl023831, 2005.

Holzinger, R., Lee, A., Paw, K. T., and Goldstein, A. H.: Observations of oxidation products above a forest imply biogenic emissions of very reactive compounds, *Atmospheric Chemistry and Physics*, 5, 67-75, 2005.

I.P.C.C.: *Climate Change 2001: The Scientific Basis -- Contribution of Working Group I to the Third Assessment Report of the Intergovernmental Panel on Climate Change*, Cambridge University Press, New York, 2001.

Kanakidou, M., Seinfeld, J. H., Pandis, S. N., Barnes, I., Dentener, F. J., Facchini, M. C., Van Dingenen, R., Ervens, B., Nenes, A., Nielsen, C. J., Swietlicki, E., Putaud, J. P., Balkanski, Y., Fuzzi, S., Horth, J., Moortgat, G. K., Winterhalter, R., Myhre, C. E. L.,

Tsigaridis, K., Vignati, E., Stephanou, E. G., and Wilson, J.: Organic aerosol and global climate modelling: a review, *Atmospheric Chemistry and Physics*, 5, 1053-1123, 2005.

Kieber, R. J., Zhou, X., and Mopper, M.: Formation of carbonyl compounds from UV-induced photodegradation of humic substances in natural waters: Fate of riverine carbon in the sea, *Limnology Oceanography*, 35, 1503-1515, 1990.

Kroll, J. H., Ng, N. L., Murphy, S. M., Flagan, R. C., and Seinfeld, J. H.: Secondary organic aerosol formation from isoprene photooxidation under high-NO_x conditions, *Geophysical Research Letters*, 32, L18808, 10.1029/2005gl023637, 2005.

Limbeck, A., Kulmala, M., and Puxbaum, H.: Secondary organic aerosol formation in the atmosphere via heterogeneous reaction of gaseous isoprene on acidic particles, *Geophysical Research Letters*, 30, 1996, 10.1029/2003gl017738, 2003.

McFiggans, G., Alfarra, M. R., Allan, J., Bower, K., Coe, H., Cubison, M., Topping, D., Williams, P., Decesari, S., Facchini, C., and Fuzzi, S.: Simplification of the representation of the organic component of atmospheric particulates, *Faraday Discussions*, 130, 341-362, 10.1039/b419435g, 2005.

Moise, T., and Rudich, Y.: Reactive uptake of ozone by proxies for organic aerosols: Surface versus bulk processes, *Journal of Geophysical Research-Atmospheres*, 105, 14667-14676, 2000.

Molina, M. J., Ivanov, A. V., Trakhtenberg, S., and Molina, L. T.: Atmospheric evolution of organic aerosol, *Geophysical Research Letters*, 31, L22104, 10.1029/2004gl020910, 2004.

Muller, J. F., and Brasseur, G.: Sources of upper tropospheric HOx: A three-dimensional study, *Journal of Geophysical Research-Atmospheres*, 104, 1705-1715, 1999.

Murphy, D. M., Thomson, D. S., and Mahoney, T. M. J.: In situ measurements of organics, meteoritic material, mercury, and other elements in aerosols at 5 to 19 kilometers, *Science*, 282, 1664-1669, 1998.

Poschl, U., Letzel, T., Schauer, C., and Niessner, R.: Interaction of ozone and water vapor with spark discharge soot aerosol particles coated with benzo a pyrene: O₃ and H₂O adsorption, benzo a pyrene degradation, and atmospheric implications, *Journal of Physical Chemistry A*, 105, 4029-4041, 2001.

Quinn, P. K., Bates, T. S., Baynard, T., Clarke, A. D., Onasch, T. B., Wang, W., Rood, M. J., Andrews, E., Allan, J., Carrico, C. M., Coffman, D., and Worsnop, D.: Impact of particulate organic matter on the relative humidity dependence of light scattering: A simplified parameterization, *Geophysical Research Letters*, 32, L22809, 10.1029/2005gl024322, 2005.

Rudich, Y.: Laboratory perspectives on the chemical transformations of organic matter in atmospheric particles, *Chemical Reviews*, 103, 5097-5124, 10.1021/cr020508f, 2003.

Singh, H., Chen, Y., Staudt, A., Jacob, D., Blake, D., Heikes, B., and Snow, J.: Evidence from the Pacific troposphere for large global sources of oxygenated organic compounds, *Nature*, 410, 1078-1081, 2001.

Singh, H. B., Kanakidou, M., Crutzen, P. J., and Jacob, D. J.: High concentrations and photochemical fate of oxygenated hydrocarbons in the global troposphere, *Nature*, 378, 50-54, 1995.

Singh, H. B., Salas, L. J., Chatfield, R. B., Czech, E., Fried, A., Walega, J., Evans, M. J., Field, B. D., Jacob, D. J., Blake, D., Heikes, B., Talbot, R., Sachse, G., Crawford, J. H., Avery, M. A., Sandholm, S., and Fuelberg, H.: Analysis of the atmospheric distribution, sources, and sinks of oxygenated volatile organic chemicals based on measurements over the Pacific during TRACE-P, *Journal of Geophysical Research-Atmospheres*, 109, D15s07, 10.1029/2003jd003883, 2004.

Staudt, A. C., Jacob, D. J., Ravetta, F., Logan, J. A., Bachiochi, D., Krishnamurti, T. N., Sandholm, S., Ridley, B., Singh, H. B., and Talbot, B.: Sources and chemistry of nitrogen oxides over the tropical Pacific, *Journal of Geophysical Research-Atmospheres*, 108, 8239, 10.1029/2002jd002139, 2003.

Tervahattu, H., Hartonen, K., Kerminen, V. M., Kupiainen, K., Aarnio, P., Koskentalo, T., Tuck, A. F., and Vaida, V.: New evidence of an organic layer on marine aerosols, *Journal of Geophysical Research-Atmospheres*, 107, 4053, 10.1029/2000jd000282, 2002a.

Tervahattu, H., Juhanaja, J., and Kupiainen, K.: Identification of an organic coating on marine aerosol particles by TOF-SIMS, *Journal of Geophysical Research-Atmospheres*, 107, 4319, 10.1029/2001jd001403, 2002b.

Tervahattu, H., Juhanaja, J., Vaida, V., Tuck, A. F., Niemi, J. V., Kupiainen, K., Kulmala, M., and Vehkamäki, H.: Fatty acids on continental sulfate aerosol particles, *Journal of Geophysical Research-Atmospheres*, 110, D06207, 10.1029/2004jd005400, 2005.

Thornberry, T., and Abbatt, J. P. D.: Heterogeneous reaction of ozone with liquid unsaturated fatty acids: detailed kinetics and gas-phase product studies, *Physical Chemistry Chemical Physics*, 6, 84-93, 10.1039/b310149e, 2004.

Wennberg, P. O., Hanisco, T. F., Jaegle, L., Jacob, D. J., Hintsala, E. J., Lanzendorf, E. J., Anderson, J. G., Gao, R. S., Keim, E. R., Donnelly, S. G., Del Negro, L. A., Fahey, D. W., McKeen, S. A., Salawitch, R. J., Webster, C. R., May, R. D., Herman, R. L., Proffitt, M. H., Margitan, J. J., Atlas, E. L., Schauffler, S. M., Flocke, F., McElroy, C. T., and Bui, T. P.: Hydrogen radicals, nitrogen radicals, and the production of O₃ in the upper troposphere, *Science*, 279, 49-53, 1998.

Wisthaler, A., Hansel, A., Dickerson, R. R., and Crutzen, P. J.: Organic trace gas measurements by PTR-MS during INDOEX 1999, *Journal of Geophysical Research-Atmospheres*, 107, 8024, 10.1029/2001jd000576, 2002.

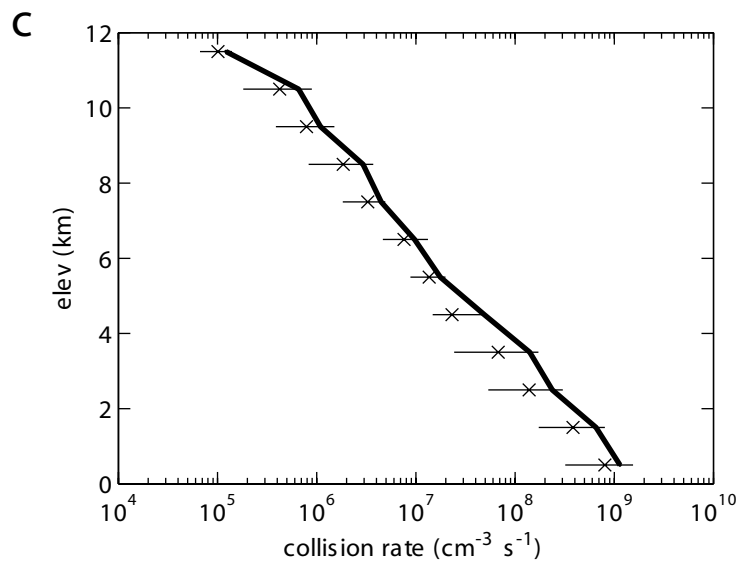
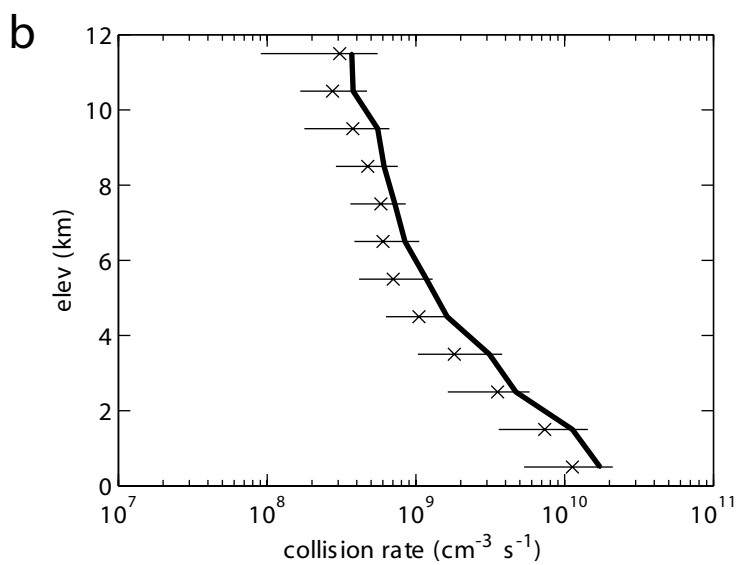
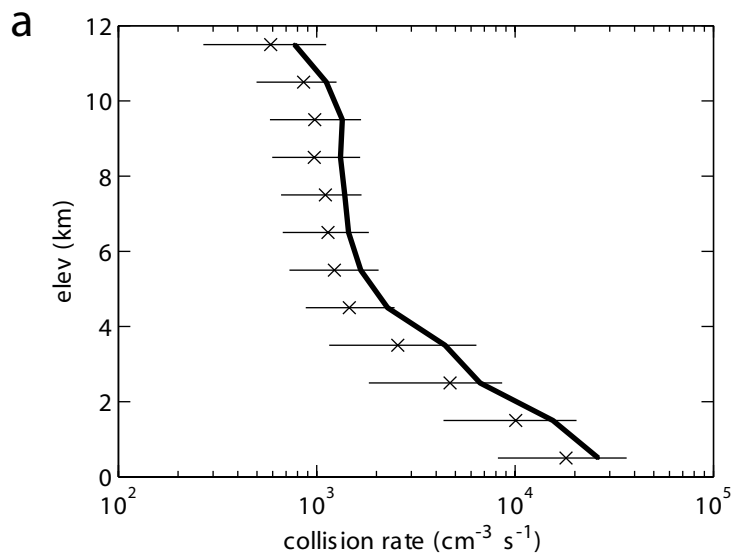


Figure 4.1. Mean elevation profiles of aerosol collision rates with a) OH, b) O₃, and c) H₂O₂. Horizontal lines show the interquartile range and x's are the elevation bin median.

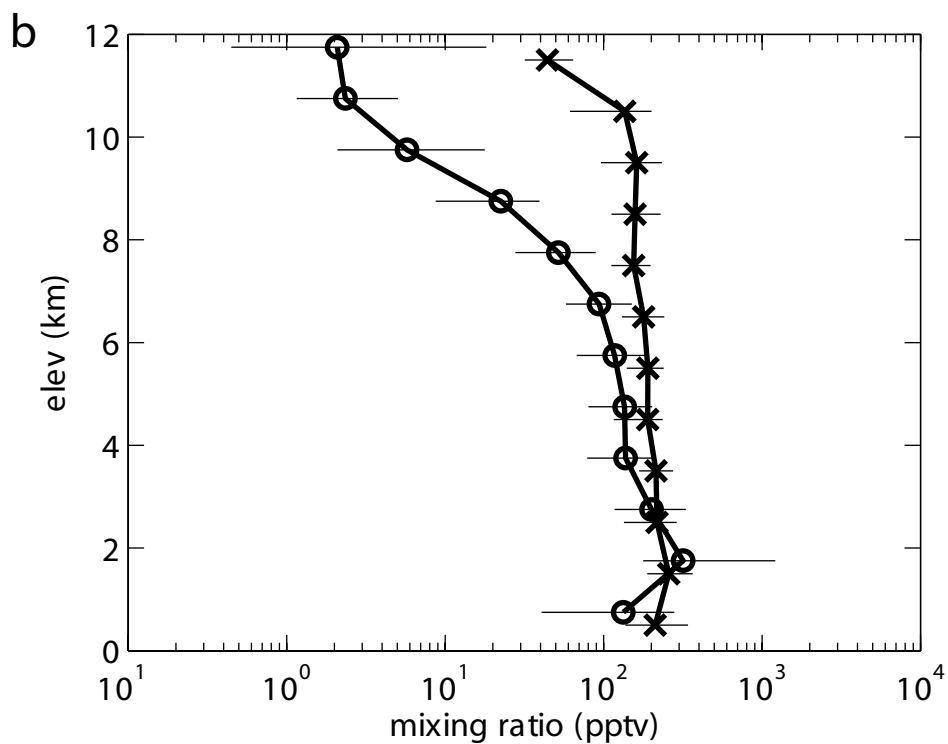
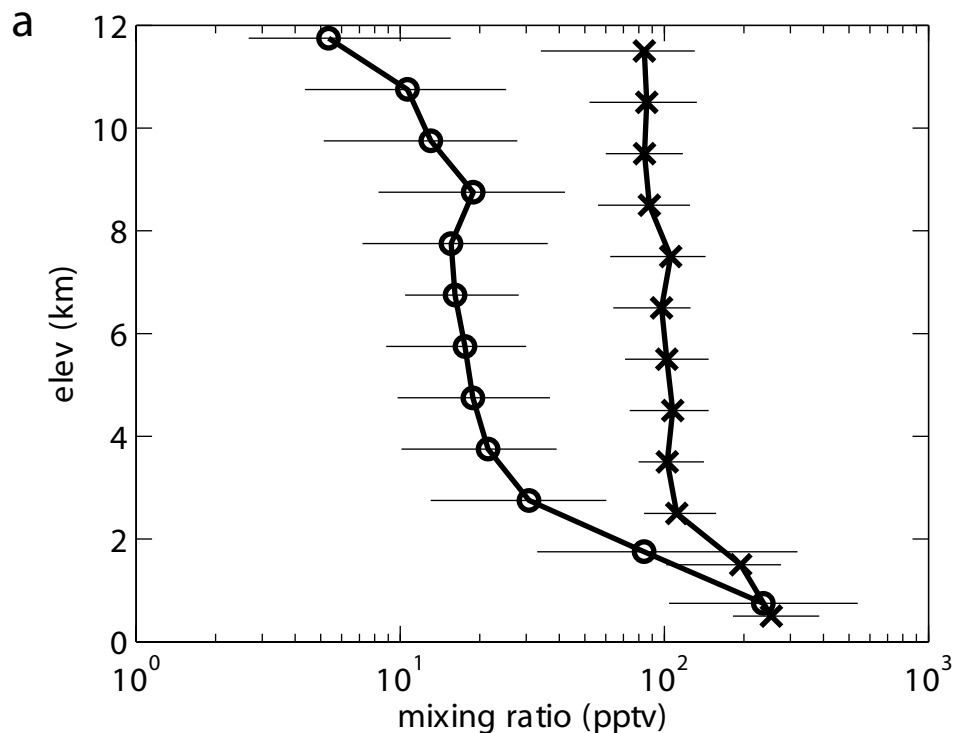


Figure 2. Modeled (circle) vs. measured (x) elevation profiles for acetaldehyde (a) and peroxyacetic acid (b). Marks are bin medians, lines are interquartile range. Model predictions offset by .25 km for clarity. Model assumes a PAA lifetime of ~ 20 days (upper limit).

Chapter 5

Conclusions and future directions

The study of organic aerosols will likely remain an active, complex, and evolving field. While this work, encompassing just a small selection of the field's analytical tools and current problems, has provided potentially important insights, it has also created many new questions deserving of further study.

In Chapter 2 we show the importance of ROOR dimers to SOA formation in laboratory studies. These compounds have generally been considered insignificant in the past, but their discovery motivates new avenues of research, in particular because SOA comprises a minor portion of VOC oxidation products, so even minor reaction pathways may be important. As ROOR dimers are novel compounds, the kinetics and mechanism of their formation are unknown even under controlled laboratory conditions, which makes predictions about their atmospheric relevance purely speculative. More studies focusing on ROOR are necessary to characterize their importance in atmospheric chemistry. Ultimately, it would be ideal to develop robust correlations between ROOR yields and measureable parameters (e.g., temperature, pressure, peroxy radical structure) for use in atmospheric models.

Even if ROOR formation were fully characterized, its full impact in the atmosphere will not be understood without knowledge of its subsequent reaction pathways. Although ROOR dimers are important SOA precursors in the laboratory, they do not lead exclusively to SOA. For many organic compounds, oxidation can either add mass and polarity, increasing the likelihood of SOA formation, or break carbon-carbon bonds, increasing volatility and decreasing the likelihood of SOA formation. Not reported in Chapter 2 is the formation of C₇ compounds in experiments where second generation chemistry is possible, i.e., where the concentration of NO₃ radical exceeds that

isoprene. These likely come from the breaking of carbon-carbon bonds of first generation C₁₀ ROOR compounds. Performing analyses of multiple oxidation steps is non-trivial because the variety of first generation products, each with their own unique second generation chemistry, leads to extremely complicated chemical evolution in the chamber. Thus, obtaining complete VOC oxidation mechanisms will require systematically stepping through single oxidation steps, which is time consuming and difficult, especially because many intermediates in the overall oxidation mechanism are not easily synthesizable or quantifiable.

Studies on ROOR formation will center on RO₂-RO₂ reactions, but as shown in Chapter 3, the current suite of experimental data provide inadequate proxies for explaining the product yield of RO₂-RO₂ (and RO₂-HO₂) reactions in the isoprene-NO₃ system, even for non-ROOR products. Flow tubes have been effective for characterizing reactions of small peroxy radicals, but the study of more complex radicals is limited by the challenges of their synthesis. It is also unclear at the moment if the conditions and analytical techniques typically employed in flow tube studies are appropriate for forming or detecting ROOR.

These fundamental studies are only a first step, because the atmosphere is a complex mixture where diverse hydrocarbons react with multiple oxidants (OH, NO₃, O₃, halogen atoms). If conditions favor RO₂-RO₂ reactions, they are likely to be cross-reactions (i.e., reactions between different peroxy radicals) rather than self-reactions (i.e., reactions between identical peroxy radicals). Peroxy radical cross-reactions are even less well understood than self-reactions.

While our work on isoprene-NO₃ is too recent for its impact to be assessed, studies addressing the issues posed in our analysis of aerosol sinks (Chapter 4) suggest that while volatilization of ambient organic aerosol does occur, it does not occur at a rate that is significant for organic aerosol budgets, or, likely, OVOC budgets. Murphy et al. (2007) report that tropospheric aerosols that reach the stratosphere, with an estimated age of ~ 4-6 months, show loss of organic matter with respect to sulfate, consistent with volatilization by heterogeneous oxidation ($\gamma > 0.1$, considering only oxidation by OH radical). The age of the particles, however, is significantly longer than the lifetime against oxidation proposed in Chapter 4 (~ 10 days), which can be explained by our key assumptions ($\gamma = 1$ and the volatilization of 6 carbons per OH collision) being overly favorable to volatilization, and the larger particles detected by the authors (> 300 nm) having lower surface area to volume ratios than fine particles and thus being more resistant to volatilization. The particle lifetimes in the study are also significantly longer than that of most tropospheric aerosol, ~ 5-10 days against deposition (Kanakidou et al., 2005). Recent laboratory and field studies of aerosol oxidation over these timescales show minor loss of carbon, and negligible loss of total mass due to increasing oxygen content in the aerosol (Capes et al., 2008; DeCarlo et al., 2008; George et al., 2008; Dunlea et al., 2009). Although heterogeneous oxidation may not be relevant to OVOC production or aerosol abundance, its impacts on aerosol chemical composition still make it worthy of further study.

Besides its exploration of scientific theories, this work also exemplifies the importance of having a diverse array of analytical techniques for addressing the complex problems of organic aerosols. In addition to the importance of ROOR dimers, recent

experiments at the Caltech environmental chamber have combined insights from CIMS and aerosol measurements to elucidate the role of peroxy acetyl nitrates and epoxydiols in SOA formation (Surratt et al., 2009; Chan et al., 2010), while field measurements with the CIMS have shown that biomass burning is at times the dominant source of organic aerosols in the Mexico City airshed (Crouse et al., 2009). Where definitive conclusions have not been achieved in this work (e.g., the parameters determining ROOR formation, how the fate of isoprene nitrooxyalkoxy radicals depends on their formation mechanism, or what the accommodation coefficient of oxidants on an organic aerosol is), it is generally due to the limitations of our analytical tools, and more studies expanding the suite of techniques and perspectives analyzing the problem may lead to more concrete explanations.

Applying the CIMS in its current configuration to study a wider variety of systems will likely produce more useful data, but in the future the CIMS will not be limited to gas-phase measurements. With a custom aerosol inlet currently under development, we will be able to apply the CIMS to direct measurements of aerosol-phase composition, enhancing the instrument's capabilities and its contributions to understanding organic aerosol chemistry.

While this work has focused on applications of the CIMS to organic aerosol studies, the instrument's qualities make it useful to address a range of other outstanding problems in atmospheric chemistry. In particular, its high time resolution makes it ideal for airplane sampling, allowing for high spatial resolution for studying small scale processes, for example the interaction of trace gases with liquid and ice cloud particles during vertical transport. Convection and frontal lofting transport surface emissions (and

their oxidation products) to the upper troposphere, where their fate and global impacts may be significantly different than in their source regions (e.g., Lacis et al., 1990). As air parcels rise, liquid and possibly ice clouds will form, providing additional media for gas scavenging or heterogeneous reactions. Of particular interest is what happens to dissolved gases when a liquid hydrometeor freezes. Thermodynamically, gases are less soluble in ice than liquid water, which implies that they would be released at the level of freezing, but kinetically, the mass transfer to the gas phase may be slower than freezing, in which case the gases will be carried with the ice and released at the elevation the ice sublimates or evaporates (Stuart and Jacobson, 2003). Although there have been numerous campaigns aimed at understanding the chemical consequences of deep convection, these campaigns have relied on traditional methods for measuring soluble acids and peroxides, which lack the resolution to reveal the detailed structure of air masses, which is important because encounters with cloud influenced air may be of short duration in an airplane.

Many challenges remain, some known, many waiting to be revealed by new discoveries or creative disruptions. No tool, no instrument – or instrument user – is perfect, and fully understanding the atmosphere and mankind's impacts on it will require continued diligent and multifaceted efforts filled mostly with dead ends and misdirections, but also, occasionally, triumph, and, always, enlightenment. It is left to future researchers to determine if this work is a dead end, a triumph, or something in between, but regardless of history's judgment it has been a worthwhile journey.

References

Capes, G., Johnson, B., McFiggans, G., Williams, P. I., Haywood, J., and Coe, H.: Aging of biomass burning aerosols over West Africa: Aircraft measurements of chemical composition, microphysical properties, and emission ratios, *Journal of Geophysical Research-Atmospheres*, 113, D00c15, 10.1029/2008jd009845, 2008.

Chan, A. W. H., Chan, M. N., Surratt, J. D., Chhabra, P. S., Loza, C. L., Crouse, J. D., Yee, L. D., Flagan, R. C., Wennberg, P. O., and Seinfeld, J. H.: Role of aldehyde chemistry and NO_x concentrations in secondary organic aerosol formation, *Atmos. Chem. Phys. Discuss.*, 10, 10219-10269, 10.5194/acpd-10-10219-2010, 2010.

Crouse, J. D., DeCarlo, P. F., Blake, D. R., Emmons, L. K., Campos, T. L., Apel, E. C., Clarke, A. D., Weinheimer, A. J., McCabe, D. C., Yokelson, R. J., Jimenez, J. L., and Wennberg, P. O.: Biomass burning and urban air pollution over the Central Mexican Plateau, *Atmospheric Chemistry and Physics*, 9, 4929-4944, 2009.

DeCarlo, P. F., Dunlea, E. J., Kimmel, J. R., Aiken, A. C., Sueper, D., Crouse, J., Wennberg, P. O., Emmons, L., Shinozuka, Y., Clarke, A., Zhou, J., Tomlinson, J., Collins, D. R., Knapp, D., Weinheimer, A. J., Montzka, D. D., Campos, T., and Jimenez, J. L.: Fast airborne aerosol size and chemistry measurements above Mexico City and Central Mexico during the MILAGRO campaign, *Atmospheric Chemistry and Physics*, 8, 4027-4048, 2008.

Dunlea, E. J., DeCarlo, P. F., Aiken, A. C., Kimmel, J. R., Peltier, R. E., Weber, R. J., Tomlinson, J., Collins, D. R., Shinozuka, Y., McNaughton, C. S., Howell, S. G., Clarke, A. D., Emmons, L. K., Apel, E. C., Pfister, G. G., van Donkelaar, A., Martin, R. V., Millet, D. B., Heald, C. L., and Jimenez, J. L.: Evolution of Asian aerosols during transpacific transport in INTEX-B, *Atmospheric Chemistry and Physics*, 9, 7257-7287, 2009.

George, I. J., Slowik, J., and Abbatt, J. P. D.: Chemical aging of ambient organic aerosol from heterogeneous reaction with hydroxyl radicals, *Geophysical Research Letters*, 35, L13811, 10.1029/2008gl033884, 2008.

Kanakidou, M., Seinfeld, J. H., Pandis, S. N., Barnes, I., Dentener, F. J., Facchini, M. C., Van Dingenen, R., Ervens, B., Nenes, A., Nielsen, C. J., Swietlicki, E., Putaud, J. P., Balkanski, Y., Fuzzi, S., Horth, J., Moortgat, G. K., Winterhalter, R., Myhre, C. E. L., Tsigaridis, K., Vignati, E., Stephanou, E. G., and Wilson, J.: Organic aerosol and global climate modelling: a review, *Atmospheric Chemistry and Physics*, 5, 1053-1123, 2005.

Lacis, A. A., Wuebbles, D. J., and Logan, J. A.: Radiative forcing of climate by changes in the vertical distribution of ozone, *Journal of Geophysical Research-Atmospheres*, 95, 9971-9981, 1990.

Mari, C., Jacob, D. J., and Bechtold, P.: Transport and scavenging of soluble gases in a deep convective cloud, *Journal of Geophysical Research-Atmospheres*, 105, 22255-22267, 2000.

Murphy, D. M., Cziczo, D. J., Hudson, P. K., and Thomson, D. S.: Carbonaceous material in aerosol particles in the lower stratosphere and tropopause region, *Journal of Geophysical Research-Atmospheres*, 112, D04203, 10.1029/2006jd007297, 2007.

Stuart, A. L., and Jacobson, M. Z.: A timescale investigation of volatile chemical retention during hydrometeor freezing: Nonrime freezing and dry growth riming without spreading, *Journal of Geophysical Research-Atmospheres*, 108, 4178, 10.1029/2001jd001408, 2003.

Surratt, J. D., Chan, A. W. H., Eddingsaas, N. C., Chan, M. N., Loza, C. L., Kwan, A. J., Hersey, S. P., Flagan, R. C., Wennberg, P. O., and Seinfeld, J. H.: Reactive intermediates revealed in secondary organic aerosol formation from isoprene, *Proceedings of the National Academy of Sciences of the United States of America*, 107, 6640-6645, 10.1073/pnas.0911114107, 2010.

Appendix: List of authored and coauthored publications

(not including manuscripts in preparation)

Bertram, T. H., Perring, A. E., Wooldridge, P. J., Crouse, J. D., Kwan, A. J., Wennberg, P. O., Scheuer, E., Dibb, J., Avery, M., Sachse, G., Vay, S. A., Crawford, J. H., McNaughton, C. S., Clarke, A., Pickering, K. E., Fuelberg, H., Huey, G., Blake, D. R., Singh, H. B., Hall, S. R., Shetter, R. E., Fried, A., Heikes, B. G., and Cohen, R. C.: Direct measurements of the convective recycling of the upper troposphere, *Science*, 315, 816-820, 10.1126/science.1134548, 2007.

Chan, A. W. H., Galloway, M. M., Kwan, A. J., Chhabra, P. S., Keutsch, F. N., Wennberg, P. O., Flagan, R. C., and Seinfeld, J. H.: Photooxidation of 2-Methyl-3-Buten-2-ol (MBO) as a Potential Source of Secondary Organic Aerosol, *Environmental Science & Technology*, 43, 4647-4652, 10.1021/es802560w, 2009.

Crouse, J. D., McKinney, K. A., Kwan, A. J., and Wennberg, P. O.: Measurement of gas-phase hydroperoxides by chemical ionization mass spectrometry, *Analytical Chemistry*, 78, 6726-6732, 10.1021/ac0604235, 2006.

Kwan, A. J., Crouse, J. D., Clarke, A. D., Shinozuka, Y., Anderson, B. E., Crawford, J. H., Avery, M. A., McNaughton, C. S., Brune, W. H., Singh, H. B., and Wennberg, P. O.: On the flux of oxygenated volatile organic compounds from organic aerosol oxidation, *Geophysical Research Letters*, 33, L15815, 10.1029/2006gl026144, 2006.

Ng, N. L., Chhabra, P. S., Chan, A. W. H., Surratt, J. D., Kroll, J. H., Kwan, A. J., McCabe, D. C., Wennberg, P. O., Sorooshian, A., Murphy, S. M., Dalleska, N. F., Flagan, R. C., and Seinfeld, J. H.: Effect of NO_x level on secondary organic aerosol (SOA) formation from the photooxidation of terpenes, *Atmospheric Chemistry and Physics*, 7, 5159-5174, 2007.

Ng, N. L., Kwan, A. J., Surratt, J. D., Chan, A. W. H., Chhabra, P. S., Sorooshian, A., Pye, H. O. T., Crouse, J. D., Wennberg, P. O., Flagan, R. C., and Seinfeld, J. H.: Secondary organic aerosol (SOA) formation from reaction of isoprene with nitrate radicals (NO₃), *Atmospheric Chemistry and Physics*, 8, 4117-4140, 2008.

Surratt, J. D., Chan, A. W. H., Eddingsaas, N. C., Chan, M. N., Loza, C. L., Kwan, A. J., Hersey, S. P., Flagan, R. C., Wennberg, P. O., and Seinfeld, J. H.: Reactive intermediates revealed in secondary organic aerosol formation from isoprene, *Proceedings of the National Academy of Sciences of the United States of America*, 107, 6640-6645, 10.1073/pnas.0911114107, 2010.